Molybdenum and arsenic behavior in a limestone aquifer in Central Florida

Dissertation

Zur Erlangung des Doktorgrades der Naturwissenschaften (Dr. rer. nat.)

am Fachbereich Geowissenschaften

der Universität Bremen

Vorgelegt von

Ali Mozaffari

Bremen, November 2016

Gutachter:

Prof. Dr. Thomas Pichler

Erklärung

Hiermit versichere ich, dass ich

i.die Arbeit ohne unerlaubte fremde Hilfe angefertigt habe,

ii. keine anderen als die von mir angegebenen Quellen und Hilfsmittel benutzt haben und

iii.die den benutzten Werken wörtlich oder inhaltlich entnommen Stellen als solche kenntlich gemacht habe.

_____ ,den _____

_____ (Unterschrift)

Table of Contents

List of Figures

List of Tables

Abstract

The mobilization of geogenic molybdenum (Mo) and arsenic (As) from the aquifer matrix sediments in Central Florida, USA has resulted in the contamination of groundwater and irrigated soils. The aquifer matrix contained up to 825 mg/kg Mo and 144 mg/kg As. The concentrations of Mo and As in groundwater reached up to 5000 µg/L and 300 µg/L which exceed the WHO guidelines of 70 µg/L and 10 µg/L, respectively. In this research, in order to evaluate the potential of Mo and As as contaminants in the aquifer matrix sediments, chemical fractionation, primary sources, and the adsorption/desorption behavior of Mo and As by/from hydrous ferric oxide (HFO) were studied. The adsorption of Mo onto organic matter (OM) was also investigated to determine its role in removing Mo from groundwater. First, a five step sequential extraction procedure (SEP) was applied to 10 aquifer matrix samples which were chosen from three cores near Lithia village in Central Florida. Then, the chromium-reducible sulfur (CRS) method was used to assess the primary sources of Mo and As. This particular method was used to determine the relationship between reduced sulfur including inorganic reduced sulfur such as sulfur content in pyrite (FeS_2) and organic sulfur (OS) and the trace elements (Mo and As) in the aquifer matrix. Finally, to assess the adsorption and desorption of Mo and As by/from HFO and humic acid (HA), a combination of batch experiments with HFO, HA and the aquifer matrix sediments were conducted.

The results of SEP showed that Mo was mainly present in the soluble fraction (step 1). For six samples, more than 80%, for two samples more than 50% and for two samples up to 20% Mo was released during the first step. About 10% Mo was leached during steps 2 and 3, which dissolve carbonates, HFO, manganese oxides and powellite ($CaMoO_4$). Approximately 25% of Mo bounded to crystalline iron oxides, pyrite and OM in steps 4 and 5. In contrast to Mo, As was present in all the extraction's steps in somewhat similar abundances: step 1 (17%), step 2 (11%), step 3 (30%), step 4 (23%) and step 5 (18%). Hydrous and crystalline iron oxides, which were dissolved in steps 3 and 4 contained the highest As concentrations. From this

procedure, it became clear that compared to As, Mo is more easily released from the aquifer matrix.

Pyrite and OM which were present in both aquifer matrix sediments underlying Lithia area and in Avon Park Formation (APF), were generally considered as source for Mo and As. To evaluate this statement, a total of 24 samples (including 10 samples which were already subjected to SEP analysis) were chosen from Lithia area and APF. The samples were selected based on the following four criteria: (1) high total Mo concentration, (2) high total As concentration, (3) high total sulfur concentration, and (4) good geographic representation of the study area. The results of CRS did not confirm the presence of Mo in pyrite in the Lithia area, though it was shown to exist as a minor constituent in the APF. The total organic carbon content in the residues of CRS (OC_{res}) method was positively correlated to Mo ($R^2 = 0.71$ and $p < 0.001$). There was no correlation between OS and Mo. Compared to Mo, As concentration in pyrite was much higher, pointing to pyrite as a major primary source for As in the aquifer matrix sediments. There was a weak correlation between As and OC_{res}. The results suggested that the Mo found in the aquifer matrix and groundwater was mainly sourced from OM rather than pyrite, whereas As originated mainly from pyrite as a primary source, in addition to iron oxides in the adsorbed forms.

The adsorption and desorption of Mo and As by/from HFO and HA indicated that HFO was not a major sink for Mo but a significant secondary source for As. Molybdenum sorption onto HFO mainly happened by the formation of inner-sphere complexes. Arsenic(III) and As(V) sorption onto HFO resulted in inner-sphere complexes. Oxygenated water had no significant effect on the mobilization of Mo and As from the aquifer matrix in the Lithia area and APF. Powellite could be considered as a minor secondary source for Mo and As. In the alkaline pH ranges (pH ranges of the study area), the adsorption of Mo on HA was too low.

Special experiments were carried out for the first time in the present study to distinguish Mo adsorption types onto HFO (inner or outer complexes). First, the aquifer matrix samples and HFO samples with specified amount of Mo adsorbed on their surfaces were dissolved in DDI

water and shaken for 48 h. Then, the first three steps of the SEP were applied to the residue of the samples. The results showed two types of Mo adsorption onto HFO, i.e. inner sphere and outer sphere complexes. Studies to date recognized only one type, i.e. inner sphere complexes, for Mo adsorption onto HFO. Therefore, this is a completely new finding stemmed from this study. In addition, our experiments also provided a precise estimation of the amount of each adsorption type. About 20% of the total Mo sorbed onto HFO were outer sphere and 80% inner sphere complexes. Such methodology is of appreciable practical application because it is quicker, cheaper and simpler with much less complexity. It is believed that the invented technique is important, not only for the study area but also for all ecological projects and environmental pollution studies which may involve Mo in one way or another.

To summarize, this study demonstrated that OM was a main primary source for Mo in the study area. Oxidation of OM led to the mobilization of Mo from strong phases to soluble phases. This process resulted in the release of Mo into groundwater. On the other hand, Mo was removed from the groundwater either through powellite precipitation or via adsorption onto adsorbents such as HFO, OM, and clay minerals. Precipitation of powellite was considered as trivial and insufficient to be a substantial sink for Mo. Also, Mo adsorption onto HFO and OM was not significant. The main reason for low Mo adsorption onto HFO was related to the point of zero charge (PZC) of HFO which roughly corresponded to the pH of the Lithia's groundwater. It was also discovered that there was a strong competition between phosphate, sulfate and molybdate for HFO sorption sites. Phosphate competed strongly with molybdate for sorption sites, while sulfate was relatively a weaker competitor.

Mo adsorption/desorption by/from other adsorbents such as clays, carbonates and their organically bounds, remain questionable. These are the areas requiring more research, since very little, if any, is known about these topics. All these considerations and findings explain why Mo was not fixed and commuted between groundwater and the exchangeable phases in Lithia area.

Kurzzusammenfassung

Die Mobilisierung von geogenem Molybdän (Mo) und Arsen (As) aus Sedimentgesteinen hat in Zentral-Florida zu Kontamination des Grundwassers und der bewässerten Böden geführt. Diese Sedimentgesteine enthalten bis zu 825 mg/kg Mo und 144 mg/kg As. Die Mo und As Konzentrationen im Grundwasser erreichen bis zu 5000 µg/L beziehungsweise 300 µg/L und übersteigen die WHO-Richtwerte von 70 µg/L und 10 µg/L erheblich.

In dieser Arbeit wurden die chemische Fraktionierung, die primären Quellen sowie die Adsorption/Desorption von Mo und As an wasserhaltiges Eisenoxid und organische Stoffe (OM) untersucht, und versucht, ihre mögliche Rolle als Kontaminanten in dem Aquifer-Matrix zu bewerten. Zuerst wurde ein fünfstufiges sequentielles Extraktionsverfahren auf 10 Aquifer Matrixproben angewendet, die aus drei Bohrkernprobe in der Nähe des Dorfes Lithia ausgewählt wurden. Dann wurde das CRS-Verfahren zur Bestimmung von Chrom-reduzierbarem Schwefel angewendet, um primäre Mo und As Quellen zu beurteilen. Diese besondere Methode wurde verwendet, um die Beziehung zwischen reduziertem Schwefel (Pyrit Schwefel und organischer Schwefel) und der Mo und As Konzentration in den sedimentären Gesteinen zu bestimmen. Schließlich wurde eine Kombination aus Batchversuchen mit synthetisiertem Ferrihydrit, Huminsäure und Aquifer-Matrix durchgeführt, um die Adsorption und Desorption von Mo und As an diese Materiale zu beurteilen. Die SEP Ergebnisse zeigen, dass Mo eine sehr lösliche Fraktion ist (Schritt 1). Bei sechs Proben wurden mehr als 80 % Mo, bei zweien mehr als 50 % und bei zwei weiteren bis zu 20 % in der Fraktion mobilisiert. Etwa 10 % Mo wurden im Schritt 2 und 3 mobilisiert, die Carbonate, HFO, Manganoxide und Powellit wurden gelöst. In den Schritten 4 und 5 wurden etwa 25 % Mo an Eisenoxiden, Pyrit und OM adsorbiert. Im Gegensatz zu Mo war Arsen in allen Extraktionsschritte etwa gleich vertreten: Schritt 1 (17 %), Schritt 2 (11 %), Schritt 3 (30 %), Schritt 4 (23 %) und Schritt 5 (18 %). Wasserhaltige und kristalline Eisenoxide, die in den Schritten 3 und 4 gelöst wurden, enthielten die höchsten As Konzentrationen. Durch dieses

Verfahren wurde deutlich, dass Mo im Vergleich zu As leichter aus der Aquifer-Matrix gelöst und mobilisiert wird.

Pyrit und OM, die in der Lithia und APF Aquifer-Matrix vorkommen, werden allgemein als Quellen für Mo und As angenommen. Um diese Möglichkeiten zu bewerten wurden insgesamt 24 Proben (einschließlich 10 Proben der SEP) aus Lithia und APF gewählt. Die Proben wurden auf Grundlage dreier Kriterien ausgewählt: (1) hohe gesamt Mo Konzentration, (2) hohe gesamt As Konzentration und (3) gute geographische Darstellung des Untersuchungsgebietes. Die Ergebnisse der CRS zeigten kein Mo in Pyrit in DEP Kernen. Es wurde jedoch als Nebenquelle in APF bestätigt. Der Gesamtgehalt an organischem Kohlenstoff in den Resten der CRS (OC_{res}) zeigt eine gute Korrelation mit Mo (R^2 = 0.65). Es gibt keine Korrelation zwischen dem organischen Schwefel (OS) und Mo. Im Vergleich zu Mo, ist die As-Konzentration in Pyrit viel höher und weist auf Pyrit als primäre Quelle für As in den Aquifer-Matrix. Es gibt eine schwache Korrelation zwischen As und OC_{res}. Die Ergebnisse zeigen, dass organisches Material und nicht Pyrit die primäre Quelle für Mo in der Aquifer-Matrix und im Grundwasser ist, während As hauptsächlich auf adsorbiertes Pyrit als primäre Quelle zurückzuführen ist sowie auf Eisenoxide in den adsorbierten Formen.

Molybdän und As Adsorption und Desorption an HFO und Huminsäure zeigen, dass Ferrihydrit keine wichtige Quelle für Mo, jedoch eine bedeutende sekundäre Quelle für As ist. Molybdän Sorption an HFO bildet hauptsächlich inner-sphärische Komplexe. Arsenic (III) und As(V) Sorption an HFO bilden inner-sphärische Komplexe. Sauerstoff angereichertes Wasser hatte keinen signifikanten Effekt auf die Mobilisierung von Mo und As in Lithia und APF. Powellit könnte als sekundäre Quelle für Mo und As in Betracht gezogen werden. Die Molybdän Adsorption an Huminsäure ist in dem untersuchten alkalischen pH-Bereich zu niedrig.

Das Ergebnis dieser Arbeit zusammenzufassen, organische Materie wurde in der Lithia-Region als primäre Quelle für Molybdän bestimmt. OM konnte oxidiert werden und Molybdän wurde in Folge dessen von der starken Phase zur löslichen Phase verschoben und ins Grundwasser freigesetzt. Denkbar sind zwei Arten, Molybdän aus dem Grundwasser zu entfernen. Erstens durch Niederschlag von Powellite, jedoch war dies nicht signifikant. Zweitens durch Adsorbenten wie HFO und OM. Jedoch war die Molybdän-Adsorption auf HFO und OM aus zwei Gründen in Bezug auf HFO nicht signifikant. Zunächst entsprach der pH-Wert des Untersuchungsgebietes etwa dem Nullpunkt von HFO. Zweitens herrschte ein Wettbewerb zwischen Phosphat und Molybdän. Selbst wenn Mo trotz dieser Beschränkungen adsorbiert werden konnte, waren 20 % des gesamten Mo-sorbierten Zustandes immer noch austauschbar. Diese könnten als äußere und innere Sphären-Komplexen betrachtet werden. Während frühere Studien nur innere Sphären-Komplexe für Mo-Adsorption auf HFO feststellten, ist dieses Erkenntniss neu. Mo-Adsorption/ Desorption mit anderen Adsorptionsmitteln wie Ton, Carbonat und dessen organischen Verbindungen müssten noch untersucht werden. Die große Menge Gesamt-Mo wurde jedoch nicht fest an diese Adsorptionsmittel adsorbiert, daher wurde es in der Lithia-Region frei und verlagert zwischen Grundwasser und austauschbaren Phasen gefunden.

Chapter 1. Introduction

1.1 Problem statement

Generally, water quality studies focus on anthropogenic sources as potential environmental contaminants. However, groundwater contamination is not exclusively due to the direct input of contaminants. Geogenic trace element enrichment in sedimentary rocks can contaminate drinking water and irrigated soils (Pichler and Mozaffari, 2015; Pichler et al., 2016). The leaching of metals from these rocks poses a threat to the groundwater resources and may persist for a long time in groundwater (e.g., Amini et al., 2008; Ferguson and Gavis, 1972). This type of contamination is a public health issue worldwide particularly for arsenic (As), but this is the first study of its kind with respect to molybdenum (Mo). Thus, in this study, emphasis was on Geogenic Mo as a potential groundwater contaminant.

In general, metals and metalloids can be divided into two groups: those which are essential for human survival like calcium (Ca), magnesium (Mg), zinc (Zn), iron (Fe), Mo, etc, and those which are less important and at the same time toxic, including among others mercury (Hg), lead (Pb) and As (Slaveykova and Wilkinson, 2005). In fact, Mo plays a unique role in the environment. In one hand, it is a cofactor of enzymes which are essential in plants, animals and for human health and it is important for the functioning of the enzyme xanthine dehydrogenase which plays key roles in human metabolism (Momcilovic, 2000; WHO, 2011). In the other hand, it has potential benefits for patients with asthma and sulfite sensitivity. High doses of Mo can damage organisms in terrestrial and aquatic environments and could cause some problems for human organs like osteoporosis, gout, liver enlargement, disorders of the gastrointestinal tract, respiratory infections, kidney diseases, increased blood levels of Mo, uric acid and increased xanthine oxidase activity (Krishnamachari and Krishnaswamy, 1974; Stiefel, 1996). Major threats to human health are associated with exposure to Pb, cadmium

(Cd), Hg, uranium (U) and As. These metals and metalloids pose serious threats to the health of millions of people around the world (O'Shea et al., 2007; Reza et al., 2010; Schreiber et al., 2000). The Lithia area in Central Florida provides an exceptional field site to study the contamination of groundwater by geogenic Mo and As in a limestone aquifer. Previous studies indicated no obvious anthropogenic or agricultural sources for Mo and As in the area (Pichler and Mozaffari, 2015; Pichler et al., 2016). The sedimentary rocks in the Lithia area contained high levels of Mo and As. The concentrations of Mo and As in the aquifers were high and exceeded the WHO guidelines of 70 and 10 µg/L, respectively (Pichler and Mozaffari, 2015; Pichler et al., 2016).

1.2 Research objectives

The central hypothesis of this study was to determine whether geogenic Mo and As are potential contaminants in a limestone aquifer. Although water quality studies focus mainly on anthropogenic sources; but terrestrial environments and groundwater may also be affected by the mobilization of geogenic trace metals such as Mo and As from sedimentary rocks. There were some studies with regard to As, but very little knowledge, if any, was available about Mo and its leaching processes from the sedimentary rocks into groundwater. Thus, the specific objectives of this work were to:

1. Assess the chemical fractionation of Mo and As in the aquifer matrix by using sequential extraction procedure (SEP),
2. Test the effect of dissolved oxygen and time on Mo and As mobilization from the aquifer matrix,
3. Determine the primary sources of Mo and As in the aquifer matrix by using the chromium reduction sulfur (CRS) method,

4. Evaluate powellite ($CaMoO_4$) as a source for Mo and As in the aquifer matrix and groundwater,

5. Evaluate Mo and As adsorption and leaching processes from hydrous ferric oxide (HFO) in the aquifer matrix, and

6. Investigate organic matter (OM) as a Mo adsorbent from groundwater.

1.3 Research outlines

The research described in this thesis is organized in 6 chapters. Chapter 1, Introduction, describes the research background, study site, problems and objectives. In Chapter 2, a review of the publications dealing with the primary sources of Mo and As, adsorption/desorption, speciation, mechanism, and model applications is presented.

The main subjects dealt with in this thesis are described in Chapters 3 to 5, which are assigned to achieve the research objectives already mentioned in the previous chapters. Chapter 3 deals with the assessment of Mo and As speciation in the aquifer matrix. This chapter describes a modified five-step SEP which was applied to 10 samples of three cores to assess the presence of Mo and As in the adsorbed/exchangeable phases, carbonates, hydrous iron oxides (HFO), crystalline iron oxides and sulfides. In addition, the effect of dissolved oxygen on the exchangeable phases is also presented. A part of this research was published in the Journal of Applied Geochemistry (Pichler and Mozaffari, 2015).

In Chapter 4, the primary sources of Mo and As in the aquifer matrix and groundwater are determined. Analysis which introduced powellite as a main secondary source for the elements in question are also described in this Chapter.

Chapter 5, discusses the adsorption of Mo and As onto two adsorbents, HFO and humic acid. Additionally, desorption experiments from HFO are also described.

Chapter 6 presents the conclusions and recommendations drawn from this investigation.

1.4 Site description

1.4.1 Location

This study was carried out in a local area (Lithia) and a regional area (Southwest Florida). Lithia is a relatively small area (3 × 4 km), located approximately 30 km southeast of Tampa city on the west coast of Florida. There are approximately 100 private water supply wells and 5 monitoring wells including DEP-1 to DEP-5 which were installed by The Florida Department of Environmental Protection (DEP) after discovering more than 5000 µg/L Mo by accident in an irrigation well in Lithia area (Fig 1.1). Previous studies collected water and drill core samples from these wells for analyses (Pichler and Mozaffari, 2015; Pichler et al., 2016). The drill cores were analyzed for total organic carbon, Ca, Mg, Si, Al, P, Sr, As, Mo, Fe, and S content (Pichler and Mozaffari, 2015). The water samples were analyzed for turbidity, pH, conductivity, dissolved oxygen, oxygen reduction potential, alkalinity, Al, Sb, As, Br, Cd, Ca, Cl, Cr, Cu, F, Fe, Pb, Mg, Mn, Mo, Ni, N, K, Se, Si, Na, Sr, SO_4, S, P, V, and Zn. Fig. 1.2 shows the 3-dimensional view of the Lithia area.

The regional area is located in the southwest Florida Water Management District between Tampa and Fort Myers. There are currently 190 Aquifer Storage Recovery (ASR) wells in Florida, at various stages of construction or operation. Of these, 15 ASR wells are not in compliance with the Federal Drinking Water Regulations due to the mobilization of trace metals such as Mo and As (Arthur et al., 2007). Of the 15 wells, 9 with the highest Mo and As concentration in aquifer matrix, were chosen for this research.

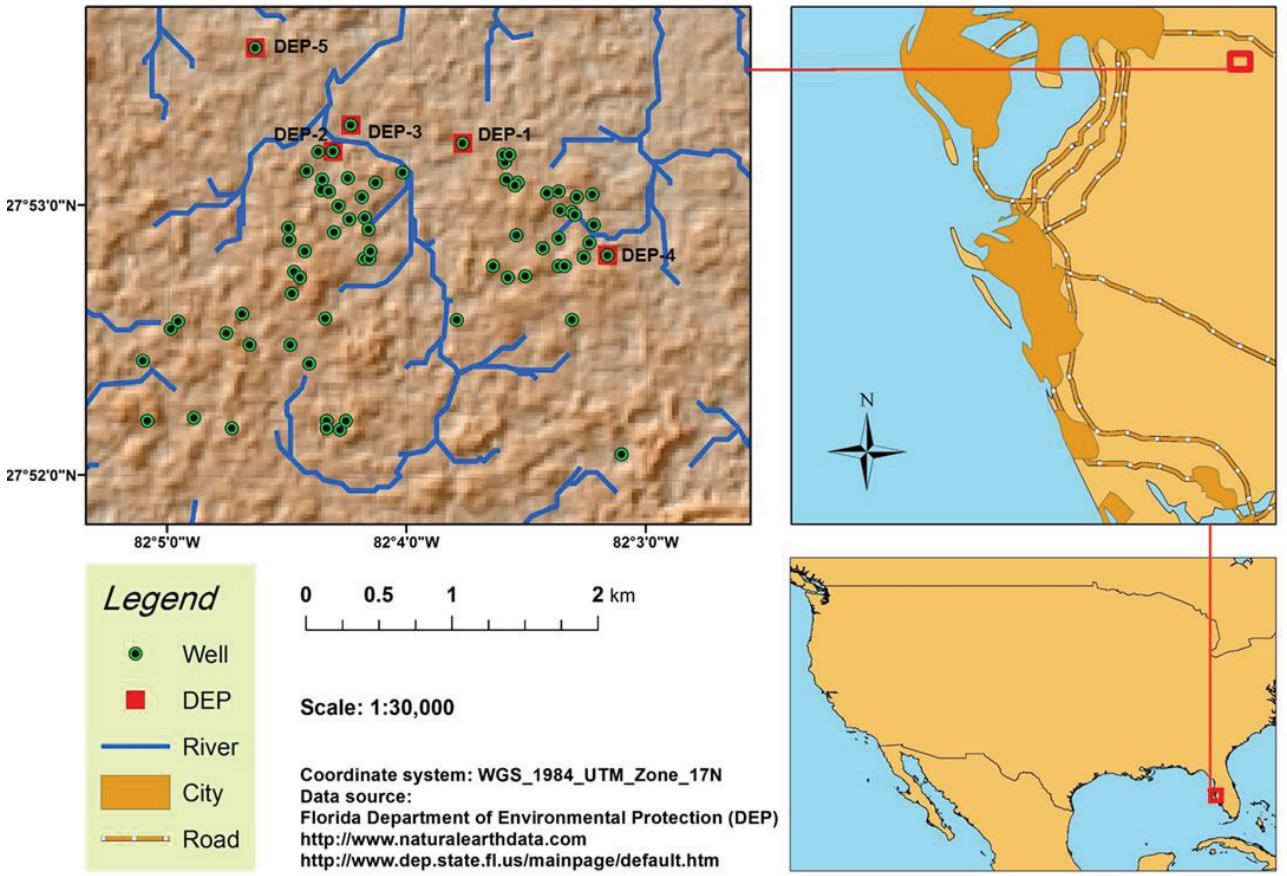

Fig. 1.1 Location of the study area showing domestic supply wells (circle) and monitoring wells (quadrangular) in Lithia area aquifer.

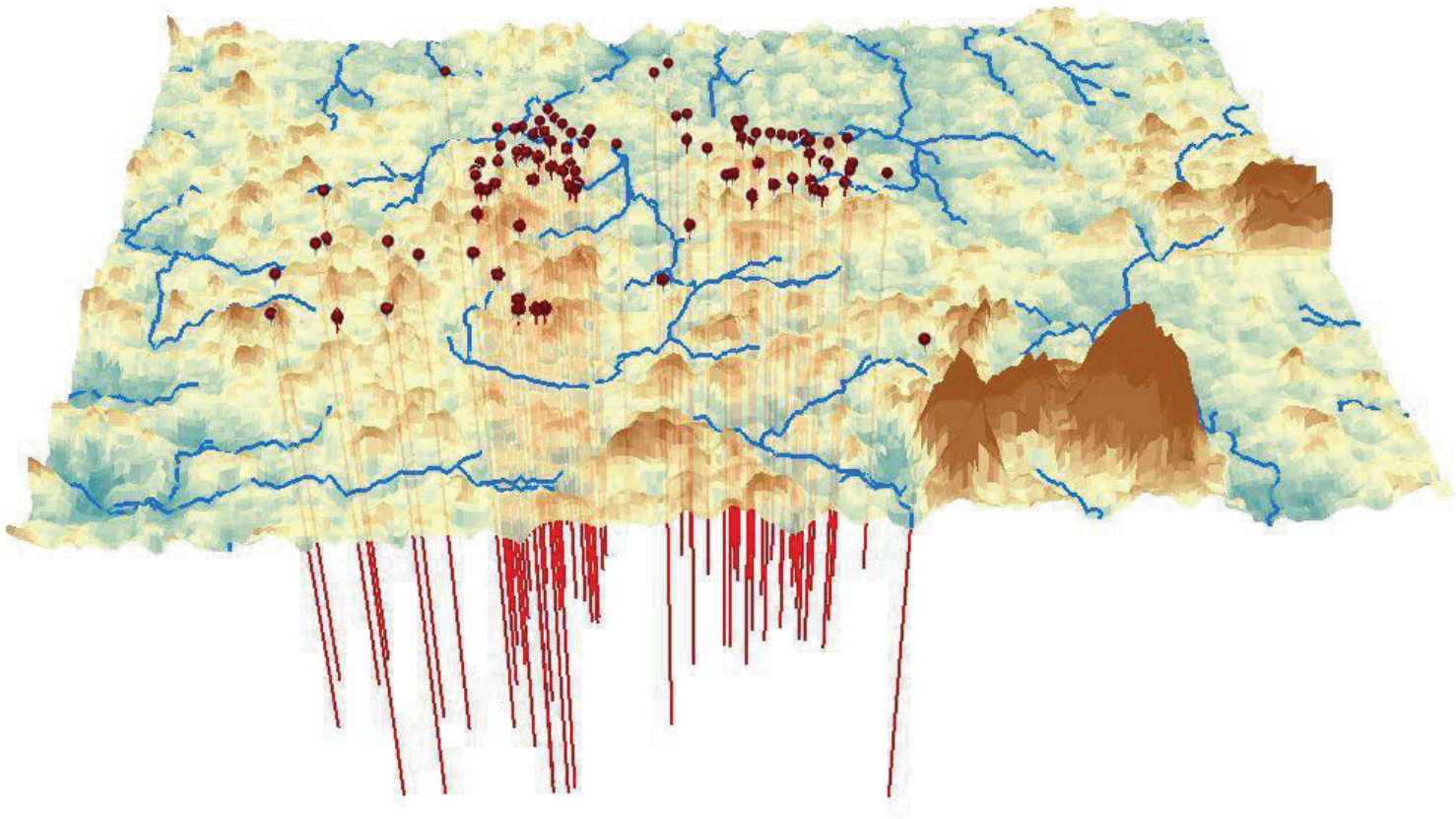

Fig. 1.2 Three dimensional view of the Lithia area and the wells.

1.4.2 Concentration of Mo and As in groundwater and sediments/rocks

The concentration of Mo and As in groundwater reached up to 5000 and 350 µg/L, respectively (Pichler and Mozaffari, 2015; Pichler et al., 2016). Approximately 50% of the groundwater in the Lithia area is contaminated by Mo and As. In Fig. 1.3, the boundary between the yellow and blue color shows the WHO guideline values for Mo and As. The supplementary data related to this work can be found in appendix 1, and Pichler et al., (2016).

The sedimentary rocks in the study area contained up to 825 mg/kg Mo and 144 mg/kg As (Pichler and Mozaffari, 2015; Pichler et al., 2016). In the core of DEP-1, the concentration of Mo increased at depths of 45 m and 70 m. In the core of DEP-2, Mo showed the same pattern as As. It varied significantly between 5 and 35 m followed by high concentrations at approximately 45 and 70 m. In the core of DEP-5, the concentration of Mo was elevated at several depths, the highest values were observed at approximately 50 and 75 m depths. In the core of DEP-1, As was high at depths of approximately 45 and 55 m. In the core of DEP-2, As concentration varied significantly between 5 and 35 m, followed by two pronounced high concentrations at 45 and 60 m. In the core of DEP-5, As was high at depths of approximately 50 and 65 m (Fig. 1.4). The specifications of the mentioned cores which are related to this work can be found in Pichler and Mozaffari (2015), and Pichler et al., (2016).

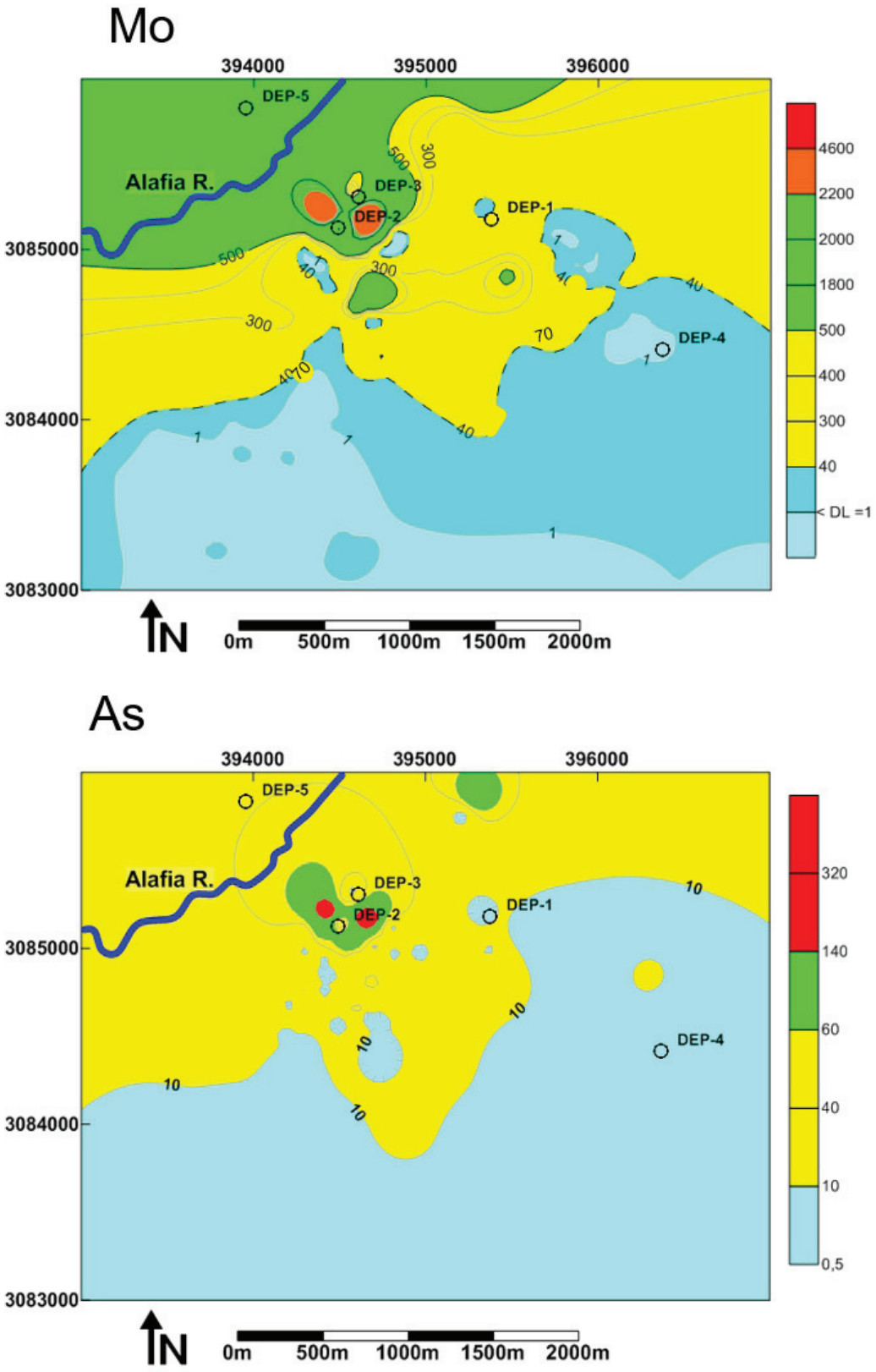

Fig. 1.3 Map of Mo and As concentrations (µg/L) in supply and monitoring wells and the locations of the monitoring wells in the Lithia area aquifer.

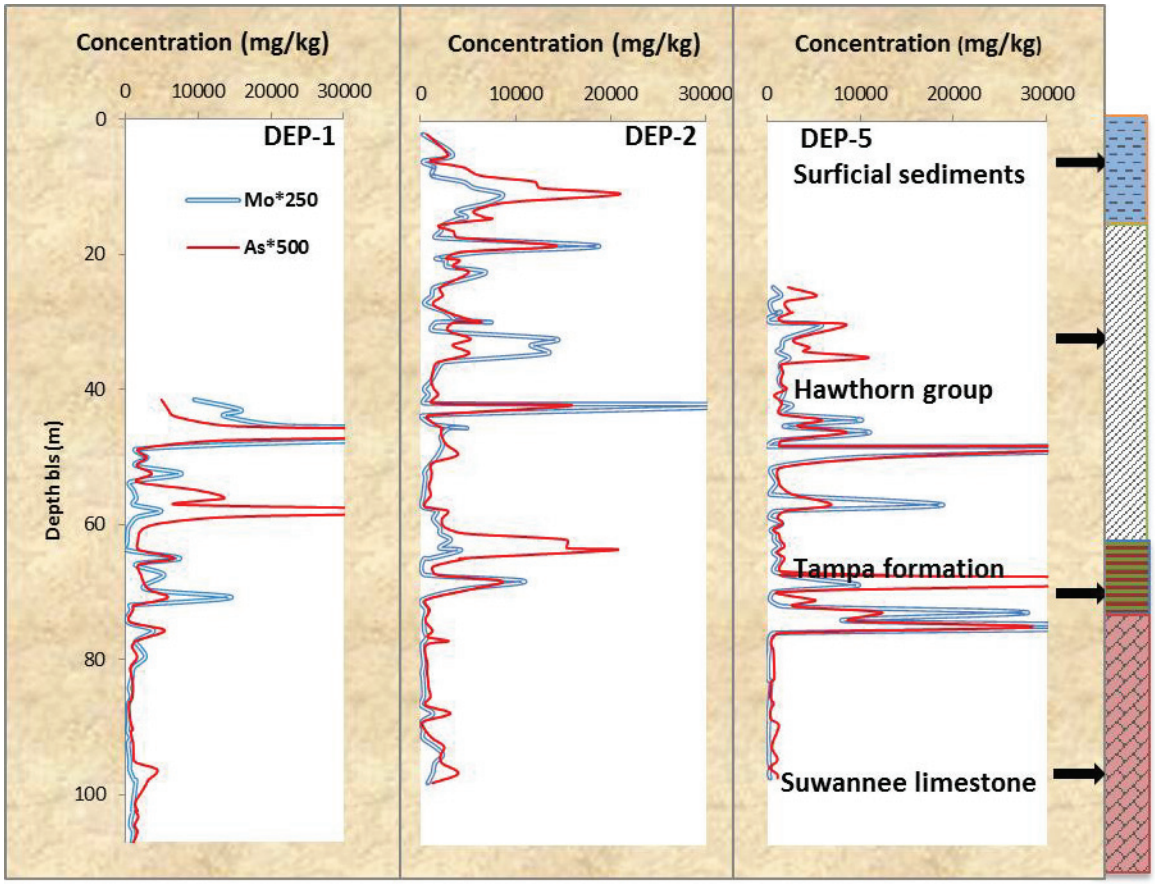

Fig. 1.4 Concentration of Mo and As in vertical profile for well clusters DEP-1, DEP-2 and DEP-5 (data from Pichler and Mozaffari, 2015; Pichler et al., 2016).

1.5 Geology and Hydrogeology

1.5.1 Regional geology of Central Florida

The similarities between the Florida basement rocks and the subsurface rocks in northwest Africa indicate that the area now known as Florida was a part of northwest Africa. The basement rocks of southeastern United States, including Florida, is a subsurface extension of the igneous, metamorphic, and sedimentary rocks that are exposed in the Appalachian Mountains. These rocks are overlain by the Cedar Key, Oldsmar, and Avon Park Formation (APF), as well as the Ocala and Suwanee limestone. These formations consist of limestone,

dolomite, anhydrite, and gypsum which were deposited when most of the Florida peninsula was below sea level. The total thickness of these formations ranges from 1675 to 3660 m (Scott et al., 1989). The overlying Hawthorn Group, deposited about 25 million years ago, represents a transition between the marine-derived and land-derived sediments. Generally, the lower layers of the Hawthorn Group are marine-derived and contain limestone, whereas the upper layers of clay, fine sand, and silt are land-derived. These upper layers of the Hawthorn Group, generally restrict groundwater movement. Overlying the Hawthorn Group and continuing upward to the present land surface are unconsolidated sediments consisting of quartz sand, clay, and some organic materials. The thickness of the Hawthorn Group, which varies greatly in central Florida, is a key element in the lake formation process. Fig. 1.5 shows the lithostratigraphic units of the regional geology of Florida.

1.5.2 Local geology of the study area

The stratigraphic column of the study area predominantly consists of Miocene Hawthorn Group, which is subdivided into a lower section comprising the undifferentiated Arcadia Formation, Tampa and Nocatee Members of the Arcadia Formation and the upper section of the Peace River Formation (Scott et al., 1989). These formations unconformably overlay the Oligocene Suwannee limestone and its thickness from the surface is about 80 m. Petrographic and mineralogy studies showed that carbonates are the dominant lithology in the Lithia area. The stratigraphic column from top to bottom is approximately as follows: 0-18 m surficial sediments, 18 - 60 m Hawthorn Group, 60-70 m Tampa Member and below 70 m Suwannee Limestone (Pichler and Mozaffari, 2015) (Fig 1.4). The Upper Pliocene to Pleistocene surficial sediments generally comprises unconsolidated to poorly indurated clastic deposits such as sand, sandy clays, phosphorite and some well-indurated carbonate rocks. The Hawthorn Group consists of layers of clay, sand beds, carbonate lenses, and phosphorite. The Suwannee limestone is a continuous sequence of carbonate rocks with generally high porosity

and permeability. The APF is comprised of interbedded limestone, dolomite and deeper beds of continuous dolomite that increase in evaporites towards the base.

1.5.3 Floridan Aquifer System

The Floridian Aquifer System (FAS) consists of thick carbonaceous units that comprise all or part of the Paleocene to Early Miocene series covering an area of 259,000 km^2 from southern South Carolina, through southeastern Georgia and part of southern Alabama to the entire state of Florida (Budd and Vacher, 2004; Williams and Paillet, 2002). The FAS is a continuous sequence of carbonate rocks with generally high porosity and permeability. Based on the hydrologic properties of the present lithological units, it is divided into the Upper Floridian Aquifer (UFA), Intermediate Aquifer System and Lower Floridian Aquifer (LFA) (Scott et al., 1989). The Upper Floridian aquifer is comprised of the Suwannee and Ocala Limestone as well as the APF (Randazzo and Jones, 1997). The upper portion of the APF comprises the lower part of the UFA system. The Tampa Member and the lower part of the Arcadia Formation of the Hawthorn Group are part of the upper section of the FAS, where it consists of permeable carbonate lenses (Randazzo and Jones, 1997).

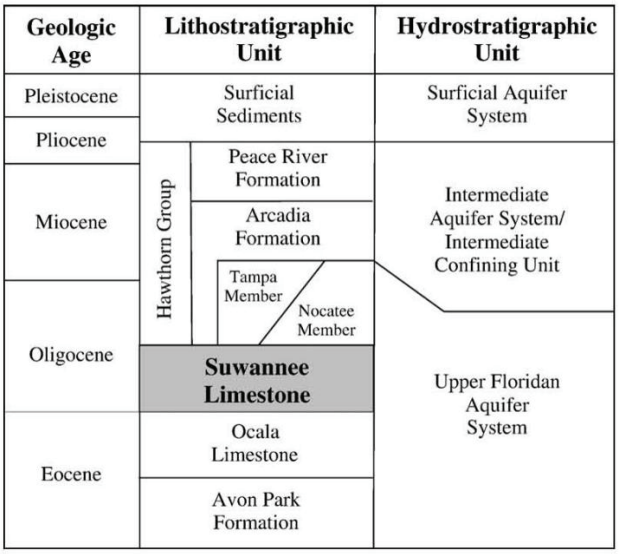

Fig. 1.5 Lithostratigraphic and hydrogeologic units of Florida defined by Scott et al., (1989).

Chapter 2. Literature review

This literature review encompasses the prominent aspects of molybdenum (Mo) investigation within this thesis, including the original sources of Mo in sedimentary rocks and Mo sorption onto sorbents in the aquatic environment. It also deals with geochemistry mineralogy and various sources of arsenic (As), especially sedimentary As.

2.1 Geochemistry, biochemistry and applications of Mo

Molybdenum plays unique roles in geochemistry and biochemistry, hence both geochemists and biochemists find this trace element interesting. In oxic waters, it is conservative and relatively unreactive, and is the most abundant transition metal with a residence time of 440,000 years (Miller et al., 2011). Under such conditions, Mo is (more likely) slowly removed from seawater by manganese oxides (Bertine and Turekian, 1973; Chappaz et al., 2014). In contrast, in anoxic/sulfidic (euxinic) settings, Mo is readily removed from solution, such that Mo enrichments in sediments are considered diagnostic of reducing depositional conditions (Chappaz et al., 2014; Adelson et al., 2002; Tribovillard et al., 2004). Few elements possess such bimodal redox behavior in the environment. This unusual chemistry serves as a palaeoenvironmental indicator of reducing conditions for sedimentary Mo.

Biochemically, Mo is a cofactor of enzymes which are essential in plants, animals and for human health (Stiefel, 1996). This element is important for the functioning of the enzymes like xanthine dehydrogenase, sulfite oxidase, and aldehyde oxidase, which play key roles in human metabolism (Momcilovic, 2000; WHO, 2011). It also has potential benefits for patients with asthma and sulfite sensitivity. However, chronic occupational exposure has been linked to a number of ailments including fatigue, lack of appetite, anorexia, joint pain, and tremor. Exposure to Mo may also give rise to Mo-induced copper deficiency and pneumoconiosis (Cot,

2003; WHO, 2011). The chemical state of Mo, route of exposure, and dietary doses of copper and sulfur all have a likely impact on its toxicity. Despite the above observations, recognized cases of Mo toxicity in humans are rare (Berislav, 1999; Cot, 2003). In considering these human health problems, the World Health Organization (WHO, 1993) recommended 70 µg/L as a guideline for Mo concentrations in drinking water.

Molybdenum has seven stable isotopes including: ^{92}Mo, ^{94}Mo, ^{95}Mo, ^{96}Mo, ^{97}Mo, ^{98}Mo and ^{100}Mo with relative abundances ranging from 9.5 to 24.13% (Fig. 2.1). Thus, from an analyst's perspective, Mo offers both an unusually large mass spread as well as a number of options for isotope ratio determination. Combined with rich redox chemistry and covalent-type bonding, both of which tend to drive isotope fractionation, these factors make the Mo isotope system a particularly promising target for stable isotope investigation (Moore et al., 1974).

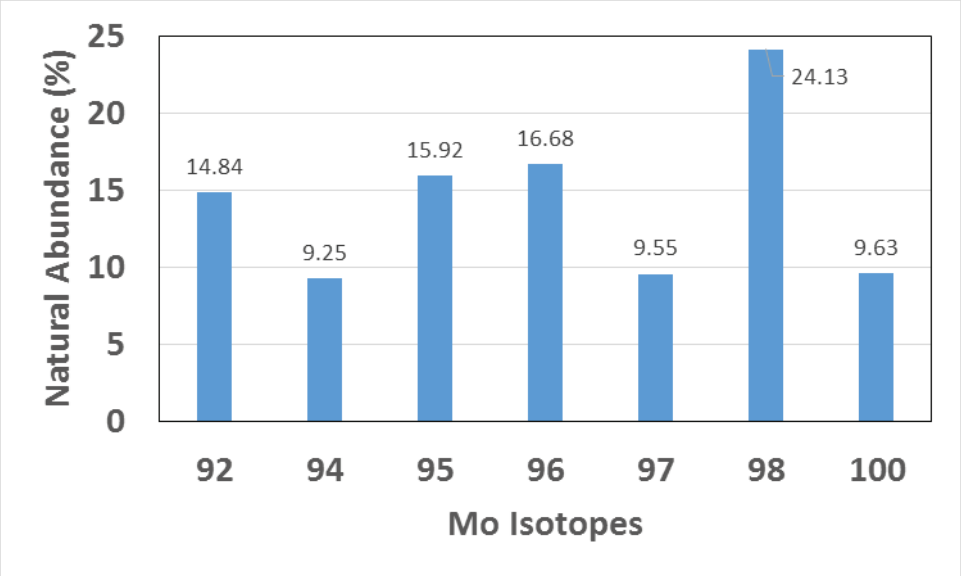

Fig. 2.1 Average natural abundances of the stable isotopes of Mo.

Molybdenum is a component of steel alloys and welding rods and it is used as an additive in lubricants, as a corrosion inhibitor and in the manufacture of tungsten, pigments and ceramics. It is added to cast iron for hardness control at concentrations of 250 to 450 mg/kg (Morrison et al., 2006). It is also used in agriculture to counteract Mo deficiency in crops (WHO, 2011).

Therefore, Mo can be distributed in the environment as a result of industrial or agricultural contamination. It can also be circulated due to fossil-fuel combustion, leaching from fly ash and release from mine wastes (Morrison and Spangler, 1992).

2.2 Natural reserves of Mo

The average concentration of Mo in the Earth's crust, as well as in igneous and sedimentary rocks can be seen in Table 1.1 (Taylor and McLennan, 1985). Being a chalcophile element, it is found mainly as molybdenite (MoS_2). Other natural mineral forms of Mo include wulfenite ($PbMoO_4$), powellite ($CaMoO_4$) and ilsmannite (Mo_3O_8). Approximately 95% of the world's Mo and 60% of the world's Cu are sourced from porphyry copper deposits (Hollister, 1978). Compared to the hundreds of porphyry copper deposits existing worldwide, climax-type porphyry Mo deposits are extremely rare. A total of thirteen deposits are known, all in western North America, ranging in age from Late Cretaceous to mainly Tertiary. The deposits are of relatively high grades (typically 0.1 to 0.3% Mo) and may be very large, typically 100 to 1,000 million tons (Clark, 1972; Hollister, 1978). Molybdenum, as MoS_2, is the primary commodity in all known deposits. The known resources of Mo amount to about 5.4 million tons of Mo in the United States and about 13 million tons in the rest of the world (Taylor et al., 2012). In addition to the occurrence and accumulation of Mo as a mineral deposit and its anthropogenic sources, it concentrates in sedimentary rocks which underwent sulfidic conditions especially in the presence of organic matter (OM) (Adelson et al., 2002; Bostick et al., 2003; Campillo et al., 2002; Chappaz et al., 2014; Das et al., 2007; Erickson and Helz, 2000; Helz et al., 1996; Kaback and Runnells, 1980; Riboulleau et al., 2000; Tribovillard et al., 2004; Vorlicek, 2004; Zheng et al., 2000). Although sedimentary Mo is not a considered Mo resource, it has the potential of contaminating aqueous environments (Pichler and Mozaffari, 2015). Therefore,

geochemical processes controlling the leaching of Mo from sedimentary rocks into the aquifer matrix, groundwater and agricultural soils need to be researched.

Table 2.1: Molybdenum concentration (mg/kg) in different rock types (Taylor and McLennan, 1985).

Upper crust	Granite	Basalt	Shale	Sandstone	Limestone	Amphibolite, Granolite
1.5	1	1.5	2.6	0.2	0.4	1.5 - 2.9

2.3 Importance of Mo in the biogeochemical cycle of nitrogen

Nitrogen is an essential component of all biopolymers such as amino acids, proteins and nucleic acids. Molybdenum plays a crucial part in trapping and fixing N_2 in biopolymers. Although N_2 accounts for roughly 80% of the earth's atmosphere, and nitrate is relatively abundant in seawater, ammonia is the only nitrogen form that can be assimilated into biomass directly. Therefore, the reduction of dinitrogen and nitrate to bioavailable ammonia, catalyzed by nitrogenase and nitrate reductase, is critical in the biological system (Kasper, 1983). Molybdenum is an essential and constitutive part of the active centers of these enzymes. As show in Fig. 2.2, the biogeochemical cycle of nitrogen generally includes several metabolic pathways including: 1) nitrogen fixation, 2) denitrification, 3) nitrification, 4) assimilation 5) dissimilatory nitrate ammonification, and 6) anaerobic ammonia oxidation (anammox). A large family of Mo enzymes is also involved in heterocyclic metabolism (Philippot and Hojberg, 1999). For instance this element is necessary for the fixation of atmospheric nitrogen by bacteria at the start of protein synthesis.

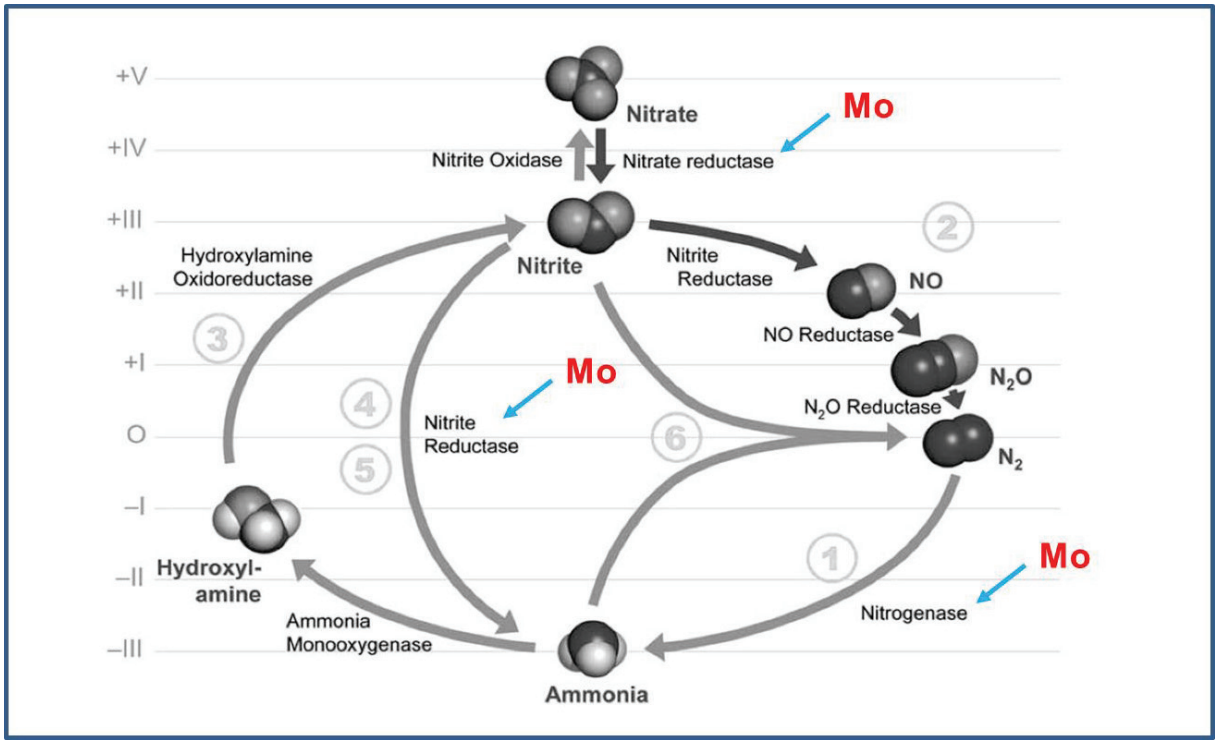

Fig. 2.2 Molybdenum and its roles in the biogeochemical cycle of nitrogen (modified after Einsle and Kroneck, 2004).

Considering the small quantity of Mo in the continental crust (Table 2.1), the question that arises is from where the Mo required for N_2 fixation comes from. Tannins in plants play an important role in accumulating Mo in the outset layer of the soil in the Earth's surface. The binding of Mo to insoluble tannins should significantly slow down the leaching rate of highly soluble molybdate, allowing Mo accumulation in topsoil layers, thereby forming an important reservoir of Mo accessible to N_2-fixing bacteria. Mo which is present in the deep soil horizons is extracted by the root network of trees, and is incorporated in leaves. When the senescent leaves fall to the ground, they provide a Mo-enriched environment for N_2-fixing bacteria living in the upper soil horizon (Kraus et al., 2003; Marks et al., 2015; Wichard et al., 2009). Despite its importance for N_2 fixation in nature, Mo appears to be toxic if its concentration in the aqueous environments exceeds the WHO guideline of 70 µg/L (WHO, 2011). It should be noted that the concentration of Mo in plants should not be higher than 5 mg/kg (Goldberg et al., 2009; Kaspar, 1983).

2.4 Molybdenum geochemistry in marine environments

The hydrogeochemical behavior of Mo has an exclusive potential to track paleodepositional conditions (Mongenot et al., 1996). Therefore, its geochemistry has been extensively studied over the last four decades (Bertine and Turekian, 1973; Goldberg et al., 1996; Erickson and Helz, 2000; Adelson et al., 2002; Bostick et al., 2003; Goldberg, 2010; Helz et al., 2011; Chappaz et al., 2014; Pichler and Mozaffari, 2015). The average crustal value for Mo in sedimentary rocks, which were deposited under oxic conditions, is 1 to 2 ppm (Wolthers et al., 2005); in anoxic/sulfidic sediments, it is up to 825 mg/kg (Lyons et al., 2003; Mitry et al., 1999; Pichler and Mozaffari, 2015). Table 2.2 shows the concentration of Mo in different sedimentary rocks and soils.

2.4.1 Molybdenum behavior in oxic conditions

The dominant species of Mo in oxic seawater is the molybdate, MoO_4^{2-}, with a modern seawater concentration of about 10 μg/L (Morford and Emerson, 1999). It is a conservative trace element and the most abundant transition metal in the modern ocean, with a residence time of 440,000 years (Miller et al., 2011). Despite the stability of molybdate in solution, Mo can be enriched up to 1000 mg/L in oxic sediments (Bertine and Turekian, 1973). In this environment, Mo can be adsorbed onto iron oxyhydroxides and manganese oxides (Crusius et al., 1996; Goldberg et al., 2009). Ferromanganese crusts and nodules are probably not the dominant sinks themselves because these sediments accumulate very slowly. Molybdenum which is associated with Mn oxides in widely disseminated pelagic sediments may be quantitatively more important, although Mo enrichment in pelagic sediments are relatively small (Anbar, 2004).

Table 2.2: Mo concentration in different sedimentary rocks and soils (mg/kg).

Rock type and soil	Concentration	Location	Age	Reference
Black shale	50 to 200	Cariaco (Venezuela)	Modern	Lyons et al., (2003)
Shale	32 to 34			Das et al., (2007)
Diatomaceous	1 to 200	Kashpir oil shale (Russia)	Late Jurassic	Riboulleau et al., (2000)
Upwelling sediments	53	Namibia	Modern	Brumsack (2006)
Soil	0.32 to 1.2	Spain		Campillo et al., (2002)
Limestone	1 to 100	Akkuyu (Turkey)	Late Jurassic	Mitry et al., (1999)
Limestone	< DL to 825	Hawthorn group (USA)	Miocene	Pichler and Mozaffari (2015)
Limestone	0 to 135	La Luna (Venezuela)	late Cretaceous	Mongenot et al., (1996)

2.4.2 Molybdenum enrichment in anoxic/sulfidic conditions

It has been revealed that Mo is systematically more enriched relative to the other redox-sensitive/sulfide forming elements such as U, V, Ni, Cu, Zn, and Cr (Adelson et al., 2002; Chappaz et al., 2014; Erickson and Helz, 2000; Glass et al., 2013; Zheng et al., 2000). It is a known indicator of reducing depositional conditions and by using this element, it is easier to characterize paleoredox conditions (Adelson et al., 2002; Brumsack, 2006; Erickson and Helz, 2000). In reducing environment, Mo(VI) is reduced to Mo(IV) and is released into the pore water as a result of the reductive dissolution of Mn and Fe in anoxic/sulfidic waters and fixed with iron sulfide and/or OM (Chappaz et al., 2014; Dahl et al., 2013; Glass et al., 2013; Helz et al., 2011; Helz et al., 1996; Lyons et al., 2003; Tribovillard et al., 2008; Tribovillard et al., 2004). There are several models for Mo enrichment in anoxic/sulfidic sediments:

1. Manganese (Mn) redox cycling has the potential to concentrate MoO_4^{2-} at the sediment-water interface. In cases where anoxia zone extends upward into the water column, Mn^{2+} oxidizes just above the chemocline to particulate MnO_x (solid). The particulate Mn settles in the anoxic waters, and redissolved Mn^{2+} diffuses back through the chemocline, thus completing a redox cycle. The concentrated molybdate at the water-sediment interface is fixed by OM and/or pyrite (Adelson et al., 2002).

2. Another model suggests that Mo fixation in the presence of dissolved sulfide does not simply result from MoS_2 or MoS_3 formation, but instead mineralization occurs through organic thiomolybdates and inorganic Fe–Mo–S cluster complexes, possibly occurring as solid-solution components in Fe sulfides (Helz et al., 1996). Helz et al., (1996) introduced the concept of a geochemical switch, which transforms Mo from a largely conservative element to a particle-reactive species in marine depositional environments. The oxygen atoms in MoO_4^{2-} are susceptible to replacement by soft ligands, such as S donors. According to Erickson and Helz et al., (2011) and Helz et al., (1996), a key step in this inorganic pathway is the reaction: MoO_4^{2-}→thiomolybdates ($MoO_xS_4^{-x}$, x=0–3), which is a reactive particle and is thus prone to

scavenging. The sulfide activation of the switch depends on the $\sum H_2S$ activity (Erickson and Helz, 2000; Zheng et al., 2000). Because each successive sulfidation reaction is about one order of magnitude slower than the previous one, thiomolybdate equilibria might not be achieved in seasonally or intermittently sulfidic waters (Erickson and Helz, 2000). Persistently, sulfidic conditions appear to be necessary. In the sediments, the transformation reactions are catalyzed by proton donors or in the presence of some active-surface minerals such as kaolinite (Erickson and Helz, 2000; Vorlicek, 2004). Once the thiomolybdate switch has been achieved, Mo is scavenged by forming bonds with metal-rich (notably Fe) particles, sulfur-rich organic molecules (Helz et al., 1996; Tribovillard et al., 2004) and iron sulfide (Vorlicek, 2004). The work of Helz et al., (1996) also suggested the formation of compact, monocrystalline Fe–Mo–S cluster compounds that are capable of surviving over geologic time periods.

3. Chappaz et al., (2014) introduced a model, which describes Mo fixation in the reducing environment by OM and pyrite. Based on this model, first Mo co-precipitates as Fe-Mo-S leading to the formation of $Fe_5Mo_3S_{14}$ in the water column. After Mo reduction in the water-sediment interface, it is fixed by OM. They argued that the dominant source for Mo in sedimentary rocks is OM, not pyrite. The correlation between Mo and OM in six different sites including 1) Cariaco Basin, 2) Posodonia Shale, 3) Doushantuo Formation, 4) Mount McRae Shale, 5) Transvaal Super group F, and 6) Transvaal Super group P was much stronger than that between Mo and pyrite (Chappaz et al., 2014; Lyons et al., 2003). Organic matter plays a powerful role in fixing and retaining Mo in a long-term sequestration. Molybdenum enrichment was positively correlated to an amount of sulfurized OM but not to pyrite abundance. However, pyrite could act as an initial trap, prior to Mo uptake by OM that is sulfurized after the pyritization step (Tribovillard et al., 2004).

2.5 Molybdenum in groundwater

The concentration of Mo in groundwater is often insignificant but depending on the aquifer matrix, lithology of the surrounding environment and anthropological contamination (related to urban, commercial, industrial, and mining activities), it may be very high locally and exceed the WHO guidelines of 70 µg/L. The mobilization of Mo under neutral and basic conditions is more prominent than under acidic conditions (Goldberg et al., 2009; Gustafsson, 2003). Under neutral or basic conditions, molybdenite (MoS_2) is weathered and oxidized. In acidic environments, molybdenite is stable or Mo in solution is immobilized by the precipitation of iron molybdate. Under neutral conditions, Mo is expected to be released into solution, where the oxidation of molybdenite occurs, leading to the formation of molybdate oxyanions (Bostick et al., 2003; Takeno, 2005). Molybdate predominates in solutions having pH values above 4. The stability diagrams of Mo are shown in Fig. 2.3.

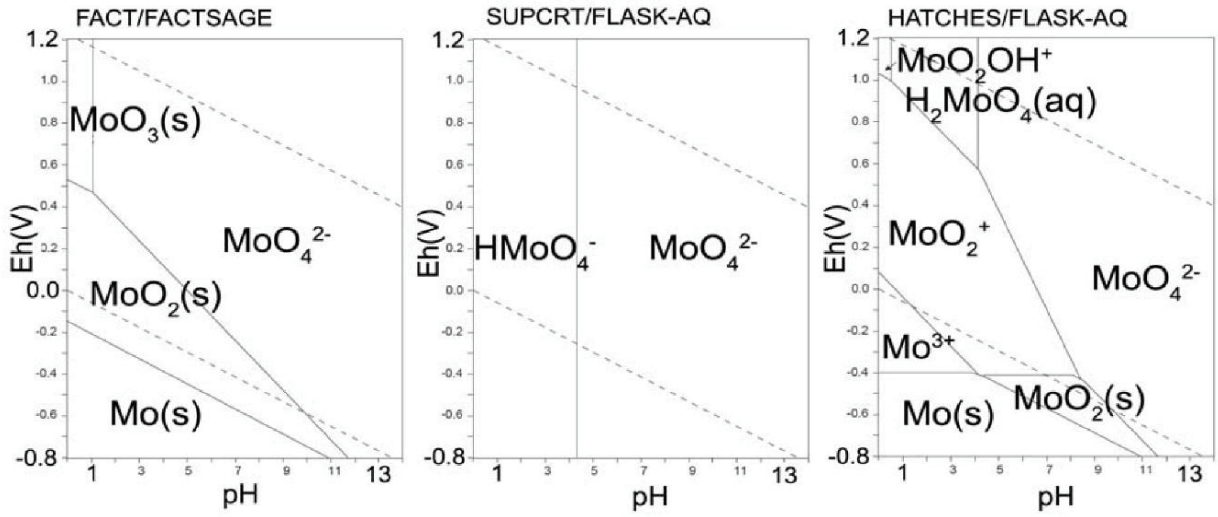

Fig. 2.3 Eh-pH diagram for aqueous and solid species of Mo (modified after Takeno, 2005).

2.5.1 Molybdenum sorption

Metal contaminants can be removed from the solutions by sorption onto the solid phases present in the system. The term sorption is defined by some authors either as adsorption or absorption. Adsorption typically refers to the accumulation of atoms or molecules of solutes, gases or vapor (sorbates) on a solid surface (sorbent), while absorption is defined as sorption in the internal region of a porous media. Sorption to surfaces may occur by physical binding forces (van de Waals force), by chemical bonding (Coulomb force) or by hydrogen bonding (Merkel et al., 2005).

The surface sites of minerals have a pH-dependent charge, which mainly controls the surface sorption behavior. For every mineral, there is a pH at which the positive and negative charges (caused by protonation and deprotonation) become equal and hence have a surface charge of zero. This pH is called point of zero charge (PZC). For instance, the PZC for quartz is 2, for kaolinite it is about 3.5, for goethite, magnetite and hematite, it is between 6 and 7, and for corundum, it is 9.1 (Drever, 1988). Table 2.3 presents the mineralogical PZC and specific surface area data for some oxides, pyrite and clay minerals. Further information about the PZC of metal oxides and related materials can be found in Kosmulski (2002).

Table 2.3: Specific surface area (m^2/g) and point of zero charge (PZC) for the oxides, pyrite and clay minerals.

Solid	Surface area	PZC	Reference
Amorphous Fe oxide	222.7	7.23	Goldberg et al., 1996
Amorphous Fe oxide	120		Qi and Pichler, 2014
Amorphous Fe oxide	750	8.1	Gustafsson, 2003
Hematite	10.9	7-9.5	Kosmulski, 2002
Hematite	30-90		Cornell et al., 1987
Goethite	63.1	8.82	Goldberg et al., 1996
Poorly crystalline goethite	148.8	7.83	Goldberg et al., 1996
Aluminium oxide	102.9	9.3	Goldberg et al., 1996
Gibbsite	56.5	9.41	Goldberg et al., 1996
Amorphous anoxide	209.9	9.3	Goldberg et al., 1996
Calcite	22	8-9.5	Somasundaran and Agar, 1967
KGa-1 kaolinite	9.14	2.88	Goldberg et al., 1996
KGa-2 kaolinite	19.3	2.93	Goldberg et al., 1996
SWy-1 montmorillonite	18.6		Goldberg et al., 1996
SAz-1 montmorillonite	48.9		Goldberg et al., 1996
STx-1 montmorillonite	70.3		Goldberg et al., 1996
IMt-1 illite	24		Goldberg et al., 1996
Anatase	7.39	6.15	Weng et al.,1997
Mn oxide (birnessite)	7.3	269	Matern and Mansfeldt, 2015
Pyrite	41.7	6.4	Borah and Senapati, 2006

Surface complexation can be defined as inner-sphere complexes in which the ions are directly bound to the surface of the solid phase and outer-sphere complexes in which a hydration layer covers the ions (Borah and Senapati, 2006; Cornell et al., 1987; Kosmulski, 2002; Somasundaran and Agar, 1967; Weng et al., 1997). In an inner-sphere complex, a cation can also be sorbed on a positively charged surface and complexes are tied much stronger (Goldberg et al., 2009; Matern and Mansfeldt, 2015; Merkel et al., 2005; Qi and Pichler, 2014). The most common and useful models are the constant capacitance model (CCM) (Schindler and Gamsjäger, 1972), the triple layer model (Davis et al., 1978), multi-site approaches (Hiemstra et al., 1989) and the generalized two-layer model (Dzombak and Morel, 1990). The generalized two-layer model is developed as two-layer model and the diffuse layer model (Dzombak and Morel, 1990). The generalized two-layer model explains the sorption of ions as a chemical reaction on a specific surface site of an oxide mineral. This surface reaction might be a proton exchange (acid-base), cation or anion binding via ligand exchange on surface hydroxyl sites. This is a simple model which can account qualitatively and quantitatively for all available model-constraining experimental data (Dzombak and Morel, 1990).

One of the main factors controlling the distribution of Mo in natural environments is its sorption on soil and sediment. The adsorption of Mo on adsorbents is a function of pH and the geochemical composition of groundwater (Stollenwerk, 1998). The significant sorption sites in the aquatic environment for Mo include hydrous ferric oxide (HFO) (Goldberg et al., 1996; Gustafsson, 2003), pyrite (Bostick et al., 2003; Xu et al., 2006), Fe and Al oxides, clay minerals (Goldberg, 1985, 2010), calcite (Goldberg et al., 1996), anatase (Prasad Saripalli et al., 2002) and OM (Bibak and Borggaard, 1994).

2.5.1.1 Molybdenum sorption on hydrous ferric oxide and goethite

The sorption of molybdate by soils involves anion exchange, primarily with surface hydroxyl groups found in the mineral part of the soil, especially those pertaining to the oxides and hydrous oxides of aluminum and iron (Dzombak and Morel, 1990; Goldberg et al., 1996;

Kaback and Runnells, 1980). Hydrous ferric oxide is one of the main adsorbents in the oxic environment. The adsorption of molybdate by adsorbents including HFO is a function of several chemical factors, including the Mo concentration in solution, the pH of the solution, the concentration of the competing anion and the adsorbent concentration in the aquifer matrix. The adsorption of Mo on HFO is maximum at low pH extending to a pH of about 4 to 5 (Goldberg et al., 1996; Gustafsson, 2003; Stollenwerk, 1998). Mo adsorption on an aquifer matrix including HFO decreases with increasing Mo solution concentration (Stollenwerk, 1998). Anions such as phosphate, arsenate and to a lesser extent, sulfate compete with molybdate for adsorption sites (Gustafsson, 2003; Stollenwerk, 1998). Gustafsson et al., (2003) showed that Mo adsorption in the presence of phosphate shifted by 2 units to the left on the pH scale. However, the percentage of its adsorption at low pH (< 4) is still over 90%. These results are similar to those of Goldberg et al., (1996). As expected, surface sites availability plays a critical role in Mo adsorption.

Molybdenum adsorption on goethite is a function of pH. Maximum Mo adsorption was recorded at low pH of 4 to 5. Adsorption decreases rapidly from pH 5 to 8 with little adsorption occurring at pH above 8. Molybdate reacts with the protonated sites of goethite but not with the neutral site. Since the PZC of goethite is about 8.4, goethite surfaces are positively charged, between pH 4 and 8 (Zhang and Sparks, 1989). Depending on the crystallization of the goethite, its PZC charge ranges from 7.83 to 8.82. Poorly crystalline goethite has a higher surface area (148.8 m^2/g) but lower PZC (Goldberg et al., 1996). Ionic strength dependence of adsorption has been used to indirectly distinguish between inner- and outer-sphere adsorption mechanisms for both cations and anions (Hayes and Leckie, 1987; Hayes et al., 1988). Ions showing little ionic strength dependence of adsorption form strong inner-sphere surface complexes; ions showing marked ionic strength dependence are considered to be weakly adsorbed as outer-sphere surface complexes. In a study by Hayes et al., (1988), Mo showed little ionic strength dependence on goethite and this was taken as an evidence for the inner-sphere surface

complexation. Zhang et al., (2000) showed that the effect of ionic strength on Mo adsorption onto goethite was minor and similar results were obtained by Hayes et al., (1988).

2.5.1.2 Molybdenum sorption on iron, aluminum, titanium, and manganese oxides

The mobility of Mo in soils and sediments depends on several factors including soil mineralogy, pH and anion competition (Bostick et al., 2003; Goldberg et al., 1996; Gustafsson, 2003; Manning and Goldberg, 1996). Studies by Ferreiri et al. (1985) showed that Mo adsorption on oxides increased from pH 2 to 4, exhibited a peak near pH 4, and decreased with increasing pH above 4. The decrease in adsorption occurred at pH above 4 more rapidly for Al oxides than for Fe oxides (Ferreiro et al., 1985). The mechanism of Mo adsorption on Al and Fe oxides was suggested to be ligand exchange with surface hydroxyl ions (Ferreiro et al., 1985; Goldberg et al., 1996). Ligand exchange is a mechanism by which ions become specifically adsorbed as inner-sphere surface complexes. Inner-sphere surface complexes contain no water molecules between the adsorbing ion and the surface functional group (Sposito, 1984). The PZC of variable charged minerals shifts to a more acidic pH value, following the specific adsorption of anions. Molybdenum adsorption lowers the PZC of goethite, indicating specific adsorption. By studying the effects of ionic strength on anion adsorption, Hayes et al., (1988) were able to distinguish between inner- and outer-sphere surface complexes. Outer-sphere surface complexes contain at least one water molecule between the adsorbing ion and the surface functional group (Sposito, 1984). Hayes et al., (1988) suggested that since selenite showed little ionic strength dependence in its adsorption behavior, it was specifically adsorbed on goethite in an inner-sphere surface complex.

Hematite: Mo adsorption onto hematite is a function of initial concentration of Mo, pH, contact time and ionic strength (Das and Jim Hendry, 2013; Ferreiro et al., 1985; Goldberg et al., 1996). The mentioned studies showed that the maximum adsorption of Mo on hematite occurred at pH 4, and dropped significantly as the pH increased beyond the maximum, thus demonstrating high sensitivity of sorption to pH changes. Because of the PZC of hematite (7.5) at low pH, the

surface of hematite has a net positive charge that would attract $HMoO_4^-$ and MoO_4^{2-} ions, thereby causing adsorption by electrostatic attraction. However, as the pH increases, the portion of positively charged surface sites on hematite decreases, increasing repulsion of anionic Mo species, and reducing adsorption. Under these conditions, Mo adsorption does not occur through electrostatic interaction, but through specific chemical interaction between the negatively charged hematite surface and Mo ions (Goldberg, 2010; Goldberg et al., 1996).

Gibbsite: Molybdenum adsorption on gibbsite has been investigated by many researchers (Ferreiro et al., 1985; Goldberg et al., 1996; Manning and Goldberg, 1996). Goldberg et al., (1996) conducted experiments and concluded that there was maximum Mo adsorption on Al oxides at low pH of about 4 to 5. At pH above 5, adsorption decreased rapidly with adsorption occurring at pH above 8. Molybdenum adsorption was higher, having a higher specific surface area and lower crystallinity. These results are similar to those of Ferreiro et al., (1985).

Manganese oxide: Anbar (2004) showed that authigenic Mo concentration of 100 to 1000 mg/kg in oxic sediments, correlated well with Mn oxides, most likely reflecting the removal of Mo from the oceans by adsorption on and/or coprecipitation with Mn oxide phases. Birnessite is one of the most common Mn oxides in soils. It has a large specific surface area (269 m^2/g) and its PZC is 7.3 (Matern and Mansfeldt, 2015). Matern and Mansfeldt (2015) conducted a series of batch expriments to determine Mo adsorption to birnessite and found that the amount of adsorbed molybdate was strongly dependent on pH and time. It reached equilibrium roughly after three days and the maximum adsorption of molybdate occurred at pH 3.

Anatase: Molybdate adsorption onto TiO_2 is strongly governed by pH of the solution and surface loading. Under acidic conditions, the sorption of Mo was higher than 95% and constant, whereas under neutral to alkaline conditions, there was a significant decrease in Mo uptake by anatase (Prasad Saripalli et al., 2002). The edge of adsorption happened approximately at pH 6.5 (Prasad Saripalli et al., 2002), which is close to the PZC (6.15) of TiO_2 (Weng et al., 1997).

2.5.1.3 Clay minerals

Molybdenum adsorption on clay minerals exhibited a peak close to pH 3 and decreased rapidly with increasing pH until the adsorption was virtually zero close to pH 7 (Goldberg et al., 1996; Jones, 1957; Motta and Miranda, 1989). The relative adsorption on clay minerals increased in the order: illite < kaolinite < kaolinite and montmorillonite < nontronite < metahalloysite (Jones, 1957; Motta and Miranda, 1989). Goldberg et al., (1996) concluded that the magnitude of Mo adsorption increased in the following order: kaolinite < illite < montmorillonite. However, it is difficult to compare the adsorption affinity per unit mass or per unit surface area, since the suspension density varies between adsorbents of different experiments.

For Mo adsorption on kaolinite, the PZC of kaolinite is shifted to a more acidic pH value by changing the amounts of ionic strength, indicating an inner-sphere adsorption mechanism for Mo on these surfaces. Adsorption may occur through a variety of mechanisms, including adsorption on the outer or inner-sphere complexes and precipitation. Outer-sphere adsorption is a weak electrostatic attraction between an ion and the surface. Goldberg et al., (1996) reported that inner-sphere adsorption occurred through the formation of one or more chemical bonds between the surface and the adsorbate.

2.5.1.4 Pyrite

The scavenging of Mo in the oceans occured primarily in anoxic/sulfidic basins where Mo was sorbed by sulfide minerals including pyrite (Chappaz et al., 2014; Helz et al., 1996). Molybdate and tetrathiomolybdate (MoS_4^{2-}) are two major Mo species in this environment; their adsorption on pyrite was shown to be a function of ionic strength and pH (Bostick et al., 2003; Xu et al., 2006). Both MoO_4^{2-} and MoS_4^{2-} adsorption are impacted by increasing ionic strength; MoO_4^{2-} adsorption is affected by the addition of salt at all concentrations, while MoS_4^{2-} adsorption is unaffected except at low ionic strength. Generally, changes in ionic strength affect outer-sphere complexes; therefore implying that a portion of adsorbed MoO_4^{2-} and MoS_4^{2-} is present

as an outer-sphere complex or at least as a labile complex. Maximum molybdate adsorption occurs at pH 5 and 6 and then adsorption decreases sharply as the pH increases.

2.5.1.5 Organic matter

Under anoxic/sulfidic (euxinic) conditions, marine sediments including limestone are known to incorporate Mo into OM and pyrite (Adelson et al., 2002; Brumsack, 2006; Chappaz et al., 2014; Dahl et al., 2013; Helz et al., 1996; Kaback and Runnells, 1980; Pichler and Mozaffari, 2015; Tribovillard et al., 2004; Vorlicek, 2004; Zheng et al., 2000). However, in comparison to pyrite, the dominant source of Mo in sedimentary rocks is OM (Chappaz et al., 2014). The correlations between Mo and OM in six different sites studied were much stronger than those of Mo and pyrite (Chappaz et al., 2014; Lyons et al., 2003).

The adsorption of Mo from aqueous solutions was determined for eight different soil types from the Atlantic Coastal Plain and Piedmont regions by Karimian and Cox (1978). The data followed the Freundlich isotherm more consistently than Langmuir. Adsorption increased as the organic matter and/or Fe oxide contents of the soils increased (Karimian and Cox, 1978). Wichard et al., (2009) used x-ray spectroscopy to examine the chemical speciation of Mo in soil samples from forests in Arizona and New Jersey. They concluded that in the leaf litter layer, most of the Mo formed strong complexes with plant derived tannins and tannin-like compounds; Mo was bound to these organic ligands across a wide pH range. In deeper soils, Mo is bound to both iron oxides and natural organic matter. Molybdenum bound to OM can be captured by small complexing agents that are released by nitrogen-fixing bacteria; the Mo can then be incorporated into a nitrogenase (Wichard et al., 2009). Bibak et al., (1994) conducted batch experiments and concluded that Mo adsorption on humic acids was a function of pH. Its adsorption envelope decreased sharply from its maximum at pH 3.5.

2.5.2 Competitive impacts of anion effect on Mo adsorption

Roy et al., (1986) showed that the mobility of Mo in aquifers depends on several factors including sediment characteristics, and the presence of other oxyanions that compete with Mo for the surface sites of the sorbents.

Phosphate: phosphate (PO_4^{3-}) concentration affects MoO_4^{2-} adsorption, although PO_4^{3-} and MoO_4^{2-} form inner-sphere surface complexes (Ferreiro et al., 1985; Goldberg, 2010; Gustafsson, 2003). Roy et al., (1986) showed that the adsorption of molybdate was noticeably reduced by the competitive adsorption of phosphate on the surfaces of clay minerals. It has been revealed that molybdate transport in groundwater was retarded by sorption, depending on the pH and phosphate concentration in the water (Diels and Vanbroekhoven, 2008). Gustafsson et al., (2003) demonstrated that sorbed P reduced Mo sorption in soils, especially at high P levels. Stollenwerk (1998) observed that a lesser quantity of MoO_4^{2-} was adsorbed from sewage-contaminated groundwater than from uncontaminated groundwater, mostly because of the competition for surface sites exerted by PO_4^{3-}. Phosphate exhibited a highly competitive behavior towards adsorption of MoO_4^{2-} and MoS_4^{2-} onto goethite and pyrite (Xu et al., 2006).

Sulfate: Sulfate formed outer-sphere adsorption complexation on goethite, while molybdate formed inner-sphere adsorption complexation; therefore, sulfate did not show significant competition effect on Mo adsorption onto goethite (Xu et al., 2006). Goldberg (2010) showed that sulfate formed inner- and outer-sphere complexes on the aluminum oxide but its concentration did not affect Mo adsorption. Molybdate adsorption onto gibbsite was not impacted by sulfate, but the adsorption of sulfate was significantly inhibited by molybdate (Wu et al., 2000).

Tungstate and Vanadium: Vanadium (V), Mo and tungsten (W) were adsorbed strongly at pH 4 by kaolin, and decreased sharply reaching zero at pH 6.5. When V, Mo, and W were

added simultaneously, the adsorption curves showed that adsorption of Mo(VI) predominated at pH 4, whereas W(VI) and V(V) predominated at pH 5 to 6 and pH over 6.5, respectively (Mikkonen and Tummavuori, 1993). Mikkonen and Tummavuori (1993) conducted further research on the effect of adsorption of V, Mo, and W on the release of phosphate to the aqueous phase. Experimental results showed that the retention of W and Mo is greatest for the most acidic samples (around pH 4), and adsorption of molybdate occurs faster than vanadate and tungstate. Furthermore, in addition to the fact that phosphate can displace adsorbed molybdate, it can also be displaced by high amounts of other specifically adsorbed anions such as V, Mo, and W in the pH range of 2.5 to 7.5. The affinity of tungstate for the goethite surface was greater than that of molybdate (Xu et al., 2006).

Other anions: Some other anions showed little effect on Mo adsorption, e.g. arsenate adsorption onto clay minerals (Goldberg and Forster, 1998), selenite adsorption onto y-Al_2O_3 (Wu et al., 2001), and silicate onto goethite and pyrite (Xu et al., 2006).

2.6 Sedimentary arsenic

Elemental As is a member of group 15 of the periodic table, together with nitrogen, phosphorus, antimony and bismuth. It has an atomic number of 33 and an atomic mass of 74.91. Arsenic is a ubiquitous element found in the atmosphere, soils and rocks, natural waters and organisms.

Arsenic in rocks and sediments: The concentration of As in sedimentary rocks typically lies within the range of 1 to 10 mg/kg (Li, 2000; Taylor and McLennan, 1985), i.e, slightly above average terrestrial abundance. On average, sediments are more enriched in As than igneous rocks. Sands and sandstones tend to have the lowest concentrations, reflecting the low As concentrations of their dominant minerals including quartz and feldspar. Average concentration

of As in sandstone is about 4 mg/kg, although Ure and Berrow (1982) reported a lower average of 1 mg/kg.

Arsenic is found in coal; coals from south-western China were reported to contain as high as 826 to 2,578 mg/kg (Nriagu et al., 2007) and up to 32,000 mg/kg was reported by Wang et al., (2006). In Germany, the As content of bituminous shale ranged from 100 to 900 mg/kg (Smedley and Kinniburgh, 2002). The As contents of American coal were reported to be up to 2,200 mg/kg (Wang et al., 2006), but the mean concentration of more than 7000 samples was 24 mg/kg. Pyrite is the main source of As in coal with high As contents, whereas in coals with lower As, the As tends to be associated with organic materials (Yudovich and Ketris, 2005).

Argillaceous deposits showed a broader range and higher average As concentration than sandstone, typically an average of about 13 mg/kg (Ure and Berrow, 1982). The higher values reflect the larger proportion of sulfide minerals, oxides, OM, and clay. Black shale typically has highest As concentrations principally because of its enhanced pyrite content. Marine argillaceous deposits have higher concentrations than non-marine deposits. This may also be a reflection on the grain-size distributions, with potential for a higher proportion of fine materials in offshore pelagic sediments as well as systematic differences in sulfur and pyrite contents. Marine shale tends to contain higher sulfur concentrations. Sediment provenance is also an important factor. Particularly, high As concentrations were measured in shales from mid-ocean settings (Mid-Atlantic Ridge average of 174 mg/kg). In this case, Atlantic Ridge gases may be the source of As. Carbonate rocks typically have low concentration, reflecting the low concentrations of the constituting minerals (approximately 3 mg/kg) (Ure and Berrow, 1982). Some of the highest observed As concentration, often several thousand mg/kg, are found in ironstone and Fe-rich rocks. Phosphorites are also relatively enriched in As (values up to approximately 400 mg/kg have been measured). Concentrations of As in unconsolidated sediments are not notably different from those in their indurated equivalents, muds and clays having typically higher concentrations than sands and carbonates. Values are typically 3 to 10

mg/kg, depending on the texture and mineralogy. Elevated concentrations tend to reflect the amounts of pyrite or HFO in the environment; high concentrations are also typically found in mineralized areas. Placer deposits in streams can have very high concentrations due to the abundance of sulfide minerals.

Average As concentration in stream sediments in England and Wales were in the range of 5 to 8 mg/kg (Johnson et al., 2005; Smedley and Kinniburgh, 2001). Similar concentrations have also been found in river sediments where groundwater As concentrations were high. Datta and Subramanian (1997) found concentrations in sediments from the River Ganges averaging 2 mg/kg (ranging from 1.2 to 2.6 mg/kg), from the Brahmaputra River averaging 2.8 mg/kg (ranging from 1.4 to 5.9 mg/kg) and from the Meghna River averaging 3.5 mg/kg (ranging from 1.3 to 5.6 mg/kg). They found concentrations in lake sediments ranging from 0.9 to 44 mg/kg (median 5.5 mg/kg) but noted that the highest concentrations were present up to a few kilometers down-slope of the mineralized areas. The upper baseline concentration of these sediments is likely to be about 13 mg/kg. They also found concentrations of 1.9 to 170 mg/kg (median 9.2 mg/kg) in glacial till and noted the highest concentrations down-ice of mineralized areas. As enrichments were observed to decrease in sediments in both near shore and continental-shelf deposits (Legeleux et al., 1994; Peterson and Carpenter, 1986). Legeleux et al., (1994) noted an increase in concentration with depth (up to 30 cm) in the continental shelf sediments due to the generation of increasingly reducing conditions; concentrations varied between sites, but generally increased with depth in the range of 2.3 to 8.2 mg/kg.

Arsenic in waters: In Wisconsin and Florida, USA, As concentration in groundwater in sandstone and limestone aquifers were as high as 100 and 344 µg/L, respectively. Oxidation of pyrite hosted by these formations was the likely source of As, the transport of which was, in some instances, retarded by its association with Fe oxyhydroxides (Pichler and Mozaffari, 2015; Thornburg and Sahai, 2004). In Florida, the anthropogenic disturbance of subsurface redox conditions in an aquifer containing pyrite as a trace mineral led to significantly elevated

As concentrations in groundwater (Price and Pichler, 2006). In the adjacent State of Michigan, USA, As concentrations in groundwater reached 220 µg/L in a sandstone aquifer (Haack and Rachol, 2000). In Australia, a combination of increased water withdrawals during development and declining recharge due to drought caused oxidation of pyrite in sedimentary aquifers, resulting in As contamination of water wells (Appleyard et al., 2006). In England, groundwater from a sandstone aquifer contained As at concentrations that spanned from 10 to 50 µg/L; the As content of the sandstone ranged from 5 to 15 mg/kg. Desorption at pH of about 8 appeared to was the mechanism for As release to groundwater (Kinniburgh et al., 2006). Water wells completed in a Mesozoic Era sandstone in northern Bavaria also contained As at concentrations ranging from 10 to 150 µg/L (Heinrichs and Udluft, 1999), although the minerals contributing As were not identified.

2.7 Geochemistry of aqueous As

Arsenic is mobilized in the environment through a combination of natural processes such as weathering reactions, biological activity and volcanic emissions as well as through a range of anthropogenic activities (Pichler et al., 2001; Price and Pichler, 2006; Smedley and Kinniburgh, 2002). Most environmental As problems are due to mobilization under natural conditions, but humans have an important impact via mining activities, combustion of fossil fuels, the use of As bearing pesticides, herbicides and crop desiccants and the use of As as an additive to livestock feed, particularly for poultry.

Arsenic occurs in nature in two primary forms, inorganic and organic. Inorganic As occurs in four oxidation states (-III, 0, +III and +V). Arsenite, As(III) and arsenate, As(V) are the dominant forms found in natural waters. Inorganic As is a metalloid widely distributed in the Earth‘s crust (Qi and Pichler, 2014). In aquatic systems, As has complex chemistry with oxidation-reduction, ligand exchange, precipitation and adsorption reactions, all taking place. Under pE conditions

occurring in oxygenated waters, As acid species ($H_3AsO_4^0$, $H_2AsO_4^-$, $HAsO_4^{2-}$ and AsO_4^{3-}) are predominant for the pH ranges encountered in surface and groundwater, although the fully dissociated arsenate ion would be rare because very few waters reach a pH higher than 11.5. At pE values characteristic for mildly reducing conditions, the fully protonated arsenite species ($H_3AsO_3^0$) is predominant over a wide pH range (1 to 9). Dissolved arsenite tends to be much more mobile than arsenate. Both $H_2AsO_3^-$ and $HAsO_3^{2-}$ become dominant at higher pH values.

Organic species of As are predominantly found in food, such as shellfish, and include forms such as monomethyl arsenic acid (MMAA), dimethyl arsenic acid (DMAA), and arsenosugars. Organic As forms may be produced by biological activity, mostly in surface waters or wetlands, but are rarely important. Under sulfidic, mainly neutral to alkaline conditions, As forms thioarsenates and thioarsenites which can become the predominant As species (Planer-Friedrich et al., 2007, 2009). The equilibrium mineral stability of As under different pE and pH values exhibits a sequence of stable minerals from fully oxidized As pentoxide to fully reduced native As in the presence of 10^{-4} M total dissolved sulfur. No mineral corresponds with arsenate oxide because of its extreme solubility (about 40 g per 100 g of solution). Some divalent cations commonly found in surface and groundwater would promote the precipitation of metal arsenates that are less soluble. Arsenate is chemically similar to phosphate and may be isomorphously substituted and enriched in phosphate minerals (Ferguson and Gavis, 1972). Arsenic can be removed from the aqueous solution by sorption and co-precipitation. Clay minerals and HFO play an important role in retarding As in the environment.

Chapter 3. Chemical fractionation of molybdenum and arsenic

Abstract

Fractionation of molybdenum (Mo) and arsenic (As) in 10 matrix samples of the Lithia aquifers- which were singled out from three drill cores near the Lithia area in Central Florida- was determined by sequential extraction procedure (SEP). The samples contained up to 825 mg/kg Mo and 144 mg/kg As. The aim of this work was to determine the proportions of Mo and As in different forms, in the matrix of Lithia aquifers. The reagents which were used in the SEP analysis included sodium acetate (NaOAc), hydroxylammonium chloride ($HONH_2 \cdot HCl$) and Aqua regia. Concentration of Mo and As was measured by inductively coupled plasma mass-spectrometry (ICP-MS); analytical quality was controlled by including a replicate and a blank in every batch. Blanks contained no detectable amount of the elements in question and replicate samples results showed high precision (average standard deviation of 2.8 and 0.86 for Mo and As, respectively). The SEP results were compared with those obtained by total digestion method. The recovery ranged from 88 to 111% for Mo and 75 to 116% for As, and the precision (RSD) in the extracts was below 10%. In most samples, up to 90% Mo was present in the very soluble fraction (step 1), indicating a major source for Mo. For six samples more than 80%, for two samples more than 50% and for the remaining two samples up to 20% of Mo was released in this fraction. About 10% Mo was leached during steps 2 and 3, through which carbonates, hydrous ferric oxides (HFO) and manganese oxides were dissolved. Approximately, 25% Mo was removed in steps 4 and 5, where crystalline iron oxides, pyrite and organic matter (OM) were dissolved. Because of the importance of powellite as a possible source of Mo and in order to better understand this hypothesis, powellite was precipitated and run through the SEP. It was completely dissolved during step 3 through which HFO was also dissolved. The results showed that a maximum 4% Mo was released from powellite and HFO. In contrast to Mo, As was present in somewhat similar abundances in all of the extraction steps, i.e. step 1 (17%), step 2 (11%), step 3 (30 %), step 4 (23 %) and step 5 (18%). Hydrous

and crystalline iron oxides which were dissolved in steps 3 and 4 contained the highest As concentrations. Arsenic was possibly present as impurity in some minerals like pyrite and powellite, and co-precipitated with HFO.

From the procedure described above, it became clear that Mo is easily mobilized from the aquifer matrix. The mobilization of Mo can proceed along several pathways which include oxidation of OM, desorption from mineral surfaces, and re-dissolution of powellite. Extraction of Mo in step 1 for 3 samples from surficial sediments was relatively low. This could be due to following three reasons:

1. Surficial sediments underwent lower water level fluctuations and less change in physico–chemical conditions and as a result, lower OM degradation.

2. Oxygenated waters caused degradation of OM and could lead to the mobilization and transport of Mo from the surficial sediments into the deeper aquifers.

3. Higher concentration of Mo in sources like phospherite, iron oxides and powellite than in OM.

To assess the effect of dissolved oxygen on the easily mobilized Mo and As, 32 aquifer matrix samples from the Lithia area and Avon Park Formation (APF) were dissolved in groundwater of a well near the Geology Department of the Bremen University and distilled deionized (DDI) water. The dissolved oxygen of the groundwater sample was low and relevant for the experiments (0.45 mg/L). The experiments for the groundwater samples were conducted under a glove box to provide an isolated conditions from the outside atmosphere. The results suggested that Mo and As extraction increased with increase in time and equilibrated after 48 h. The amount extracted when both solutions were used was almost the same after 48 h, indicating no oxygen effect on Mo and As desorption from the aquifer matrix.

3.1 Introduction

Molybdenum is an important nutrient for a range of biological functions in animals, plants, human body and microorganisms (Stiefel, 1996). However, very large doses of Mo can damage organisms in terrestrial and aquatic environments (Cornell et al., 1987; Krishnamachari KA, 1974; WHO, 1993). Therefore, geochemical processes governing Mo leaching from contamination sources and sedimentary rocks into the groundwater resources are of significance and need to be addressed.

Numerous research were conducted to assess the geochemistry of Mo in marine sediments (Bertine and Turekian, 1973; Chappaz et al., 2014; Crusius et al., 1996; Glass et al., 2013; Helz et al., 1996; Kaback and Runnells, 1980; Lyons et al., 2003; Miller et al., 2011; Tribovillard et al., 2008; Werne et al., 2008). However, no attempt has been made to investigate the fractionation and mobilization of Mo in/from sedimentary rocks.

The behavior of the elements in the environment (e.g., bioavailability, toxicity and distribution) cannot be reliably predicted on the basis of their total concentration. Chemical speciation is of interest in environmental analytical chemistry because the behavior of trace elements in natural systems depends on the forms as well as on the amounts available for consumption or taking part in chemical reactions. This is often undertaken by single or sequential extraction. These procedures involve subjecting a solid sample such as soil or sediment to successive attacks with reagents possessing different chemical properties (acidity, redox potential or complexing properties). In this study, SEP was carried out for determination of Mo and As in sedimentary rocks following the procedure recommended by Pichler et al., (2001). Samples subjected to the SEP were from three drill cores (DEP-1, DEP-2 and DEP-3) in the Lithia area. The SEP was selected to provide information about soluble phases, adsorption, desorption and sulfides/OM which is attributed to the primary and secondary sources of Mo and As in sedimentary rocks. In addition, some samples from Lithia area and APF formation were

dissolved in groundwater and DDI water to assess the dissolved oxygen effect on Mo and As desorption from the aquifer matrix. Molybdenum mineral, powellite ($CaMoO_4$), was also synthetically prepared to evaluate how it is dissolved during the SEP.

3.2 Materials and methods

3.2.1 Materials and reagents

All chemicals used in these experiments were of analytical grade, and used without any further purification. Distilled deionized water was used to prepare solutions and dilute the samples. The reagents which were used in the SEP are listed in Table 3.1.

Powellite was precipitated by mixing 1 M $Ca(NO_3)_2.4H_2O$ and 1 M Na_2MoO_4-$2H_2O$ solutions in equal Ca/MoO_4 molar proportions. To test the influence of dissolved oxygen on the weak bond of Mo and As, groundwater and DDI water were added to some samples of the Lithia area and APF formation and shaken for 48 h.

3.2.2 Sample selection, preparation and analytical methods

The samples were chosen from DEP-1, DEP-2, and DEP-5 in Lithia area and APF drill cores. All the samples were selected based on three criteria including high Mo concentration, high As concentration and good geographic representation of the study area. The samples were powdered with an agate mortar and pestle which were thoroughly rinsed with ethanol in between samples to prevent cross contamination. An electronic scale was used to weigh out 1 ± 0.005 g of powdered sample by pouring it into 50 mL centrifuge tube for the experiments. Fifty mg of each sample were used to measure total content of the elements. The total concentrations of major elements were measured by inductively coupled plasma optical emission spectrometry (ICP-OES) using an Optima 7300 instrument (Perkin Elmer). Trace

elements of Mo and As in different phase of the SEP were determined by using inductively coupled plasma mass spectrometry (ICP-MS) using an iCAP-Q instrument (Thermo Fisher). The detection limits for Mo and As were 1 and 0.5 μg/L, respectively.

Table 3.1: A summary of the SEP.

Steps	Phases	Reagents	Procedure
Step 1	Adsorbed/exchangeable	20 mL 1 M NaOAc (pH 8.1)	2 h leach, 2×5 mL H_2O rinse
Step 2	Carbonates	20 mL 1 M NaOAc (pH 5)	2 h leach, 2×5 mL H_2O rinse
Step 3	Hydrous iron oxides	20 mL 0.25 M $NH_2OH.HCl$ in 0.25 M HCl	2 h bath at 60°C, 2×5 1 mL H_2O rinse
Step 4	Crystalline iron oxides	30 mL 1 M $NH_2OH.HCl$ in 25% HOAc	3 h bath at 90°C, 2×5mL 25% HOAc rinse
Step 5	Sulfides and organics	8 mL Aqua Regia (6 mL HCl, 2 mL HNO_3)	Approximately 3 h bath (1 h at 90°C)

3.2.3 Sequential extraction procedure

Step 1. Twenty mL of 1 M NaOAc (at pH 8.1) were added to 1 g of powdered sample in a 50 mL screw cap centrifuge tube. The contents were shaken for 2 h at room temperature by a mechanical shaker operating at 250 RPM. The solutions were centrifuged for 10 min at 4000 RPM and separated from the solids , decanted into another 50 mL labeled tube, diluted to 50 mL and was finally prepared for analysis after filtering. The residues were rinsed with 5 mL DDI water and centrifuged again, and the washings were discarded.

Step 2. Another 20 mL of 1 M NaOAc adjusted to pH 5 and were added to the residues of the first step and the procedure continued similar to step 1.

Step 3. Twenty mL of a freshly prepared 0.5 M $HONH_2 \cdot HCl$ in 0.25 M of HCl were added to the residues of the second step, capped and shaken for 5 to 10 seconds. The samples were then placed in a hot block at 60°C for 2 h with the cap loosened. Every 30 min interval, the caps were tightly closed and the contents were shaken for 5 to 10 seconds. The samples were then centrifuged and the extracts were separated as described above.

Step 4. Thirty mL of 1 M $HONH_2 \cdot HCl$ in 0.25% HOAc were carefully added to the residues of the third step, capped and shaken for 5 to 10 seconds. Then, the samples were placed in the hot block at 90°C for 3 h, capped and the contents were shaken every 20 min. The samples then centrifuged for 10 min, the supernatant liquids were decanted in 50 mL centrifuge tubes and topped up to 50 mL and filtered. The residues were rinsed with 5 mL 25% HOAc and the washings were discarded.

Step 5. Six mL HCl and 2 mL HNO_3 (8 mL Aqua regia) were added to the residues of the forth step, capped and shaken for 5 to 10 seconds. The samples were placed in the hot block for 3 h and the contents were shaken for 5 to 10 seconds every 30 min. The liquid supernatants

were separated after centrifuging samples for 10 min, transferred to 50 mL centrifuge tube, and finally prepared for analysis after filtering.

3.2.4 Powellite precipitation

Powellite ($CaMoO_4$) was precipitated to test its behavior during the SEP. It was prepared by the same general procedure described by Andrew et al., (1992). Calcium molybdate [$CaMoO_4$(c)] was prepared by mixing 1 M $Ca(NO_3)_2.4H_2O$ and 1 M Na_2MoO_4-$2H_2O$ solutions in equal Ca/MoO_4 molar proportions. A white precipitate was generated upon mixing. The suspension was allowed to react by constantly mixing it for 48 h. The white precipitate was removed from the solution by vacuum filtration and washed with copious amounts of DDI water and by pure ethanol thereafter. The solid was oven-dried at 115° C for 24 h. The precipitate was analyzed by X-ray diffraction technique which showed it contained no impurities (Fig. 3.1).

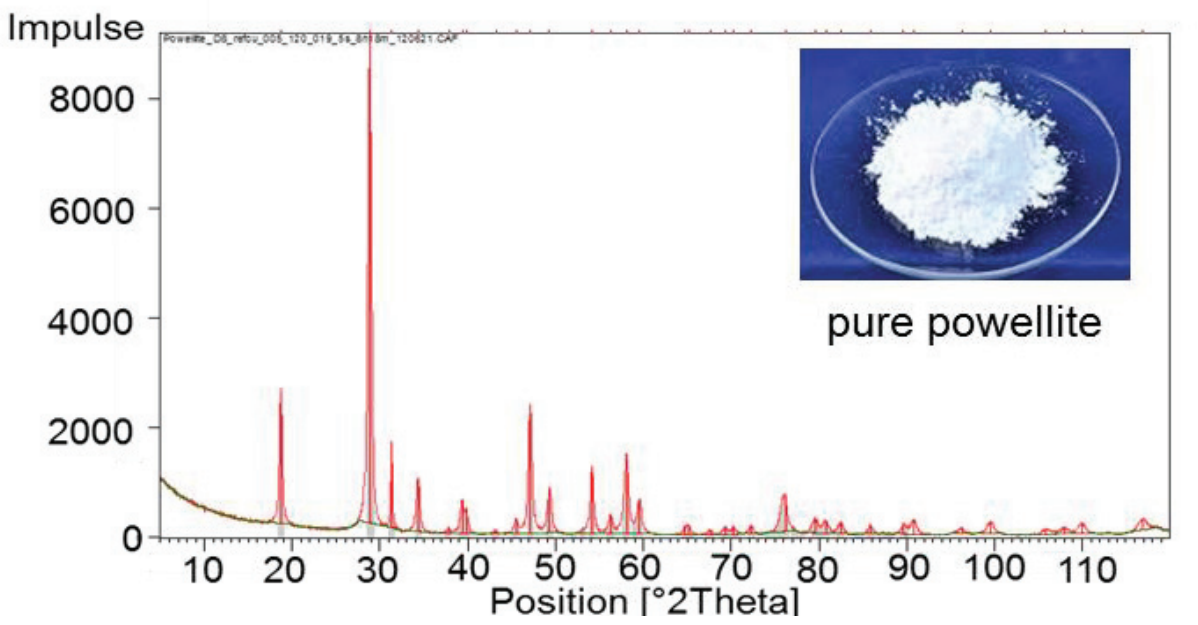

Fig. 3.1 X-ray diffractometer patterns for precipitated powellite

3.2.5 Mobilization test for weakly bound Mo and As

To test the influence of dissolved oxygen on the easily mobilized Mo and As in the Floridian aquifer matrix, 32 samples were selected from the Lithia area drill cores and the APF. Then, 40 mL water with a background electrolyte of 0.01 M $NaNO_3$ were added to 1 g of each sample and shaken for 48 h. In addition, 40 mL groundwater with low dissolved oxygen content which was collected from a water well near the Geology Department of the Bremen University (0.45 mg/L) was added to 1 g of the samples in a glove box. The samples were then shaken for 1, 4, 12, 24, and 48 hours at room temperature by a mechanical shaker operating at 250 RPM. The extract were separated from the solid residues by centrifugation at 4000 RPM for 10 min. The supernatants were decanted into a 50 mL tube, diluted to 50 mL and prepared for chemical analyses (i.e., filtration, dilution if necessary).

3.3 Results

3.3.1 Sequential extraction procedure results

Sequential extraction procedure takes the advantage of using increasingly stronger solvents, each targeting a specific host mineral fraction (Table 3.1) and enabling us to subdivide the bulk trace element (in this case Mo and As) content of a sample into proportions of different extractabilities. This exercise provides an estimation of the potential mobility of Mo and As and is thus more valuable for ecological considerations than the bulk content. In the present research, A SEP recommended by Pichler et al., (2001) was used to assess Mo and As mobility from the aquifer matrix sediment. Analytical quality of the SEP was controlled by including a replicate and a blank in every batch. The results showed high precision for replicate samples with average standard deviation of 2.8 for Mo and 0.86 for As, and the blanks contained no detectable concentration of the elements in question. The accuracy of measurements was verified by comparing the sum of the fractions in the extracts with the total

content in the sample. Good agreement was observed between the two with recoveries ranging from 88 to 111% for Mo and 75 to 116% for As.

3.3.1.1 Molybdenum

Results of Mo fractionation by the SEP experiments are shown in Tables 3.2. A majority (up to 90%) of Mo was removed in the first step i.e., adsorbed/exchangeable phase. About 10% Mo was leached during the second and third steps, which relate to carbonates, HFO, manganese oxides and powellite dissolution. Approximately 25% Mo was released during steps 4 and 5 that dissolve crystalline iron oxides, pyrite and OM.

Excluding sample 10-11 which contained the lowest Mo concentration of 25 mg/kg, up to 90% Mo was removed in step 1, whereas much lower Mo was removed during the other steps (Table 3.2 and Fig. 3.2). More than 80% Mo was removed from samples 45-46, 46-47, 70-71, 31-32, 42-43 and 51-52. Approximately 65 to 70% Mo was removed from samples 18-19 and 75-76. In contrast to these samples, samples 10-11 and 69-70 showed much lower extraction rate of 5 and 21%, respectively. In step 2, about 3 to 4% Mo was removed from almost all the samples. Samples 10-11, 18-19, 31-32, 50-51 and 69-70 did not release any Mo in this step. Insignificant amount of Mo was removed during step 3; Mo extraction ranged from 2 to 4% for all the samples. In step 4, more than 20% Mo was released from Sample 10-11. For the remaining samples, including samples 18-19, 69-70 and 75-76, about 2 to 17% of the total Mo contents were extracted. In step 5, little Mo was removed from samples 45-46, 50-51, 75-76, 31-32 and 42-43. However, the extraction rates for samples 10-11, 46-47, 69-70 and 70-71 were relatively high i.e., 17, 11, 20 and 8%, respectively.

Table 3.2: Summary of the results of Mo (mg/kg)[a] extracted by the five-step SEP, and the total content of element in the samples.

Core	Sample	Step 1	Step 2	Step 3	Step 4	Step 5	Σ 1+2+3+4+5	Total	Rec[b] %
DEP-1	**45-46**	114	8.3	1.9	1.0	1.8	127.4	122	104.7
DEP-1	**46-47**	750	49.0	32.0	23.4	115.0	969.2	825	110.8
DEP-1	**70-71**	399	15.8	1.3	14.7	62.0	492.4	499	89.0
DEP-2	**10-11**	1	3.0	10.0	4.0	2.0	20.1	25	92.0
DEP-2	**18-19**	21	1.8	8.8	3.2	1.0	35.9	38	102.4
DEP-2	**31-32**	52	2.0	1.2	1.0	1.0	56.8	53	104.3
DEP-2	**42-43**	76	6.0	2.2	1.0	1.0	86.1	78	109.4
DEP-5	**50-51**	30	2.9	1.5	1.0	1.1	36.3	36	100.7
DEP-5	**69-70**	6	4.0	3.9	3.0	6.0	22.8	30	88.2
DEP-5	**75-76**	85	12.0	15.0	4.0	1.0	116.7	136	105.5

[a] Average value of two replicate samples
[b] Rec. =Recovery = (Σ 1 + 2 + 3 + 4 + 5 / total content) × 100%.

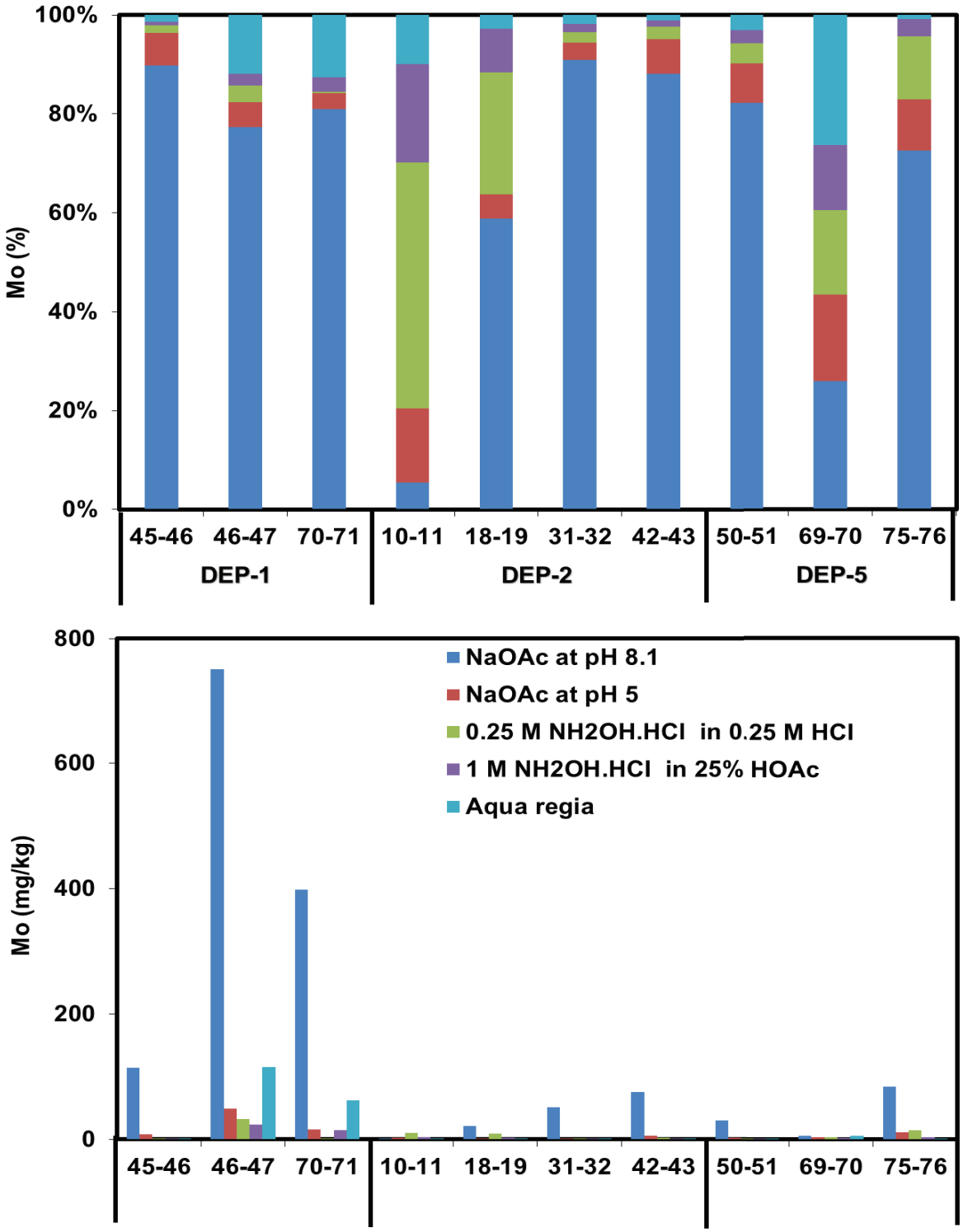

Fig.3.2 Percentage and concentration of Mo removed during the SEP. The amount leached in steps 1 to 5 corresponds to those listed in Table 3.2.

3.3.1.2 Arsenic

Arsenic extraction rate was lower than Mo in step 1. As shown in Table 3.3 and Fig. 3.3, approximately 33 to 45% As was removed from samples 45-46, 46-47, 70-71 and 31-32. About 10 to 24% As was removed from samples 42-43 and 50-51. Virtually no As was extracted from the remaining samples. There was no extraction of As in step 2 for samples 10-11, 18-19, 31-32, 50-51 and 69-70. The highest As removal (About 30%) was for sample 45-46. On average 30% As was recovered while dissolving HFO in step 3. This was the highest extraction rate for As during the SEP. With the exception of sample 10-11 whose removal rate was 64%, only 3 to 30% As was removed in step 4. Arsenic percentage rate was very low of 3% for sample 46-47. Arsenic extraction rate was much higher than that of Mo in step 5. Although, there was no extraction for samples 45-46, 46-47 and 31-32, up to 51% As was removed from the rest of the samples. Samples from DEP-5 including 50-51, 69-70 and 75-76 exhibited higher As extraction rate 22, 5 and 18%, respectively. With the exception of sample 18-19 whose extraction rate was 41%, the As extraction for samples 70-71, 10-11 and 42-43 were lower at 11, 7 and 9%, respectively.

Table 3.3: Summary of the results of As (mg/kg)[a] extracted using a five-step SEP, and the total content of the element in the samples.

Core	Sample	Step 1	Step 2	Step 3	Step 4	Step 5	Σ 1+2+3+4+5	Total	Rec.%
DEP-1	**45-46**	11.4	8.7	6.4	4.1	n.d.	31.0	29.6	104.6
DEP-1	**46-47**	71.7	28.6	45.6	4.6	n.d.	151.5	143.9	105.3
DEP-1	**70-71**	28.4	13.8	25.7	21.7	9.9	99.5	131.7	75.6
DEP-2	**10-11**	n.d.	n.d.	9.0	21.1	2.1	33.6	28.8	116.6
DEP-2	**18-19**	n.d.	n.d.	4.8	3.8	6.2	15.3	17.8	85.7
DEP-2	**31-32**	2.7	n.d.	3.1	1.4	n.d.	9.6	9.3	103.6
DEP-2	**42-43**	4.1	2.7	4.2	5.8	1.9	18.8	19.8	94.7
DEP-5	**50-51**	1.8	n.d.	7.8	5.7	5.2	22.4	29.8	75.1
DEP-5	**69-70**	n.d.	n.d.	17.5	5.5	24.3	48.5	59.9	81.0
DEP-5	**75-76**	1.5	2.1	24.9	11.9	11.2	51.7	52.2	99.0

[a] Average value of two replicate samples

[b] Rec. = Recovery = (Σ 1 + 2 + 3 + 4 + 5 / total content) × 100%.

n.d. = not detected

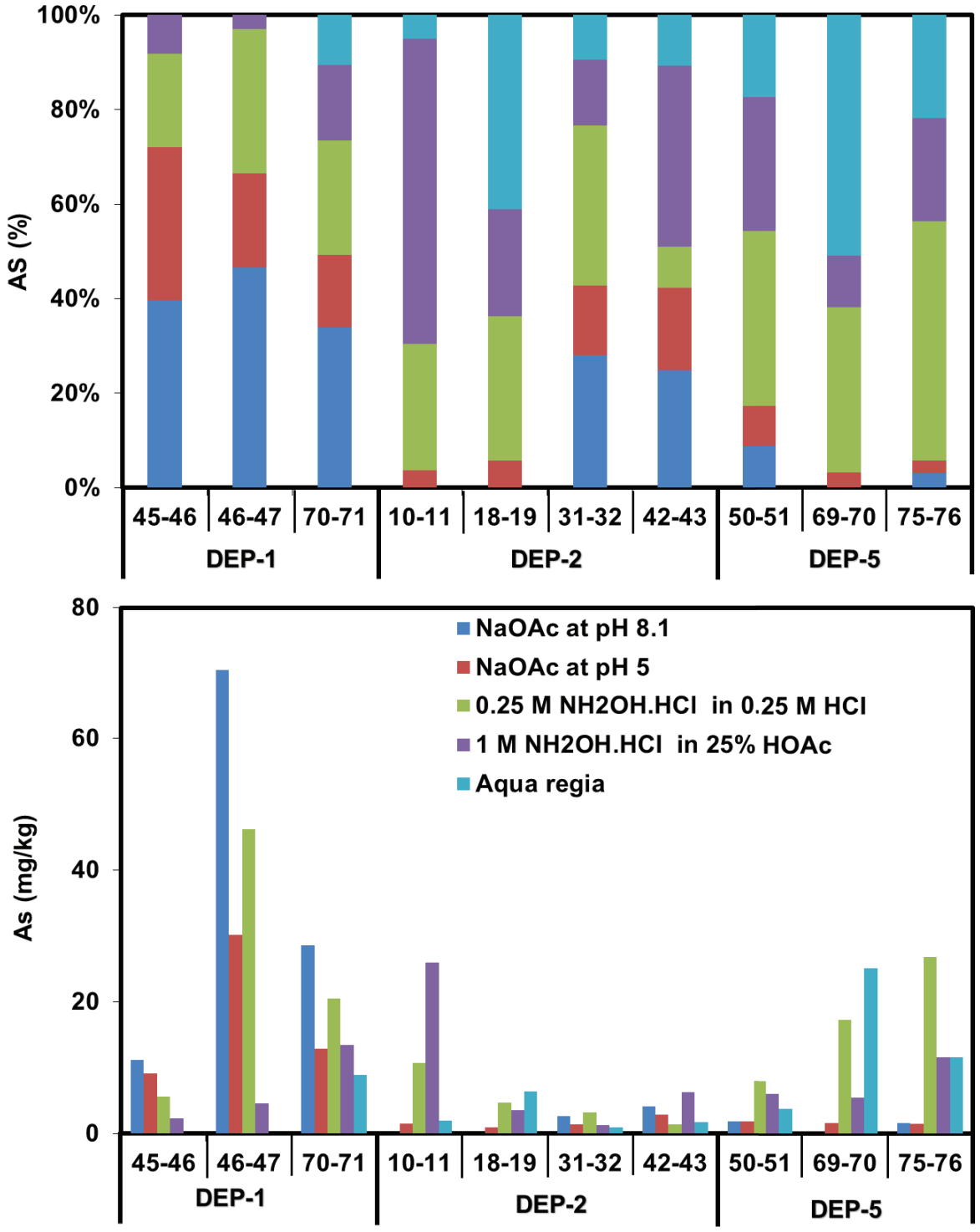

Fig.3.3 Percentage and concentration of As removed during the SEP. The amount leached in steps 1 to 5 corresponds to those listed in Table 3.3.

3.3.2 Dissolving aquifer matrix samples in groundwater and DDI water

The aquifer matrix samples from the Lithia area and APF were dissolved in groundwater and DDI water at pH 6.5 and shaken in a mechanical shaker operating at 250 RPM with different contact time of 1, 4, 12, 24 and 48 h. The groundwater sample used in this analysis (pH = 6.35 and O_2 = 0.48 mg/L) was taken from a water well near the Geology Department of Bremen University. The results of these experiments are shown in Tables 3.4 and 3.5. The experiments with groundwater and DDI water were undertaken to 1) identify the kinetic of readily mobilized Mo and As from the aquifer matrix and 2) assess the effect of dissolved oxygen on Mo and As mobilization. It took 48 hours to release all easily bound Mos. No significant difference was observed between results from groundwater and DDI water (Fig. 3.4 and Fig. 3.5). The amount of Mo and As extracted with both solvents were in good agreement with the amount released during the first step of the SEP results.

Table 3.4: Amounts of Mo (mg/kg) mobilized from the aquifer matrix by reaction with groundwater and DDI water at pH 6.5 in different mixing times as compared to total Mo.

Core	Sample	Total	Groundwater (pH = 6.35 and O_2 = 0.48 mg/L)					DDI water (pH 6.5)
			1 h	4 h	12 h	24 h	48 h	48 h
DEP-1	**45-46**	122	28	32	45	59	72	91
DEP-1	**70-71**	639	167	216	286	335	357	357
DEP-2	**10-11**	25	n.d.	n.d.	n.d.	n.d.	n.d.	n.d.
DEP-2	**18-19**	38	4	5	9	11	14	15
DEP-2	**42-43**	78	38	49	66	63	75	74
DEP-5	**44-45**	41	18	21	30	34	44	38
DEP-5	**46-47**	44	10	12	18	21	22	25
DEP-5	**50-51**	202	101	107	122	122	128	126
DEP-5	**56-57**	75	23	25	32	34	38	39
DEP5	**69-70**	39	n.d.	n.d.	n.d.	n.d.	n.d.	1
DEP-5	**72-73**	112	13	16	18	21	20	31
DEP-5	**74-75**	33	11	16	18	20	26	37
DEP-5	**75-76**	197	70	76	78	80	86	89
DV1	**72**	39	n.d.				1	2
DV1	**256**	26	6				n.d.	1
R13	**415**	3800	13				71	150
R13	**425**	108	n.d.				10	12
R13	**452**	235	1				50	43
R20	**368**	71	n.d.				13	36
R20	**376**	138	1				34	45
R20	**406**	329	1				100	112
R20	**408**	135	3				44	67
R22	**306**	109	n.d.				12	21
R25	**299**	29	n.d.				1	6
R25	**313**	42	n.d.				10	12
R25	**315**	48	n.d.				8	9
R28	**354**	50	10				14	24
R28	**373**	49	1				15	24
R28	**374**	118	n.d.				91	89
R39	**306**	66	n.d.				23	32
R39	**515**	97	19				28	24
TRSH-1	**313**	36	n.d.				2	3

n.d. = not detected

Table 3.5: Amounts of As (mg/kg) mobilized from the aquifer matrix by reaction with groundwater and DDI water at pH 6.5 in different mixing times as compared to total As.

Core	Sample	Total	Groundwater (pH = 6.35 and O_2 = 0.48 mg/L)					DDI water (pH 6.5)
			1 h	4 h	12 h	24 h	48 h	48 h
DEP-1	**45-46**	29.7	2.4	3.6	1.8	3.3	5.0	6.0
DEP-1	**70-71**	131.7	12.5	13.1	18.3	20.7	21.6	25.0
DEP-2	**10-11**	28.8	1.0	n.d.	1.1	n.d.	1.0	1.8
DEP-2	**18-19**	17.8	n.d.	n.d.	n.d.	1.0	1.0	1.4
DEP-2	**42-43**	19.8	1.0	n.d.	1.2	1.0	2.2	3.0
DEP-5	**44-45**	11.7	1.0	1.4	1.8	1.0	1.2	3.0
DEP-5	**46-47**	16.9	n.d.	1.7	1.0	1.0	1.5	2.0
DEP-5	**50-51**	77.4	n.d.	1.8	2.2	1.0	2.0	1.5
DEP-5	**56-57**	13.8	n.d.	n.d.	n.d.	1.0	n.d.	2.9
DEP5	**69-70**	66.8	1.7	1.0	1.0	1.0	1.0	2.8
DEP-5	**72-73**	24.7	1.0	n.d.	1.0	n.d.	n.d.	2.4
DEP-5	**74-75**	17.9	1.6	1.0	1.1	2.9	2.7	4.0
DEP-5	**75-76**	56.8	1.1	1.6	2.9	1.7	3.1	4.0
DV1	**72**	5.0	1.0				n.d.	n.d.
DV1	**256**	1.9	3.5				n.d.	n.d.
R13	**415**	15.0	1.1				11.0	8.0
R13	**425**	16.7	1.1				1.8	2.0
R13	**452**	22.9	1.0				1.0	1.0
R20	**368**	9.9	n.d.				3.0	3.3
R20	**376**	8.1	n.d.				2.0	3.1
R20	**406**	27.5	3.1				n.d.	n.d.
R20	**408**	21.4	1.4				1.6	1.7
R22	**306**	16.9	1.0				1.2	2.0
R25	**299**	30.8	1.0				1.8	1.6
R25	**313**	5.1	1.0				2.0	2.0
R25	**315**	5.7	n.d.				1.5	1.4
R28	**354**	11.1	n.d.				1.2	1.2
R28	**373**	20.5	n.d.				1.5	1.4
R28	**374**	18.3	1.0				3.0	2.0
R39	**306**	8.4	1.0				2.0	2.8
R39	**515**	7.9	n.d.				2.0	1.5
TRSH-1	**313**	3.3	1.0				1.0	1.0

n.d. = not detected

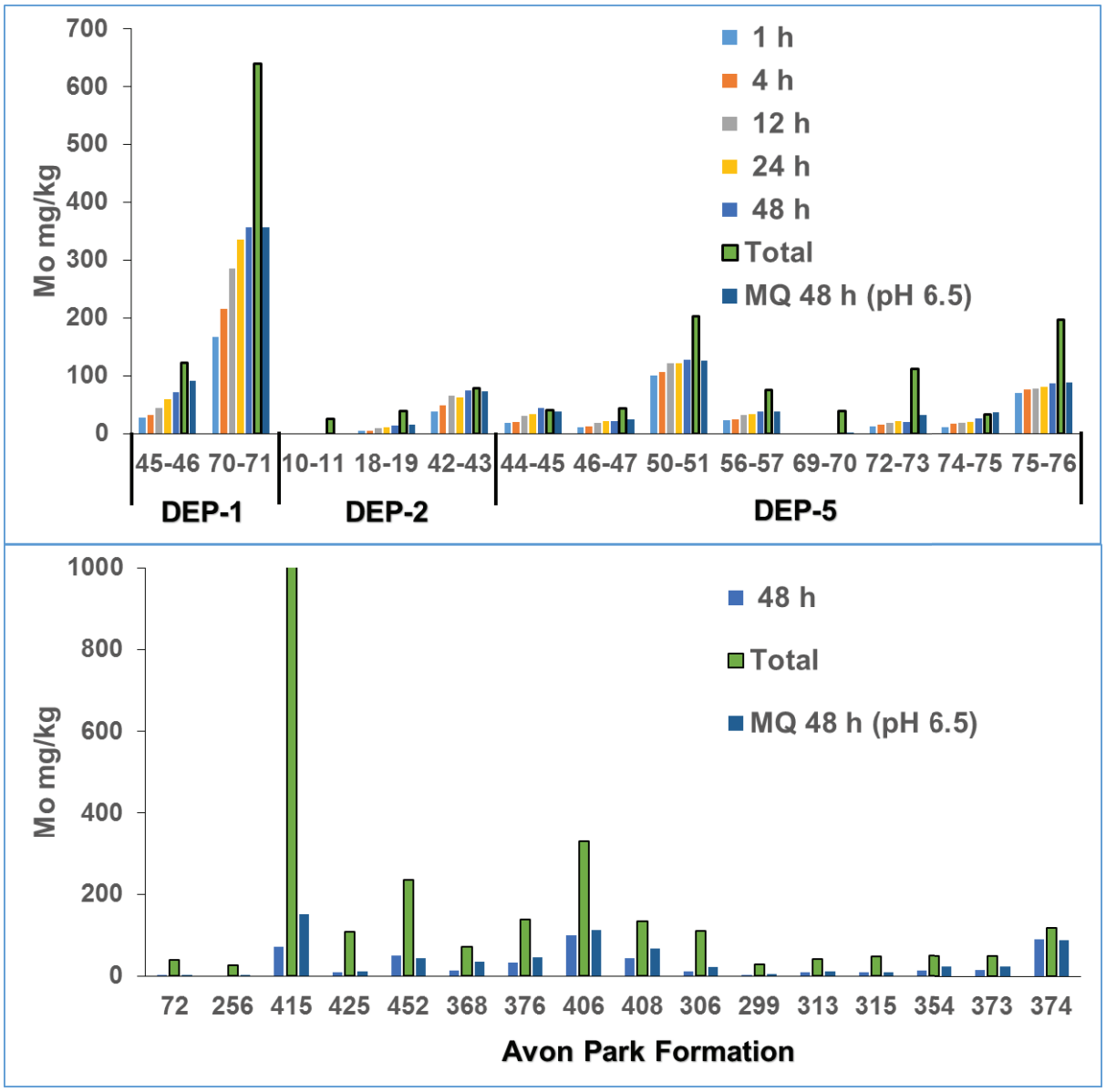

Fig. 3.4 Amount of Mo mobilized during the reaction with groundwater and DDI water in different mixing times. The data corresponds to Table 3.4.

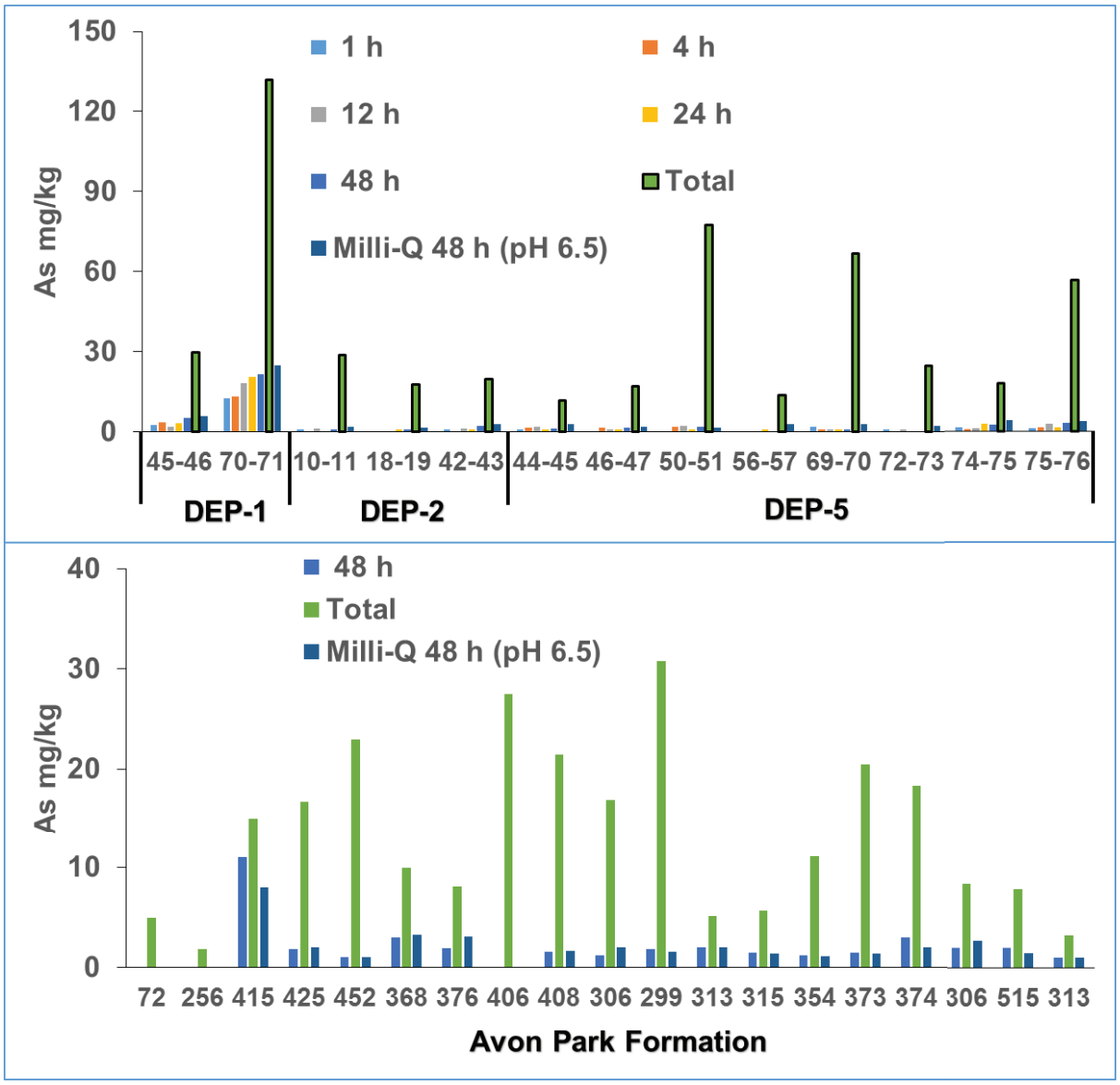

Fig. 3.5 Amount of As mobilized during the reaction with groundwater and DDI water in different mixing times. The data corresponds to Table 3.5.

3.4 Discussion

3.4.1 Estimation of the potential mobility of Mo and As

In order to evaluate potential mobility of Mo and As in the aquifer matrix sediments, a slightly modified five-step SEP recommended by Pichler et al., (2001) was applied to 10 drill core samples of the Lithia area. Molybdenum was mostly present in very soluble phases, while As had somewhat equal extractions in all fractions.

Step 1: In this step, NaOAc at pH 8.1 was used as a solvent. As shown in Figures 3.2 and 3.3, most Mo and up to 45% As were discovered to be in adsorbed/exchangeable phase. Only, three samples including 10-11, 18-19, and 69-70 yielded virtually no Mo and As. This might be due to the different conditions that these samples underwent rather than having different sources of Mo and As. Two possible reasons for the high Mo and As extracted in step 1 of SEP are as follows:

1. Specific factors such as temperature, humidity or drying condition are capable of influencing extraction phases in anoxic sediments (Hall et al., 1996). For instance, Goldberg et al., (1996) compared the phase distribution of iron (Fe) and cadmium (Cd) in the anoxic sediments extracted (a) immediately upon collecting sediments and (b) after oven drying and exposure to air. Oxidation of the sediments caused shifting of Cd (circa. 50%) from the sulfide phase to the more labile exchangeable and reducing fractions. It is well known that Mo enrichment mostly happens in the anoxic sediments and the sediments deposited beneath oxygen-deficient marine waters are enriched in Mo relative to normal (oxic) marine sediments and continental crust. In such sediments, Mo bonds to OM and/or sulfide minerals (Chappaz et al., 2014; Dahl et al., 2013; Tribovillard et al., 2004). Thus, oxidation of these materials and minerals has likely moved these phases of Mo and As to the weaker exchangeable and reducible phases and finally released them into groundwater.

2. Molybdenum and As in groundwater may be adsorbed by sorbents. An electrostatic adsorption modeling with PHREEQC showed that molybdate (MoO_4^{2-}) was the dominant Mo

species in the groundwater samples. The predicted speciation of Mo in the alkaline pH range of groundwater was 65% MoO_4^{2-}, 19% $MgMoO_4$, 14% $CaMoO_4$, and a negligible amount of other species (Fig. 3.6). This finding was in good agreement with what was reported by (Carroll et al., 2006). In fact, the result of our modeling exercise matches well with what happens in various environments including hydrosphere. This is why molybdate is referred to as the dominant species of Mo in the literature. All significant sorption sites for Mo and As in the aquatic environment include HFO (Goldberg et al., 1996; Gustafsson, 2003), pyrite (Bostick et al., 2003; Xu et al., 2006), Fe and Al (aluminum) oxides and clay minerals (Goldberg, 1985, 2010), calcite (Goldberg et al., 1996), Mn oxides (Matern and Mansfeldt, 2015), and OM (Bibak and Borggaard, 1994). Among these, Mo adsorption on Mn oxides and calcite was ruled out due to the low adsorption capacity of Mo onto calcite and low Mn concentration throughout the aquifer matrix (Goldberg et al., 1996; Pichler and Mozaffari, 2015). Molybdenum adsorption on clay minerals is a function of pH. Its adsorption on these minerals exhibited a peak near pH 3 but decreased rapidly with increasing pH until the adsorption was virtually zero near pH 7 (Goldberg et al., 1996). Molybdenum adsorption onto the Al and Fe oxides extended from pH 3 to 5 (Ferreiro et al., 1985). Limestone clearly showed the ability to remove As from groundwater (Cederkvist et al., 2010). Arsenic displayed high affinity on iron oxides and hydroxides such as HFO, goethite, and hematite (Lenoble et al., 2002; Pichler et al., 2001; Pierce and Moore, 1982).

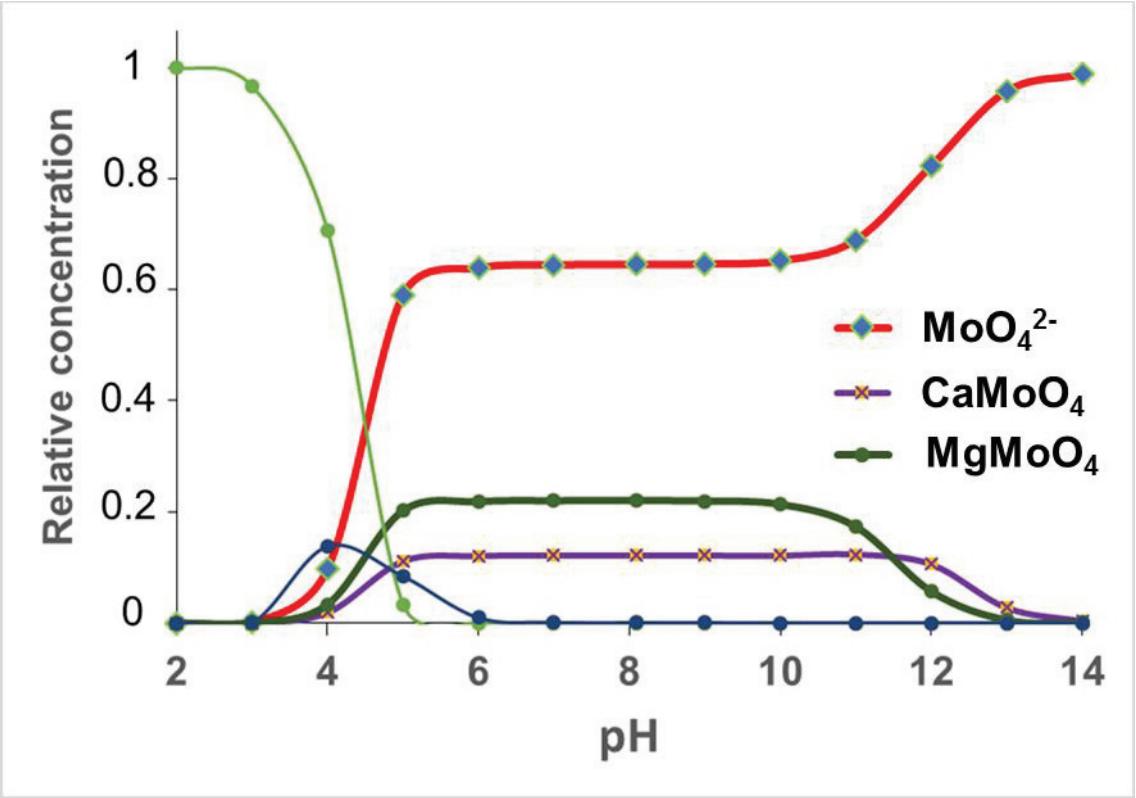

Fig. 3.6 Results of PHREEQC model for aqueous species distribution for a range of pH values within the groundwater of Lithia area.

Approximately 2-10% Mo was removed during the second step of the SEP, which extracts carbonates (Fig. 3.2). Since Mo was not found to be co-precipitated with carbonates and also its adsorption on calcite and calcareous soils is low (Goldberg et al., 1996), its extraction from samples 149-152 (30 mg/kg), 228-232 (12 mg/kg), and 144-149 (9 mg/kg) in the second step of the SEP could not be related to carbonates. These extracts should have been shifted from the stronger phases which were oxidized to the labile fractions (Fig. 3.2). As it is seen in Fig. 3.3, in this step, up to 30% As was removed pointing to carbonates as a potential site for As adsorption or coprecipitation. Limestone acts not only as a pH buffer, but may also promote the removal of As by Fe-mineral (McNeill and Edwards, 1995; Shan et al., 2013). McNeill and Edwards (1995) reported that calcium can react with As (e.g. AsO_4^{3-}) to form a sparingly soluble calcium compound. Shan et al., (2013) showed that the dissolution of limestone adjusted the pH value of the reaction system to form a weakly alkaline environment. Their

results suggested that complex mechanisms including 1) As(III) adsorption onto Fe-minerals, 2) As(III) oxidation to As(V) by iron minerals, and 3) precipitation of Ca – As(V) with Ca released through limestone dissolution collectively played the main role in removing As from the solution.

An insignificant amount (4%) of Mo was removed during the third step of the SEP (Fig. 3.2). Hydrous ferric oxides, Mn oxides, and powellite dissolved in this step all contributed to this removal. Considering the low concentration of Mn in the study area (Pichler and Mozaffari, 2015), Mo is therefore believed to either adsorbed to or scavenged with HFO or precipitated as powellite. Therefore, HFO and powellite could be considered as minor secondary sources for Mo released during the third step of the SEP. The adsorption of Mo onto HFO is a function of several chemical factors including Mo concentration in the solution, solution's pH, competing anion concentration, and Fe concentration in the aquifer matrix. It was demonstrated that Mo adsorption on Fe oxides was at its maximum at pH lower than 4 and 5 (Goldberg et al., 1996; Stollenwerk, 1998). The extraction of As in this step was much higher than Mo. Of the two naturally occurring forms of As (arsenite, As(III) and arsenate, As(V)), arsenate exhibited maximum sorption onto HFO at pH values of 4 while arsenite at pH range of 7 to 8.5 (Pierce and Moore, 1982; Qi and Pichler, 2014). Arsenate formed inner sphere surface complexes on amorphous iron oxides and showed very little ionic strength dependence as a function of the solution's pH. In contrast, arsenite formed outer sphere surface complexes with HFO and could be desorbed easier than arsenate into the environment (Goldberg and Johnston, 2001). This indicates that those As which were adsorbed on HFO and other sorbents could also be released in both steps 1 and 2 of the SEP as arsenite. The suitability of a wide range of pH for As adsorption, high affinity of As to adsorb on HFO, and low concentration of ions which have the potential to compete for surface sites, all imposed no limitation for As to be adsorbed in the study area. However, inadequate surface availability of HFO restricted As adsorption.

In step 4 of SEP, crystalline Mn as well as Fe oxides including goethite, lepidocrocite, pyrolusite, hematite, and other partially oxidized sulfide minerals and the degrading fraction of organic materials were all dissolved. A series of processes and reactions need to be taken into account to enable us to explain the encountered situation. First, Mo enrichment in oxic sediments were found to be attributed to its adsorption onto Mn and Fe oxides (Crusius et al., 1996; Goldberg et al., 2009). Under normal conditions at the time of sediment deposition, Mn refluxing has the potential to concentrate dissolved MoO_4^{2-} at the sediment-water interface. In cases where anoxia zone extends upward into the water column, Mn^{2+} is oxidized to particulate MnO_x (solid) just above the chemocline. The particulate Mn settled into the anoxic waters and re-dissolved Mn^{2+} diffused back through the chemocline, thus completing a redox cycle (Adelson et al., 2002). This type of Mo enrichment can be ruled out because the concentration of Mn in the aquifer matrix of the study area was shown to be too low (Pichler and Mozaffari, 2015). Secondly, Goldberg et al., (1996) found that Mo adsorption onto iron oxides was a function of pH, surface area, and the degree of crystal development. Maximum Mo adsorption happened at low pH of about 4 to 5. Adsorption decreased rapidly as pH increased from 5 to 8. Negligible adsorption occurred at pH above 8. Molybdenum adsorption increased in the order: hematite < goethite < amorphous Fe oxide < poorly crystalline goethite. Therefore, the relatively high Mo extractions in samples 10-11, 18-19, 69-70 and 75-76 can be associated with poorly crystalline to crystalline iron oxides (Fig. 3.2). Finally, the other possible sources for Mo in this step of the SEP are partially oxidized OM and sulfide minerals including pyrite.

With the exception of sample 10-11 (64% As removal), approximately 30% As was removed in step 4 (Fig. 3.3). The sorption of As on iron oxides depends on its oxidation state and the mineralogy of the iron oxides. It was found that at neutral pH, more than 80% As can be adsorbed onto hematite and goethite (Mamindy-Pajany et al., 2009). Arsenic (III) sorption on goethite decreased at neutral to alkaline pH ranges (Giménez et al., 2007). Maximum As adsorption on hematite took place at pH 4.2 (Singh et al., 1996). Arsenic (III) sorption on

magnetite increased to pH 9 and at higher pH its adsorption decreased (Giménez et al., 2007). All these considerations justified the relatively high As extraction rate in this step (Fig. 3.3).

As shown in Fig. 3.2., Mo extraction in step 5 of the SEP, which was released from sulfide minerals, OM and other possible sources, was low. Extraction of Mo and As in step 5 is related to the primary sources of these elements. Organic matter, and to a lesser extent pyrite, in karstified and fractured limestone could easily oxidize, degrade and shift the metals such as Mo and As to the weaker exchangeable and reducible phases. Therefore, the lower extraction rate of Mo in this step might be due to its lower OM content, because OM is oxidized and degraded easier than pyrite. This is supported with higher As extraction than Mo in this step, and it showed that pyrite is the main primary source of As in the Lithia area.

3.4. 2 Exchangeable phase of Mo and As

In Lithia area, each resident has its own water well. Thus, extensive groundwater pumping took place to meet the water demand for agriculture and drinking purposes. This may introduced oxygen-depleted water from the deep aquifer into the shallow aquifer and vice versa (Pichler et al., 2016). In addition, large fractures and karsts in the local limestone aquifers may enhanced infiltration of O_2 into the deeper groundwater environment. Oxidation of OM which could be the main primary source of Mo, mobilized and released Mo into the environment. But from the leaching experiment in the present study, it became clear that O_2 played no role in releasing loosely bound Mo and As (Fig. 3.4 and 3.5). Molybdenum and As which are released to the groundwater, may be adsorbed onto mineral surfaces such as clay minerals and/or co-precipitated with powellite and HFO (Pichler et al., 2001). The cation-exchange capacity of clay minerals is very high. These extremely high exchange capacities are due to the extremely large surfaces and electric charges of the surfaces. Mo removal from the solution occurs through a variety of mechanisms, including adsorption as outer-sphere and inner-sphere complexes, and precipitation as a secondary minerals (Goldberg et al., 1996). Outer-sphere adsorption is a weak electrostatic attraction between an ion and the surface.

Inner-sphere adsorption occurs through the formation of one or more chemical bonds between the surface and the adsorbate. Thus, Mo which is adsorbed as outer-sphere complexes, could be easily released into the environment. Considering the fact that carbonate is not a significant sorption site for Mo (Ferreiro et al., 1985), the competition between anions such as phosphate, arsenate, sulfate, and molybdate for the available sorption sites in Lithia area including HFO, clay minerals, and OM was the main reason for the existence of weakly bound Mo in the aquifer. Molybdenum and As could also be released from powellite dissolution. Electron microprobe analyses of powellite as a minor mineral in the Lithia area revealed that it contained up to 17,600 mg/kg or 42 wt% Mo (Pichler and Mozaffari, 2015).

3.5 Conclusions

Molybdenum and As were at elevated levels in the aquifer matrix of the study area in central Florida, USA. The presence of Mo as a very soluble form pointed to the anthropogenic disturbance of subsurface redox conditions which was caused by oxygenated surface water penetrating into the deeper aquifers. As a result, Mo was first transferred from the strong phase to the more labile form and was finally released into the groundwater system. Therefore, in most of the studied samples, up to 90% Mo was present in the adsorbed/exchangeable fraction (step 1) whereas relatively much lower Mo was removed during the other steps. Little Mo was extracted during the second and third steps of the SEP, which dissolve minerals like carbonates, HFO, and powellite. Crystalline iron oxides, pyrite and OM were dissolved in steps 4 and 5 and were responsible for a wide range of Mo extraction rates from 4 to 55%. Arsenic was distributed in different phases in the study area and its extraction was in somewhat similar abundances in different steps of the SEP. However, hydrous and crystalline iron oxides which dissolve in steps 3 and 4 of the SEP contained the highest As concentrations.

A considerable amount of Mo (50 to 90%) was removed from the aquifer matrix by dissolving the relevant samples in DDI water and groundwater. Mo extraction increased with increasing contact time and reached equilibrium after 48 h. The amount extracted with both solutions were almost the same after 48 h, showing that dissolved oxygen played no role in the release of Mo and As from the aquifer matrix.

Chapter 4. Primary sources of molybdenum and arsenic

Abstract

In this chapter we explain how the chromium-reducible sulfur (CRS) method was used to determine the relationship between reduced sulfur including pyritic sulfur and organic sulfur (OS), molybdenum (Mo) and arsenic (As) concentrations in marine sediments in the Lithia area and Avon Park Formation (APF) in Central Florida. A total of 24 samples -including 10 samples which were already subjected to the sequential extraction procedure (SEP) analysis (Chapter 3)- were chosen from Lithia area and APF, and were analyzed by the CRS technique. The samples were chosen based on the following four criteria: (1) high total Mo concentration, (2) high total As concentration, (3) high total sulfur (S) concentration, and (4) good geographic representation of the study area. In order to remove all other types of sulfur, the samples were first dissolved in acetone. The residues of the samples were then dissolved in 0.5 M hydroxylamine hydrochloride in 0.25 M HCl (step 3 of the SEP) to remove any possible secondary source of Mo and As. After washing the residue of the samples for three times with distilled deionized (DDI) water, they were dissolved in an acidic chromium (II) solution. The H_2S which was evolved from the samples was transferred via N_2 carrier into 30 mL of 3% zinc acetate with 10% NH_4OH and trapped as ZnS for quantification by iodometric titration. After chromium reduction, the residues were washed three times with water, filtered and dried in a desiccator and were finally analyzed for Mo, As, and sulfur concentration by inductively coupled plasma–optical emission spectrometer (ICP-OES).

Groundwater and DDI water samples were added to a small amount of powellite which was already mixed with sample R13 1090 (Mo and As free sample) to assess the behavior of powellite in the natural environment. The content was shaken in a mechanical shaker at room temperature for 1, 5, 10, 24, and 48 hours at pH 5, 6, 7, and 8 hours. Finally, the samples were centrifuged and the extracts were analyzed for Mo and As by ICP-OES.

Pyrite, which is present in the matrix of the aquifer underlying Lithia area and in the APF, is generally regarded as a source of Mo and As. However, the results of CRS did not confirm the presence of Mo in pyrite, though it was shown to exist as a minor constituent in the APF. The total organic carbon content in the residues of CRS (OC_{res}) showed a positive correlation with Mo ($R^2 = 0.71$ and $p < 0.001$). However, no correlation was found between OS and Mo. The concentration of As in pyrite was much higher as compared to Mo, pointing to pyrite as a major primary source for As in the aquifer matrix. There was a weak correlation between As and OC_{res}. The results suggested that the primary source of Mo found in the aquifer matrix and groundwater is mainly related to organic matter (OM) rather than pyrite, whereas As originated mainly from pyrite as a primary source as well as from iron oxides in the adsorbed forms. Powellite could only be considered as a minor secondary source for Mo and As.

4.1 Introduction

Molybdenum is a trace constituent of the upper crust, with an average abundance of 1 to 2 mg/kg (Taylor and McLennan, 1985). Geochemically, it is relatively unreactive in oxygenated, aqueous solutions, and hence it is a nominally conservative element in the oceans. In fact, Mo is removed so slowly from the seawater that it is considered as the most abundant transition metal in the oceans despite being a ppm-level constituent of the crust. In oxic environment, manganese (Mn) redox cycling has the potential to preconcentrate MoO_4^{2-} at the sediment-water interface (Adelson et al., 2002). Molybdenum may be adsorbed onto Mn and iron (Fe) oxyhydroxides (Chappaz et al., 2014; Crusius et al., 1996; Dahl et al., 2013; Zheng et al., 2000). Its adsorption to aluminum (Al) and Fe oxides extends from pH 3 to 8 (Goldberg et al., 2009; Gustafsson, 2003; Stollenwerk, 1998). In contrast, Mo is readily removed from the solution in anoxic-sulfidic settings, so that Mo enrichment in sediments is considered diagnostic of reducing depositional conditions. Molybdenum has two major primary sources in

anoxic-sulfidic environment namely pyrite and OM (Bertine and Turekian, 1973; Chappaz et al., 2014; Crusius et al., 1996; Das and Jim Hendry, 2013). Pyrite and OM have high capability to fix Mo from seawater and retain it during the digenesis stages of sedimentary rocks (Adelson et al., 2002; Dahl et al., 2013; Helz et al., 2011; Tribovillard et al., 2008; Tribovillard et al., 2004). Recently, a case study that used laser ablation-inductively coupled-plasma mass spectrometry (LA-ICP-MS), showed that pyrite from six different locations of modern and ancient sediments is not the dominant host for Mo (Chappaz et al., 2014). In contrast to pyrite, a clear relationship was found between Mo and OM for five of the same six locations which were studied. Although, OM is regarded as the main host for Mo in anoxic/sulfidic sediments, the relevant processes through which OM adsorbs Mo are not well understood as yet (Glass et al., 2013; Lyons et al., 2003; Meng et al., 2000). The sulfidation of OM reduces lability and enhances the preservation of OM (Tribovillard et al., 2004; Werne et al., 2008). According to Adelson et al., (2001), the organic thiomolybdates are presumed to be formed through replacement of oxygen in the first coordination sphere of Mo by macromolecular S, thereby producing covalent S bridges between Mo and the sulfurized macromolecules. This assumption was proved by studying six Mesozoic geological formations which underwent anoxic/sulfidic conditions during the deposition (Tribovillard et al., 2004).

Arsenic is an element that occurs naturally in the sedimentary rocks including shales, clays, phosphate rocks, as well as sedimentary Fe and Mn oxides (Couture et al., 2013; Kinniburgh et al., 2006; Lenoble et al., 2002; Peterson and Carpenter, 1986; Shimp et al., 1971; Wang et al., 2006). In nonmarine clays and shales, As is more enriched in clay minerals (Kinniburgh et al., 2006; Lenoble et al., 2002), whereas a substantial proportion of the As in offshore marine sediments is present as pyrite (Yudovich and Ketris, 2005). Couture et al., (2013) found a correlation between As and OM in sedimentary rocks. A similar correlation was found by Shimp et al., (1971) for unconsolidated sediments of Lake Michigan.

In this study, the CRS method was applied to 24 samples to determine the relationship between Mo, and sulfurized OM, and pyrite. Before applying this technique, all secondary Mo sources including powellite (as a secondary mineral), and Mo adsorbed onto clay minerals, manganese and iron oxyhydroxides were removed from the samples. This was done by dissolving the samples in acetone, followed by dissolving the residues instep 3 of the SEP. In order to determine the role of powellite as a source for Mo, a small quantity of powellite already mixed with one -Mo and As free- sample (sample R13 1090), was dissolved in groundwater and DDI water and was shaken for 1, 5, 10, 24, and 48 hours at pH 5, 6, 7, and 8.

4.2 Materials and methods

4.2.1 Selection and preparation of samples for CRS method

The CRS is a well-known method for the determination of reduced inorganic sulfur and OS compounds in modern and ancient sediments. With this method, it is possible to quantify both pyritic sulfur and organic sulfur and uncover their relationships with Mo and As. The CRS method was applied to 24 samples of the aquifer matrix samples -including 10 samples which were already subjected to sequential extraction procedure analysis in Chapter 3- from Lithia area and APF. Lithia area samples included DEP-1, DEP-2 and DEP-5 cores. The samples were chosen based on the following four criteria: (1) high total Mo concentration, (2) high total As concentration, (3) high total sulfur concentration, and (4) good geographic representation of the study area. These experiments were conducted to investigate the role of sulfurized OM, OM and pyrite in serving as hosts for Mo and As in the sedimentary rocks. Before using the CRS method, elemental sulfur, powellite as a secondary mineral and all those Mos which were adsorbed on various sorbents such as clay minerals, Fe and Mn oxides were removed. The following steps were carried out to achieve this:

1. In order to obtain the total elemental composition of samples, 50 mg of each sample was digested in the Milestone Ethos system with a microwave power of 1000 W and temperature control.

2. Elemental sulfur was extracted with acetone. About 75 mL acetone were added to 3 g of sediment and shaken for 4 h at room temperature in a mechanical shaker operating at 250 RPM. The produced extract was separated from the solid residue by centrifuging at 4000 RPM for 20 min. The supernatant was then decanted into a 100 mL Erlenmeyer flask and prepared for chemical analyses. To wash the residues, they were suspended in 5 mL DDI water, centrifuged, and the supernatant was discarded thereafter.

3. The residues of acetone extraction were oven-dried at 40° C and powdered with an agate mortar and pestle that was cleaned with pure quartz sand and rinsed with DDI water between consequential samples to prevent cross contamination. An electronic scale was used to weigh 2 g of the powdered sample which was subsequently poured into a 50 mL screw cap centrifuge tube. Thereafter, 40 mL of freshly prepared hydroxylamine hydrochloride and 0.5 M in 0.25 M HCl (Step 3 of the SEP) were added to the centrifuge tube. The samples were then placed in a hot block at 60°C for 2 h with the cap loosened. At every 30 min interval the cap was tightly closed and the contents were shaken. In the subsequent step, the samples were centrifuged and the extracts were separated as described earlier. By adopting this procedure, powellite and the adsorption forms of Mo and As were removed from the samples.

4.2.2 Chromium-reducible sulfur method

To prepare the Cr(II) solution, first a glass bottle with two outlets was filled with Zn-shot to about one-tenth full (Fig. 4.1). Then, 2 M $CrCl_3.6H_2O$ which was prepared with 0.5 M HCl, was slowly added to the Zn-shot, that is, 20 g of Zn-shot per 100 mL of acidic Cr(III) solution (Burton et al., 2008; Manning and Goldberg, 1996; Mohan and Pittman Jr, 2007). The screw cap of the bottle was not firmly tightened to allow releasing excess pressure from the pyrex bottle. A tube

was attached to one of the outlets for air gas (N_2) and the other outlet was sealed for removing Cr(II) solution from the glass bottle. For a period of 2 to 3 h, Cr(III) was completely reduced to Cr(II), until a clear bright blue color appeared (Fig. 4.1)..

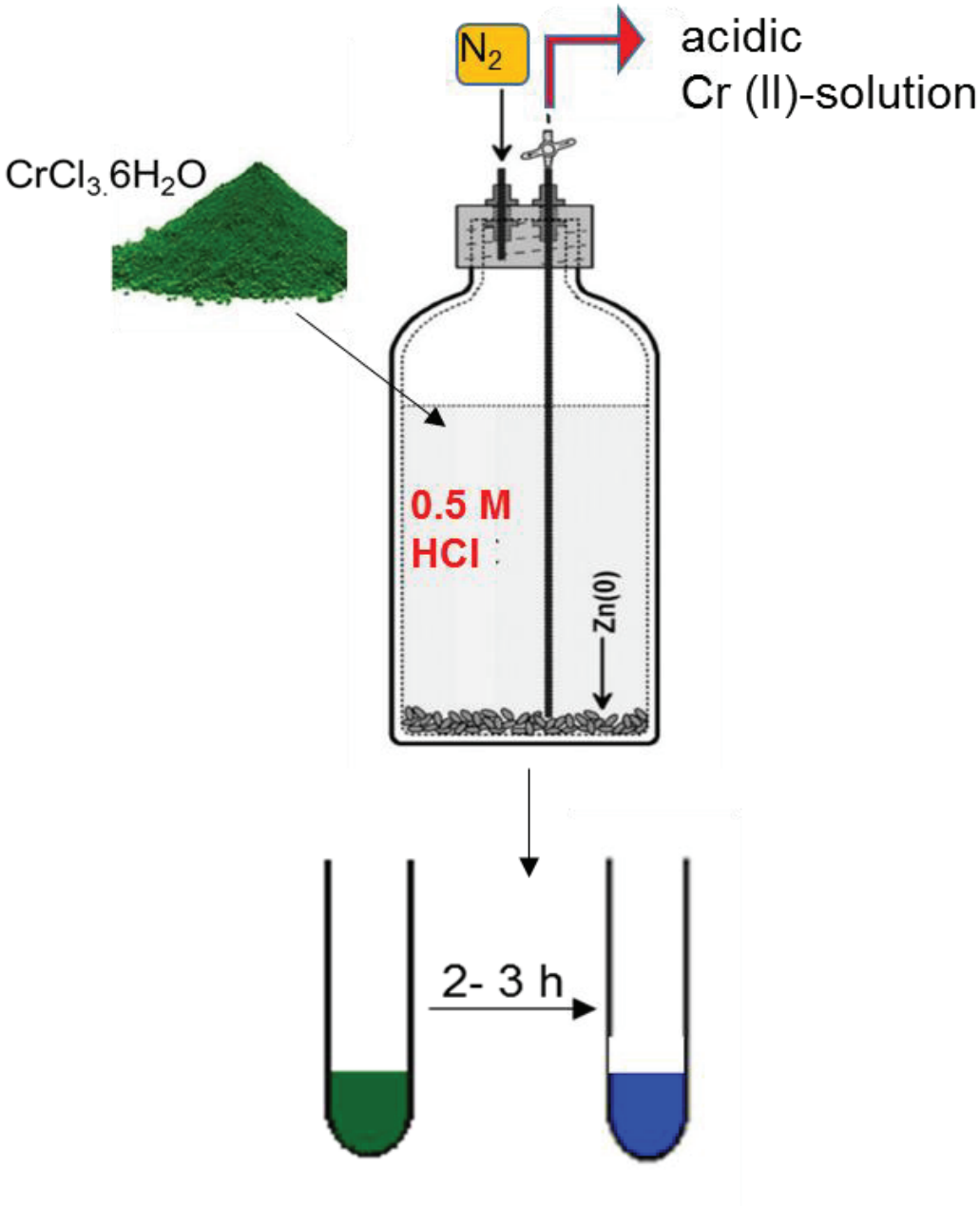

Fig. 4.1. Apparatus for preparation of the acidic Cr (II) solution used for extraction in the CRS method (modified after Borton et al., 2008).

Pyritic sulfur (S_{pyr}) was extracted from the samples using the method described by Canfield et al., (1986). The residues of step 3 of the SEP were washed 3 times with DDI water and oven-dried at 40° C, and powdered by an agate mortar and pestle which were cleaned as described earlier. One gram of powdered sample was transferred to a 100 mL Erlenmeyer flask and stirred to disaggregate any large clumps. Ten mL ethanol were added to the sample, and attached to a trapping vessel which contained 30 mL of a 3% m/v zinc acetate (Fig. 4.2). The system was flushed with N_2, and a plastic syringe was used to add 40 mL Cr(II) solution and 20 mL concentrated HCl to each flask. As the ethanol solution was purged with N_2, the reagent mixture was added to the flask. About 2 h contact period was needed to liberate pyritic sulfur, and trap it as H_2S in the Zn-acetate trapping vessel.

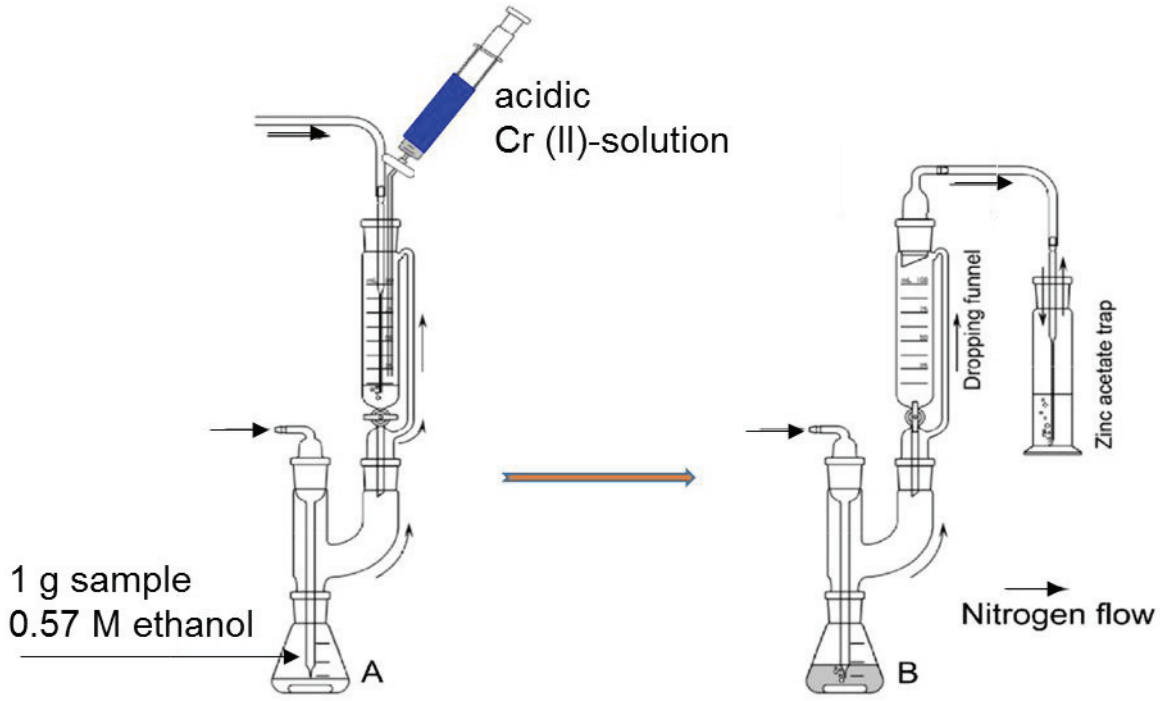

Figure 4.2. Apparatus used in the CRS method: (A) Purging acidic Cr (II) solution and ethanol to the sample, (B) Release of sulfur from the solution and transferring it to the zinc acetate trapping vessel (modified after Gröger et al., 2009).

4.2.3 Quantification of CRS

The trapped sulfide was quantified by iodometric titration. The reverse titration of the excess iodine was conducted with a thiosulfate solution following the procedure described by Burton et al., (2008). The residues of the Cr(II) reduction precipitates were washed with DDI water for 5 times. This residue contained only OS because sulfate salts, pore water sulfur, elemental S, polysulphide, acid-volatile sulfides and pyritic sulfur were all removed during the course of acetone extraction, step 3 of the SEP, and the CRS method.

A total of 50 mg of each sample, before and after applying CRS, was weighted to measure the total content of the elements in pyrite. The sulfur content in the sample after applying CRS is abbreviated as OS and the difference between two measurements (before and after applying CRS) yields pyritic sulfur. A digestion system (Milestone Ethos) with a microwave power of 1000 W and temperature control, was used to digest the sediments. After digestion, elemental analysis was carried out by inductively coupled plasma–optical emission spectrometer (ICP-OES).

4.2.4 Powellite

Powellite was freshly prepared as described earlier in Chapter 3 (Wasay et al., 1996). In order to evaluate the powellite dissolution, an appropriate amount of powellite was added to 1 g of a Mo free aquifer matrix sample and allowed to dissolve with the groundwater and DDI water samples. The samples were shaken for 1, 5, 10, 24, and 48 hours and subsequently centrifuged and analyzed for Mo and As. To assess the impact of pH on the behavior of powellite, the pH of four samples were adjusted to 5, 6, 7, and 8 by adding HNO_3 or NaOH and the samples were shaken for 48 h.

4.3 Results

4.3.1 Chromium reduction sulfur results

The concentration of pyritic sulfur (S_{pyr}) was determined by two different approaches: (1) the difference between sulfur content in the samples before and after CRS method and (2) directly by titration. The results of both methods were in good agreement. Compared to the Lithia area samples, those from APF contained lower S_{pyr}. The concentration of S_{pyr} was highest in core DEP-5 at depth 67 to 68 m (Table 4.1). Sample R-20 with 11.6 mg/kg Mo, contained the highest Mo concentration in pyrite. With the exception of samples 46-47 and 70-71, no Mo was released from pyrite in Lithia. In contrast to Mo, the concentrations of As in pyrite were much higher. Among all 21 samples of the Lithia Area and APF, only sample DEP-5 from the depth of 73-74 m had no As in pyrite. For the rest of the samples, the concentrations of As in pyrite ranged from 0.9 to 27.5 mg/kg. Some samples contained significant amounts of organic carbon (C_{org}), with a maximum of 1.55% in sample 70-71. The concentration of OS compounds -which were isolated in the residue of pyrite extracted samples- ranged from 111.7 to 14153 mg/kg (Table 4.1). The concentration and percentage of Mo and As in pyrite is illustrated in Figs 4.3 and 4.4.

Table 4.1 Geochemical data of CRS.

Core	Sample	S_T	$S(Titr)_{Pyr}$	$S(Titr)_{Pyr}$	OS_{res}	OS_{res}	TOC_{res}	Mo_T	Mo_{Pyr}	Mo_{res}	Mo_{Pyr}	Mo_{res}	As_T	As_{Pyr}	As_{res}	As_{Pyr}	As_{res}
		mg/kg	mg/kg	%	mg/kg	%	%	mg/kg	mg/kg	mg/kg	%	%	mg/kg	mg/kg	mg/kg	%	%
DEP-1	**45-46**	1037	250	24.1	129	12.4	0.19	121.7	n.d.	1.9	n.d.	1.5	29.7	7.8	0.9	26.3	3.2
DEP-1	**46-47**	1431	17	1.2	253	17.7	1.40	825.1	10.7	155.0	1.3	18.8	143.9	8.4	16.5	5.8	11.4
DEP-1	**70-71**	30126	4650	15.4	12601	41.8	1.55	499.0	8.6	74.5	3.7	31.7	132.0	32.0	0.1	34.9	0.5
DEP-2	**10-11**	2650	1400	52.8	250	17.8	0.17	25.0	n.d.	n.d.	n.d.	n.d.	28.8	16.5	1.7	57.1	5.7
DEP-2	**18-19**	4464	88	2.0	1071	24.0	0.29	38.4	n.d.	n.d.	n.d.	n.d.	17.8	6.8	1.2	38.2	6.5
DEP-2	**31-32**	559	219	39.1	155	27.7	0.15	53.3	n.d.	n.d.	n.d.	n.d.	9.3	4.0	0.0	42.0	0.0
DEP-2	**42-43**	904	323	35.7	185	20.5	0.22	77.7	n.d.	n.d.	n.d.	n.d.	19.8	7.1	4.0	35.6	20.0
DEP-2	**63-64**	12168	2987	24.5	1922	15.8	0.10	17.0	n.d.	n.d.	n.d.	n.d.	40.9	16.0	4.7	39.1	11.5
DEP-5	**48-49**	5353	2356	44.0	695	13.0	0.30	202.1	n.d.	8.0	n.d.	4.0	77.4	13.0	3.0	16.8	3.9
DEP-5	**50-51**	2696	327	12.1	566	21.0	0.43	35.9	n.d.	n.d.	n.d.	n.d.	29.8	6.5	1.5	21.9	5.1
DEP-5	**67-68**	77158	5895	7.6	14153	18.3	0.21	21.0	n.d.	n.d.	n.d.	n.d.	123.3	27.5	17.5	22.3	14.2
DEP-5	**69-70**	8996	3450	38.3	1633	18.1	0.19	29.9	n.d.	n.d.	n.d.	n.d.	59.9	19.0	10.6	12.4	17.6
DEP-5	**72-73**	528	123	23.3	190	36.0	0.11	6.8	n.d.	n.d.	n.d.	n.d.	5.7	1.4	0.0	24.0	0.0
DEP-5	**73-74**	690	65	9.4	112	16.2	0.16	111.8	n.d.	n.d.	n.d.	n.d.	24.7	n.d.	n.d.	n.d.	n.d.
DEP-5	**75-76**	8701	2345	26.9	1891	21.7	0.12	135.6	2.4	5.3	1.8	3.9	52.3	12.0	3.9	8.1	7.4
R-13	**452**	4835	300	6.2	1514	31.3	0.20	638.9	3.5	51.0	0.5	8.0	131.7	0.9	11.6	0.6	8.8
R-20	**406**	2790	2150	77.1	898	50.0	1.01	328.5	11.6	110.5	3.5	33.6	27.5	14.7	0.0	53.5	0.0
R-20	**407**	1692	27	1.6	717	42.4	1.14	104.3	1.1	50.0	1.1	47.9	10.1	7.9	n.d.	79.0	n.d.
R-28	**374**	5349	45	0.8	384	7.2	0.35	117.5	5.0	17.4	4.2	14.8	18.3	4.6	1.9	25.0	10.6
R-39	**305**	5496	1300	23.7	1011	18.4	0.45	179.3	3.5	10.6	2.0	5.9	30.4	10.0	5.2	16.4	17.2
TR-2	**236**	2628	564	21.5	512	19.5	0.12	151.5	4.2	7.7	2.8	5.1	11.0	6.6	n.d.	59.7	n.d.

S_T represent Total sulfur in the sample; S_{py} the Sulfur determined by CRS and OS_{res} the organic sulfur; the same for Mo, As and OC. n.d. = not detected.

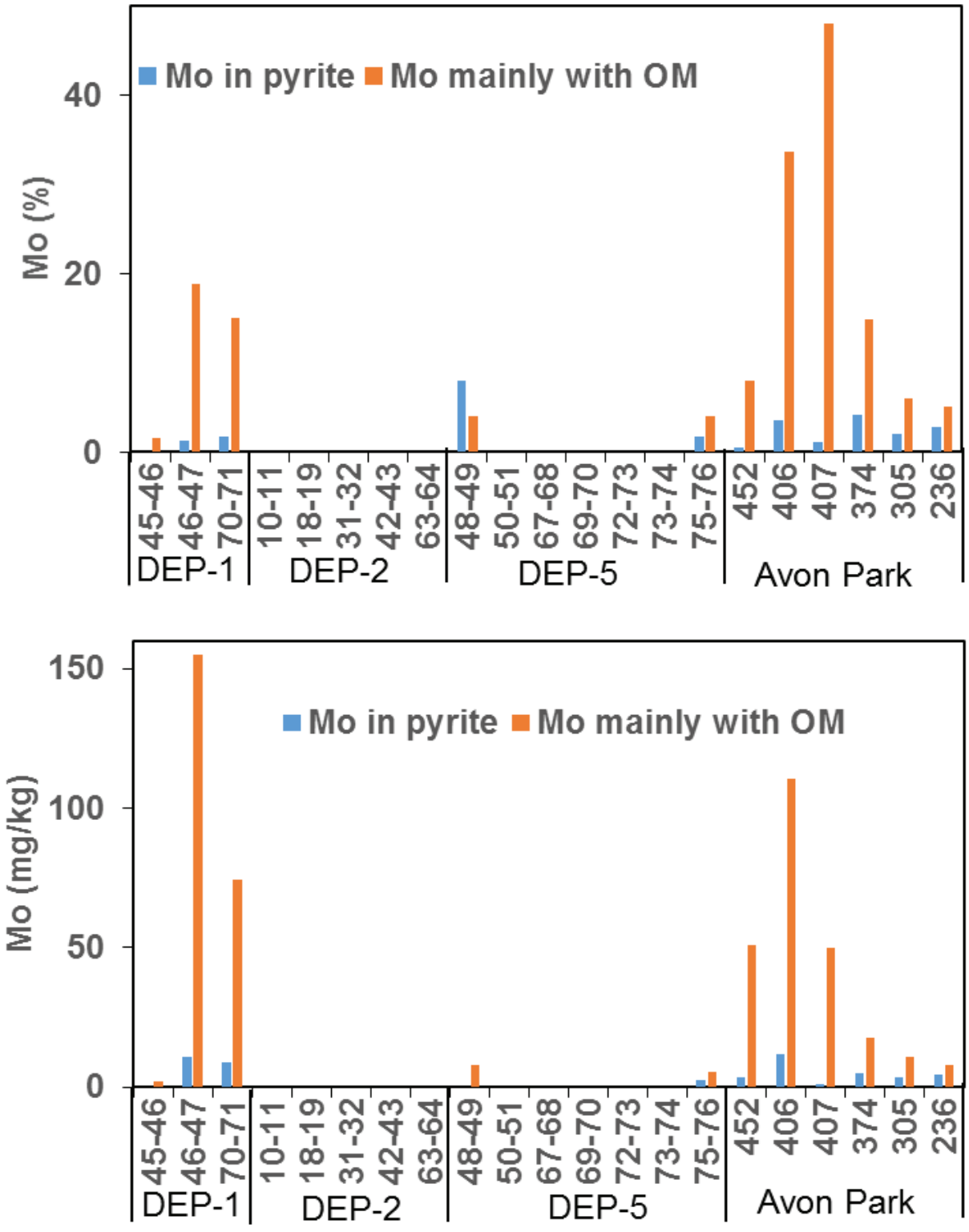

Fig.4.3 Percentage and concentration of Mo in pyrite and in Cr (Ⅱ) residue.

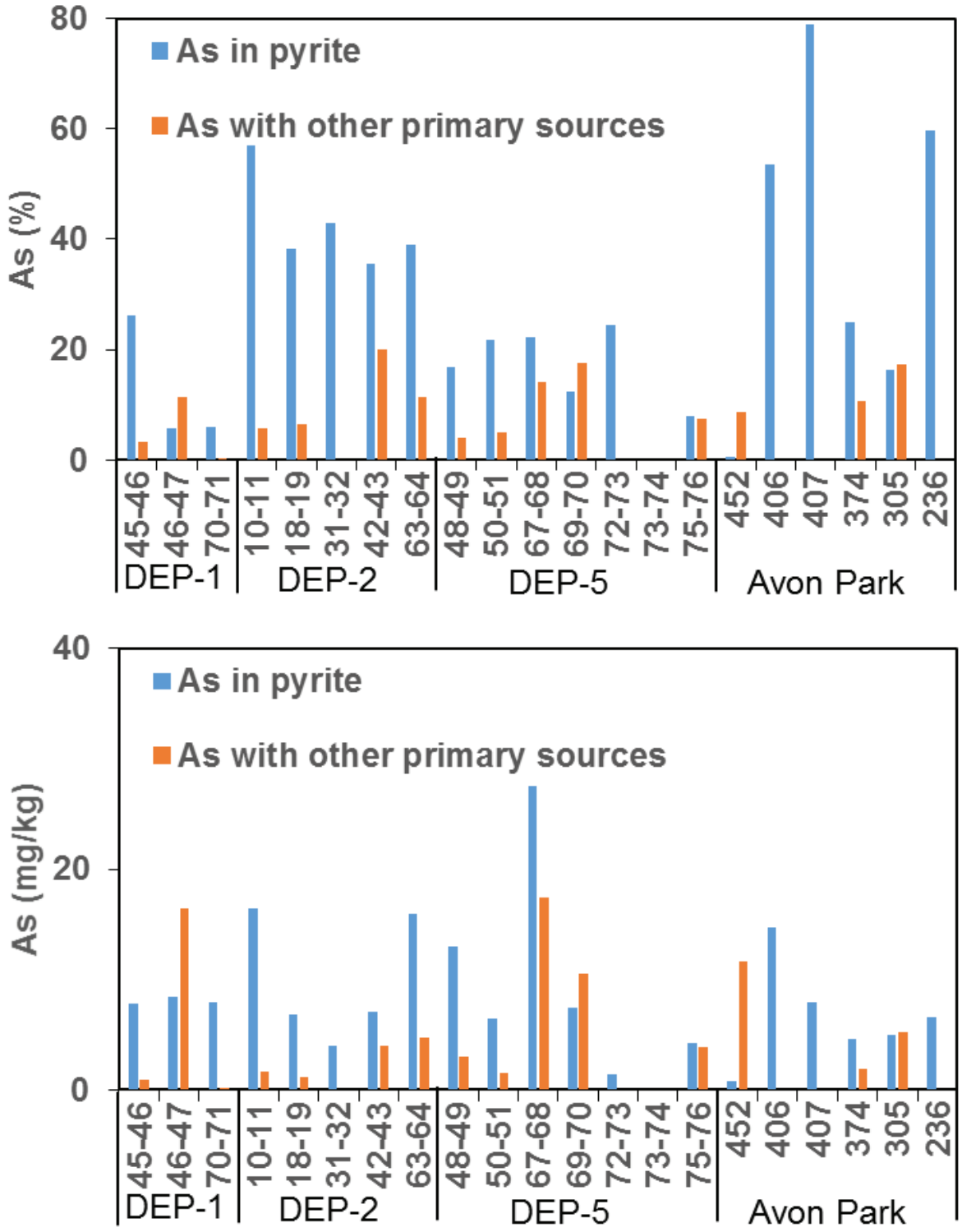

Fig.4.4 Percentage and concentration of As in pyrite and in Cr (Ⅱ) residue.

4.3.2 Comparing the results obtained by CRS method with SEP

Neither the adsorption form nor the secondary and co-precipitated minerals including HFO and powellite were considered as the primary sources of Mo and As. One way to remove these fractions from the aquifer matrix samples is to apply the first three steps of the SEP (Chapter 3) on the samples. The other approach which was used in this study was to dissolve the samples in acetone (Canfield et al., 1986; Passier et al., 1999) followed by step 3 of the SEP. To test and validate this procedure, the results obtained by applying the first three steps of the SEP were compared with those obtained when acetone and the step 3 of the SEP was applied. The amounts of Mo and As extracted in steps 4 and 5 of the SEP must also be comparable with those extracted with CRS method and the element content in the residue of the CRS method. Fig.4.5 shows that the results of the two techniques were in good agreement for Mo (Figure 4.5A) but differed for As (Figure 4.5 B); the amount of As extracted in steps 4 and 5 of the SEP was lower than the amount extracted by the CRS method and the residue of the CRS method.

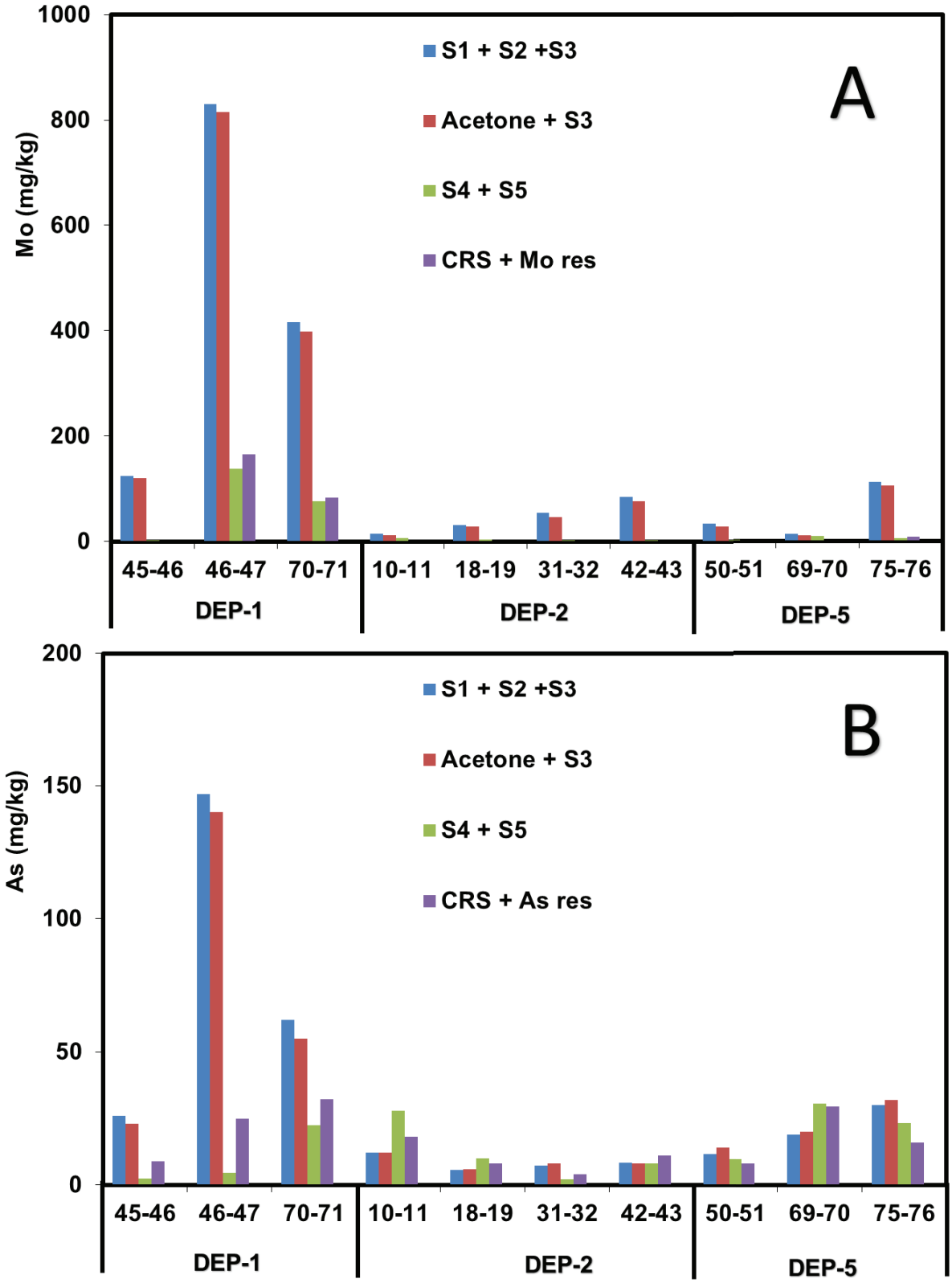

Fig. 4.5 Comparison of the results obtained by the CRS method and the SEP.

4.3.3 Dissolving the synthesized powellite in groundwater and DDI water

The results of powellite dissolution in groundwater and DDI water at different periods and at different pH ranges are shown in Fig. 4.6. The maximum amount of Mo mobilized from powellite was 0.7% of the total Mo content of the sample. Molybdenum dissolution at pH 5 and 6 was 0.8% and 0.85%, respectively. At pH 7 and 8, no Mo was released from powellite.

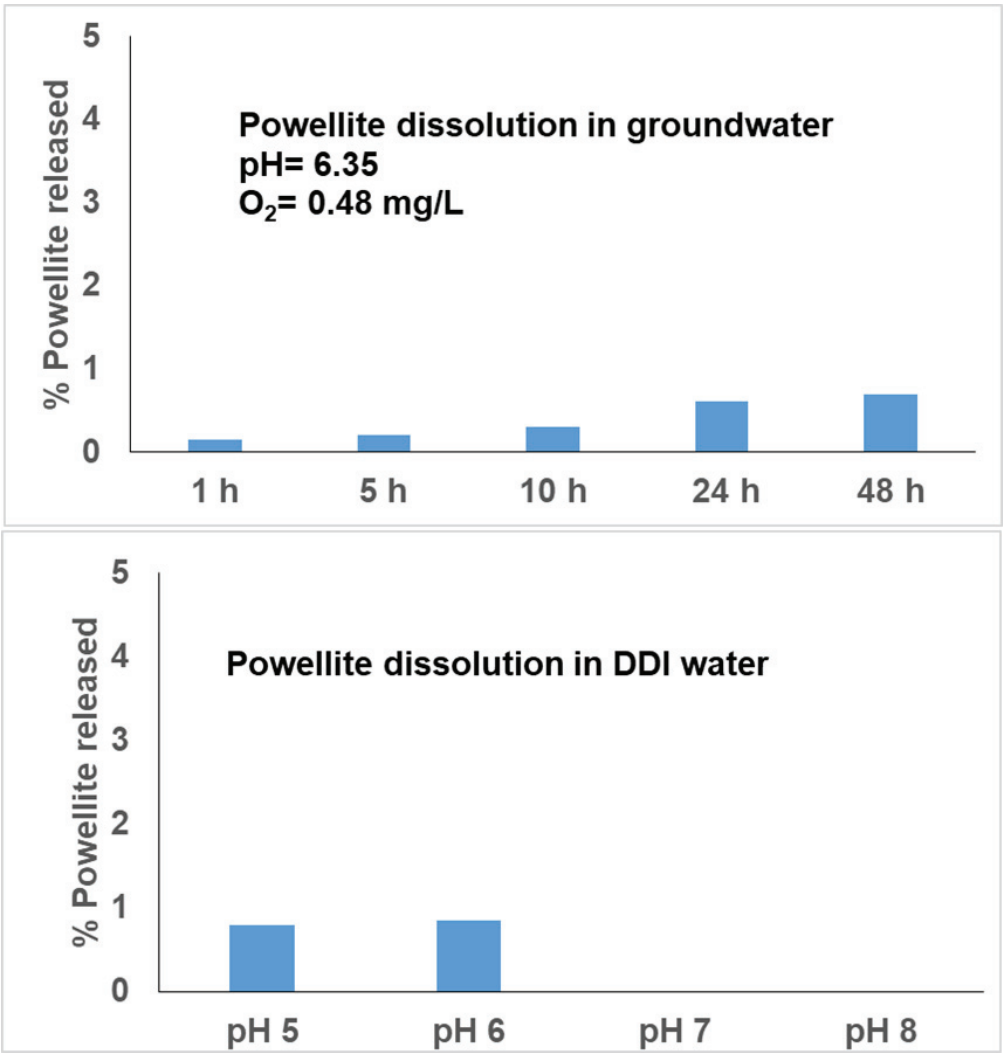

Fig. 4.6 Percentage of Mo released from powellite during reaction with groundwater and DDI water.

4.4 Discussion

4.4.1 Possible sources of Mo and As in sedimentary rocks

In total, three different sources could be considered for Mo and As in the aquifer matrix, which include OM, pyrite and powellite. Among these sources, pyrite and OM were considered as the main primary sources. In sulfidic environment, pyrite and OM have the capability to fix Mo from seawater and retain it over geological time scales (Chappaz et al., 2014; Tribovillard et al., 2004). The enrichment of Mo in sediments by pyrite and OM can be described by three models:

1. Manganese plays a crucial role in the first model. Its redox cycling has the potential to concentrate MoO_4^{2-} at the sediment-water interface. In cases where anoxia zone extends upward into the water column, Mn^{2+} is oxidized to particulate MnO_x (solid) immediately above the chemoline. The particulate Mn settles into the anoxic waters and redissolved Mn^{2+} diffuses back through the chemocline, thus completing a redox cycle (Adelson et al., 2002; Helz et al., 1996). Concentrated MoO_4^{2-} at the water-sediment interface could be fixed by OM and/or pyrite.

2. In a reducing environment, Mo is first co-precipitated as Fe-Mo-S, leading to the formation of $Fe_5Mo_3S_{14}$ in the water column. After Mo is reduced in the water-sediment interface, it is fixed by OM and pyrite (Chappaz et al., 2014). Chappaz et al., (2014) proved that OM, compared to pyrite, is the dominant source for Mo in sedimentary rocks.

3. Helz et al., (1996) introduced the concept of “geochemical switch”, through which dissolved sulfide transforms Mo from a largely conservative element to a particle-reactive species in marine depositional environments. According to Erickson and Helz (2000) a key step in this pathway is the reaction: $MoO_4^{2-} \rightarrow$thiomolybdates ($MoO_xS_4^{-x}$, x=0–3), which is particle reactive and thus prone to scavenging. The sulfide activation of the switch depends on $\sum H_2S$ activity

(Erickson and Helz, 2000; Helz et al., 2004; Zheng et al., 2000). Because each successive sulfidation reaction is about one order of magnitude slower than the previous one, dithio -→ trithio - and trithio → tetra - thiomolybdate equilibria might not be achieved in the seasonally or intermittently sulfidic waters (Erickson and Helz, 2000). Therefore, sulfidic conditions seem to be required. Of the three possible primary sources for Mo, pyrite and OM are more effective in fixing Mo from seawater at the time of sediment deposition. There was no evidence to show that Mo is co-precipitated with Mn in the study area. The Mn concentrations were rather low with more or less uniform distribution throughout the study area with median values of 24, 37 and 34 mg/kg for Cores DEP-1, DEP-2 and DEP-5, respectively. The possible explanation is that the physicochemical conditions in the sedimentary environment did not change sufficiently.

Compared to Mo, the main primary host for As in sedimentary rocks is pyrite. Under reducing conditions, As can be sequestered by co-precipitation with, or adsorption onto Fe sulfides such as, pyrite and mackinawite (Wolthers et al., 2005). In OM-rich sediments, organic substances compete with reactive iron for incorporating the reduced sulfur of the sediments. In cases where the amount of reactive iron is limited, bisulfide concentrations in the pore waters increase, and OM is believed to become a significant sink for reduced sulfur. Under these conditions, sulfurization of OM plays an important role in the formation of thiol-bound with As (Couture et al., 2013).

4.4.2 Pyrite

Although pyrite is regarded as one of the two main sources of Mo in the marine environment (Chappaz et al., 2014; Lyons et al., 2003), the concentration of Mo in pyrite was too low in the study area (Fig. 4.3). None of the samples of DEP-2 and DEP-5 contained any Mo in pyrite. Among the APF samples, sample R-20, and among the DEP samples, sample 46-47 contained the highest Mo concentration in pyrite (11.6 and 10.7 mg/kg receptively). DEP-2, which is located in the central part of the area with the highest groundwater pumping rate (Pichler et

al., 2016), underwent more anthropogenic perturbation compared other wells. Therefore, a change in the physico-chemical condition could be a reason for mobilization of Mo from pyrite. Also, the pyrite minerals in DEP-5 core -which was drilled at a far distance as a reference well- contained no Mo. This clearly indicated that pyrite could not be a significant primary source for Mo. This finding is in excellent agreement with the results reported by Pichler and Mozaffari (2015). They found no Mo in the selected pyrite minerals using microprobe analysis. Chappaz et al., (2014) showed that pyrite acts as a minor source for Mo in marine environments. Similarly, Tribovillard et al., (2004), argued that pyrite in the marine environment acts as an initial trap for Mo, while Mo may be remobilized from pyrite during digenesis. A report compiling published data of Mo, pyrite, and total organic carbon (TOC) concentrations for six study sites clearly showed a better correlation between Mo-TOC than between Mo-pyrite in 5 of the sites (Chappaz et al., 2014; Dahl et al., 2013; Tribovillard et al., 2004; Zheng et al., 2000).

It is well known that pyrite is the main primary source for As in the sediments and sedimentary rocks. The As content in the aquifer matrix and its fraction in pyrite are shown in Fig. 4.4. These results showed that the main origin of As in the aquifer matrix was pyrite. A clear positive correlation ($R^2 = 0.85$ and $p < 0.002$) was observed between As enrichment in pyrite and the sulfur extracted by the CRS method (Fig. 4.7). Pichler and Mozaffari (2015) found highly varying concentrations of As in pyrite ranging from approximately 200 to 9000 mg/kg. Assuming that pyrite is the source of As, four scenarios needed to be considered to explain the high concentrations of As. Each of these scenarios involves a change of hydraulic conditions in the Lithia area, causing the rapid introduction of oxygenated groundwater into the Upper Floridan aquifer where most of the supply wells are screened:

1. The removal of clays during the phosphate mining process in a location to the east of the Lithia area, which is hydraulically up gradient of the site, allowed water with different geochemical characteristics from the ambient surface/surficial aquifer to flow into the deeper aquifer.

2. Water from a gypsum stack which is associated with a former phosphate plant is drained into a creek that straddles the up gradient extent of the site. This creek may be a surface reflection of a fracture that allows drainage water with different characteristics to flow quickly into the deeper aquifer.

3. The extensive pumping from the well field that is located on the western portion of the study site significantly altered the hydraulic head between surficial/intermediate aquifer and the underlying Floridan aquifer providing more potential for waters from the shallow intervals to flow into the deeper aquifer.

4. There could be a combination of one or more of the aforementioned scenarios.

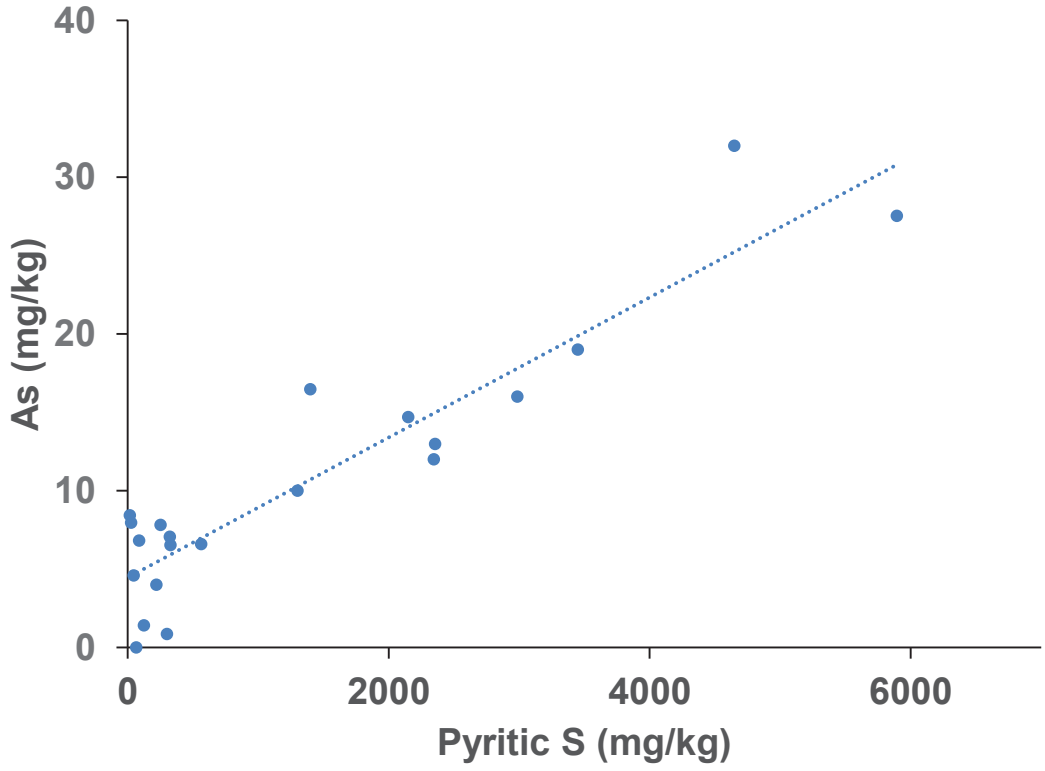

Fig. 4.7 Correlation between As concentration in pyrite and sulfur extracted by the CRS method.

4.4.3 Organic matter

If the role of pyrite as a sink for Mo does not explain most of the data obtained through this research, then some other alternative pathways for Mo burial in euxinic settings must be proposed. It is well known that Mo may be enriched in the sediments by incorporating into OM (Adelson et al., 2002; Chappaz et al., 2014; Crusius et al., 1996; Dahl et al., 2010; Tribovillard et al., 2008; Vorlicek, 2004; Werne et al., 2008; Wilde et al., 2004; Zheng et al., 2000). In the present case, a statistically significant correlation (R^2 = 0.71 and $p < 0.001$) was observed between Mo and OC_{res} (Fig. 4.8), which suggested that OC_{res} was a major primary source for Mo. Tribovillard et al., (2004) argued that sulfurized OM has a great capability to incorporate Mo and retain it over a geological time scale as well as during digenesis. However, no correlation was found between Mo and organic sulfur which indicated that sulfurized OM played no role to enhance the trapping of Mo at the time of sediment formation. There were no significant relationships between As, OC_{res} and OS. This indicated that OM and its sulfurized form did not insert significant impact on the groundwater quality with respect to As.

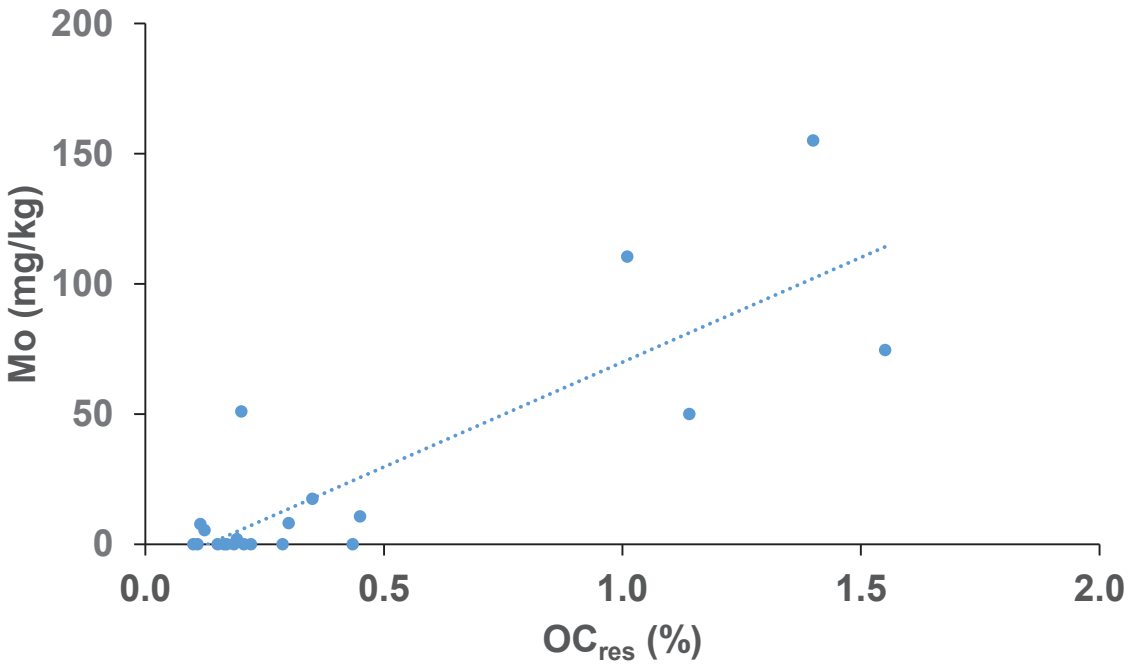

Fig. 4.8 Correlation between Mo concentration in the residue of the CRS and the OC_{res}.

4.4.4 Powellite

Molybdenum and As could be released by powellite dissolution. Based on the average of 5 Electron microprobe analyses of powellite, its chemical composition (by mass) was approximately 21% Ca, 42% Mo and 1.76% As, while other elements were less than 0.2% (Pichler and Mozaffari, 2015). Results from geochemical modeling showed that powellite was supersaturated and the precipitation of powellite in the alkaline pH range was likely when Mo concentration reached 3250 µg/L in the groundwater sample of Lithia area. On the other hand, dissolution of the synthesized powellite in DDI water and the groundwater sample of Bremen demonstrated that only minor amounts of powellite could be released in the natural system (Fig.4.6). Hence, neither precipitation nor dissolution of powellite is likely to happen at a considerable rate in the Lithia area and consequently powellite was regarded as a minor sink for Mo and As, if any.

4.5 Conclusions

The results obtained by applying steps 4 and 5 of the SEP in Chapter 3 which were considered to be related to the primary sources of Mo and As including OM and pyrite were found to be in good agreement with the CRS results. The positive correlation between OC and Mo in the residues of CRS, with little Mo in pyrite, proved that OM was the main primary source for Mo. Organic sulfur which was assumed to have a substantial ability to trap Mo in sediments played no role to fix Mo at the time of deposition. The presence of Mo in a very soluble form pointed to the anthropogenic disturbance of subsurface redox conditions which was caused by the penetration of oxygenated surface water into deeper aquifers. As a result, Mo was first shifted from the organic phase to the more labile form and subsequent released into the groundwater. Molybdenum on the other hand, appeared to be adsorbed onto mineral surfaces. Its adsorption

on calcite and HFO was too low. Some loosely bound Mo in the aquifer matrix could be attributed to clay minerals, which are coated with organic materials.

Pyrite was found to be the main primary source of As in the study area. There was no significant relationship between As and OM in the CRS residuals. Precipitation of powellite was controlled by the concentration of Mo in groundwater samples in the Lithia area. Geochemical modeling showed that powellite as a secondary Mo mineral was super-saturated when Mo concentration in the groundwater of Lithia was higher than 3250 µg/L (Chapter 3). On the other hand, the dissolution of synthesized powellite in DDI water and groundwater demonstrated that only minor amounts of powellite could be released from the aquifer matrix. Thus, the precipitation and dissolution of powellite was insignificant in the Lithia area.

Chapter 5. Impact of adsorption (hydrous ferric oxides and humic acid) and desorption (hydrous ferric oxides) reactions on the mobilization of molybdenum and arsenic from the aquifer matrix

Abstract

In order to assess the adsorption and desorption behavior of molybdenum (Mo) and arsenic (As) by/from hydrous ferric oxides (HFO), a series of batch experiments on the synthesized HFO samples were carried out. Four core samples from the exploration boreholes of the Lithia area were also included in the desorption experiments to determine the role of HFOs present in the study area in retaining Mo and As. All the experiments were undertaken using distilled deionized (DDI) water. The results showed that the adsorption affinity of Mo on HFO was very high at low pH, but very low at pH above 8. Similarly, adsorption of As(III) and As(V) onto HFO was very high at low pH; but compared to Mo, both As(III) and As(V) were stronger adsorbed to HFO at pH 7 to 9, which coincide with the pH range of the study area. In addition to the batch experiments, a surface complexation model was run to simulate the adsorption of Mo and As onto HFO. The model findings were supportive of the experiments results. Desorption experiments were carried out by dissolving HFO and core samples in DDI. The experiments showed that about 50 to 96% Mo in the core samples were released, but no Mo from those absorbed onto the HFO during the adsorption experiments was liberated. The removal of Mo from the core samples was not pH dependent. In contrast to Mo, As was mobilized to a lesser degree; in 3 of the 4 core samples less than 30% were removed, and a maximum 50% was released from the fourth sample. No As was released from HFO samples when DDI water was used as solvent.

Following desorption experiments, the residues of the core and HFO samples were sequentially dissolved through the first 3 steps of the sequential extraction procedure (SEP)

which were described in Chapter 3. These were carried out to identify the type of the adsorption, i.e. whether it is inner or outer sphere complexes. About 20% Mo was removed from the HFO samples during step 1 but little Mo was leached in the second step and the rest of Mo (≈ 80%) was dissolved in the third step where HFO itself was also dissolved. Little As was released during steps 1 and 2 of the SEP, but almost all of the As was released during step 3. The experiments showed that Mo sorption onto HFO was mainly through forming inner-sphere complexes which is a stronger bond than outer-sphere complexes. An isotherm modeling proved that anions such as phosphate and to lower degree sulfate competed with Mo for sorption sites. In contrary to Mo, As competed better with the mentioned ions and sat on a considerable number of HFO sites; something that was also proved by the high extraction rate of As in the third step of SEP which was described in Chapter 3.

In addition to HFO, humic acid (HA) adsorption test was carried out to evaluate the role of organic matter (OM) in removing Mo from groundwater. In the alkaline pH ranges (pH ranges of the study area), Mo adsorption onto HA was low. Thus, OM had no significant impact on the Mo behavior in the study area.

5.1 Introduction

Adsorption/desorption by/from the surface of solid minerals and OM are the dominant reactions controlling the fate of many heavy metals in terrestrial and aquatic environment. Knowledge of these phenomena is essential for understanding retention and transport of heavy solutes in soils and geological media. It is also crucial for assessing the environmental risk of contamination and pollution provoked by these elements. Therefore, most investigations regarding environmental concerns have been focused on describing the sorption and transport of heavy metals under field conditions as well as in the laboratory experiments. Elevated Mo

and As in Lithia area in both aquifer matrix and groundwater provided an exceptional field site to deepen these investigations.

Molybdenum adsorption onto soils and soil minerals has been well studied (Das and Jim Hendry, 2013; Goldberg, 2010; Gustafsson, 2003; Prasad Saripalli et al., 2002; Stollenwerk, 1998; Zhang and Sparks, 1989). Iron (Fe), aluminum (Al) and, to some extent, titanium (Ti) oxides may be important adsorbent minerals for Mo, as they may acquire a positive charge at low to medium pH values (Ferreiro et al., 1985; Manning and Goldberg, 1996; Matern and Mansfeldt, 2015). Among them, HFO is one of the main adsorbent in the oxic environments and has relatively huge surface area of about 600 m^2/g. In practice, the mobility of heavy metals in water depends on several factors including soil and sediment characteristics, ionic strength and concentration of oxyanions that compete with each other for soil or sediment retention sites. Goldberg et al., (1996) reported that ionic strength had a minor impact on Mo adsorption onto HFO. Few researchers investigated the influence of multiple anions on Mo adsorption (Bostick et al., 2003; Goldberg and Forster, 1998; Gustafsson, 2003; Hiemstra et al., 1989; Roy et al., 1986; Wu et al., 2000; Wu et al., 2001). Phosphate strongly competes with molybdate for adsorption sites and sulfate also competes for sorption sites but to a lesser degree than phosphate (Goldberg, 2010; Gustafsson, 2003). Sulfate forms outer-sphere complexes during adsorption on goethite, while molybdate forms an inner-sphere complex (Goldberg et al., 1996). The affinity of tungstate is greater than molybdate for the goethite surface (Xu et al., 2006). There is only one relatively old research regarding Mo adsorption onto OM (Bibak and Borggaard, 1994). These workers found that Mo adsorption decreases rapidly from its maximum at pH 3.5, indicating a different mechanism, probably complex formation between carboxyl and phenol groups on HA and Mo in octahedral coordination.

Arsenic is a trace element that is toxic to animals including humans (Abernathy et al., 1999). The concentrations of As in soils and waters can be elevated due to mineral dissolution, use of arsenic bearing pesticides, disposal of fly ash, mine drainage, and geothermal discharge

(Banning and Rüde, 2010; Price and Pichler, 2006). Presently, there is a widespread concern about elevated concentrations of As in the aquifers of Bangladesh (Harvey et al., 2002; Nickson et al., 1998; Nickson et al., 2000). Of the two naturally occurring forms of As, arsenate, As(V), and arsenite, As(III), trivalent As is considerably more toxic. These species can be removed from the solutions by sorption onto the solid phases present in the system. Both arsenite and arsenate are adsorbed onto soil mineral surfaces, but show very different adsorption behaviors. Clay minerals and HFOs play an important role in the retardation of As in the environment (Kersten et al., 2014; Manning and Goldberg, 1996).

In this study the adsorption/desorption of Mo and As onto/from two-line HFO at different pH ranges was investigated. The samples (HFO samples and core samples) were first dissolved in DDI water. The first three steps of the SEP were then applied to the residue of the samples to evaluate the surface complexes formed during the adsorption experiments. Experiments were also carried out to study adsorption of Mo onto HA to assess the role of organic materials in removing Mo from groundwater. An isotherm modeling exercise using three competing anions including molybdate, phosphate, and sulfate which were present in the Lithia area was performed to evaluate their role in the adsorption behavior of molybdate onto HFO in Lithia groundwater.

5.2 Materials and methods

5.2.1 Reagents, sample selection and analytical methods

Distilled deionized water with a resistivity less than 18 MΩ/cm was used to prepare all of the solutions. Stock Mo and As(III, V) solutions were prepared by dissolving $Na_2MoO_4.2H_2O$ (Sigma-Aldrich, Spain), As_2O_3 (for As(III)), and $HAsNa_2O_4.7H_2O$ (for As (V)) (Sigma-Aldrich, Spain) in DDI water, respectively. To maintain a relatively constant ionic strength, all working

Mo and As solutions were freshly prepared with a background electrolyte concentration of 0.01 M of $NaNO_3$.

Four samples from DEP-1, DEP-2, and DEP-5 cores were chosen for desorption experiments. The samples were selected by taking into account three criteria including high Mo concentration, high As concentration, and appropriate geographic representation of the study area. The samples were powdered by hand with an agate mortar and pestle and rinsed with ethanol to prevent cross contamination. An electronic scale was used to weigh out 1 ± 0.005 g of powdered sample which was subsequently poured into 50 mL centrifuge tubes for the experiments. Fifty mg of each sample were used to measure the total content of the elements.

5.2.2 Preparation of HFO

Two-line HFO was synthesized following the procedure described by Swedlund and Webster (1999). Four M NaOH solution (Sigma-Aldrich, Germany) were added drop-wise, under constant stirring, to a solution containing 18.44 mM of $Fe(NO_3)_3.9H_2O$ (Alfa Aesar, Germany). The resulting suspension was kept for 20 h at about 20^o C. Iron (hydr)oxide particles from similar suspensions were previously examined by Fe K-edge EXAFS spectroscopy and found to be 2-line ferrihydrite (Gustafsson, 2003; Swedlund and Webster, 1999; Tiberg et al., 2013). Prior to the batch experiments, the suspension was back-titrated to pH 4.6 by adding specified volumes of 0.1 M HNO_3 which was followed by strongly stirring for 30 min to prevent buildup of excessive CO_2 in the suspension.

5.2.3 Batch experiments

In this section, batch experiments which were set up to assess Mo, As(III) and As(V) adsorption onto HFO as well as Mo adsorption onto HA are described. Molybdenum, As(III) and As(V) adsorption experiments were conducted by mixing a background electrolyte of 0.01 M $NaNO_3$ with appropriate amounts of the HFO suspension. Then various volumes of acid (HNO_3) or base (NaOH, prepared the same day) were added to the suspension to produce a wide range

of pH, from 3 to 10. In the next step, few aqueous solutions including $Na_2MoO_4.2H_2O$, As_2O_3 (As (III)), and $HAsNa_2O_4.7H_2O$ (As (V)) were added to each suspension. The final concentration for Mo was 10 mg/L, while that of both As(III) and As(V) was 15 mg/L. Approximately 40 mL sample from the suspensions were taken and transferred to the polypropylene centrifuge vials. The suspensions were shaken for 48 h by a mechanical shaker operating at 250 rpm at room temperature; they were then centrifuged for 20 min at 4000 rpm and separated from the solids. The supernatants of all the samples were filtered by either 0.2 µm cellulose acetate filters (Membrex, Germany) or 0.45 µm Sabina membrane filters. The percentage of adsorbed Mo and As was simply calculated by computing the difference between the initial and final Mo concentrations using Equation (5.1):

Absorption (%) = (Ci −Cf/Ci) ×100 Equation 5.1

where Ci and Cf are the concentration of element in the initial and final solutions, respectively.

Desorption batch experiments were performed to determine whether the sorption is reversible or not. The experiments were carried out by adding 40 mL DDI water with a background electrolyte of 0.01 M $NaNO_3$ to the residue of centrifuged HFO (This is for those samples which adsorbed all Mo and As from the solutions during the 48 h contact time). The solutions were shaken for 48 h and subsequently centrifuged and analyzed for Mo and As content. To compare these results with the Floridian aquifer matrix, 4 samples from the Lithia cores were selected. First, 40 mL DDI water with a background electrolyte of 0.01 M $NaNO_3$ were added to 1 g of each sample, and subsequently shaken in the same manner as the HFO samples.

Two humic acids were used for this study including humic acid sodium salt from Sigma Aldrich (HA) and purified humic acid (PHA). For preparation of HA stock solution, commercial HA was dissolved in DDI water at pH above 10, followed by filtering through 0.45-µm acetate cellulose membranes. Purified humic acid was prepared by washing HA with 1 M NaOH in a glove box and were purged with nitrogen for 12 h. It was then precipitated with HCl at a pH between 1

and 2, centrifuged, rinsed three times with 0.1 N HCl in order to remove the fulvic and hydrophilic acid compounds, and finally rinsed with DDI water to remove excess salt. The percentage of Mo and As adsorbed onto HA and PHA was simply determined by computing the difference between the initial and final Mo concentration using Equation 5.1.

5.2.4 Sorption type of Mo and As onto HFO

Desorption batch experiments were carried out to determine the adsorption type of Mo and As onto HFO. Firstly, the core and HFO samples (residuals of the samples after adsorbing all Mo and As from the solutions following 48 h contact time) were dissolved in 40 mL DDI water, and subsequently shaken for 48 h. Secondly, the residues of the first step were dissolved in 20 mL 1 M sodium acetate (NaOAc) adjusted to pH 8.1 and shaken for 2 h at room temperature by a mechanical shaker operating at 250 RPM, i. e. step 1 of the SEP. Thirdly, the experiments were repeated on the residues of the second step with the same reagent at pH 5, i.e. step 2 of the SEP. Finally, 20 mL of a freshly prepared, 0.5 M hydroxylamine hydrochloride in 0.25 M HCl were added to the residues of the third step, capped and shaken for 5 to 10 seconds. The samples were then placed in a hot block at 60°C for 2 h with the cap loosened. At 30 min intervals, the caps were tightly closed and the contents shaken for 5 to 10 s, i.e. step 3 of the SEP. The filtrates (after 10 min centrifuge) of each step were analyzed to measure Mo and As concentration.

5.2.5 Modelling

The diffuse layer model (DLM) (Dzombak and Morel, 1990) was run to predict the adsorption of Mo and As onto HFO. The same DLM parameters as Dzombak and Morel (1990) were used, i.e. a) an specific surface area of 600 m^2/g was assumed, b) the site density was fixed at 0.205 mol/mol Fe, and c) the log K's of the surface complexation reactions defining the formation of the protonated $FeOH_2^+$ species and the deprotonated FeO^- species were set at 7.29 and -8.93, respectively.

In the modeling exercise, the protonation reactions of molybdate were considered as:

$K_1 = HO_4^-/ H^+ + XO_4^{2-}$ Equation 5.2

$K_2 = XO_3(H_2O)_3/ 2H^+ + 2XO_4^{2-} + 2H_2O$ Equation 5.3

where X is Mo, K_1 and K_2 are equilibrium constants. Log K_1 and log K_2 were set at 4.24 and 8.24, respectively.

A second modeling code was used to evaluate the impact of phosphate and sulfate concentrations on the molybdate sorption onto HFO in the Lithia area. For this model, the DEP-1 well data was used by varying concentrations of these ions. The concentrations were gradually altered as such to resemble the concentration of anions ranges in the study area. The competitive sorption data for molybdate and phosphate were fitted to the multi-component Freundlich equations (Equations 5.4 and 5.5) using PHREEQC code. The same equations can be written for molybdate and sulfate:

$S_{Mo} = a_{Mo} C_{Mo} / (C_{Mo} + K_{Mo, P} C_P)^{1-bMo}$ Equation 5.4

$S_P = a_P C_P / (C_P + K_{P, Mo} C_{Mo})^{1-bP}$ Equation 5.5

where S_{Mo} is the amount of sorbed Mo per unit mass of the sorbent (HFO) in the presence of competitor P, S_P is the amount of sorbed P per unit mass of the sorbent in the presence of competitor Mo, a_{Mo} and a_p are the single solute Freundlich constants for solutes Mo and P, C_{Mo} and C_P are the equilibrium concentrations of the solutes, $K_{Mo,P}$ is the competition coefficient of P on Mo, and $K_{P,Mo}$ is the competition coefficient of Mo on P. Sorption was calculated by taking into account the change in Mo, P and S concentrations. A summary of the input data for the two-site diffuse layer model is presented in Table 5.1.

Table 5.1 Surface complexation reactions for the two-site diffuse layer model (data from PHREEQC database).

Reactions	Log K
$SurfwOH + H^+ = SurfwOH_2^+$	6.3
$SurfwOH = SurfwO^- + H^+$	-7.1
$SurfwOH + MoO4^{2-} + H^+ = SurfwMoO_4^- + H_2O$	8.2
$SurfwOH + MoO_4^{2-} = SurfwOHMoO_4^{2-}$	2.4
$SurfwOH + PO_4^{3-} + 3H^+ = SurfwH_2PO_4^0 + H_2O$	27.8
$SurfwOH + PO_4^{3-} + 2H^+ = SurfwHPO_4^- + H_2O$	21.6
$SurfwOH + PO_4^{3-} + H^+ = SurfwPO_4^{2-} + H_2O$	16.5
$SurfwOH + SO_4^{2-} = SurfwOHSO_4^{2-}$	0.7
$SurfsOH + H^+ = SurfsOH_2^+$	6.3
$SurfsOH = SurfsO^- + H^+$	-7.1
$SurfsOH + MoO_4^{2-} + H^+ = SurfsMoO_4^- + H_2O$	10.3
$SurfsOH + MoO_4^{2-} = SurfsOHMoO_4^{2-}$	4.2
$SurfsOH + PO_4^{3-} + 3H^+ = SurfsH_2PO_4^0 + H_2O$	27.8
$SurfsOH + PO_4^{3-} + 2H^+ = SurfsHPO_4^- + H_2O$	21.6
$SurfsOH + PO_4^{3-} + H^+ = SurfsPO_4^{2-} + H_2O$	16.5
$SurfsOH + SO_4^{2-} = SurfsOHSO_4^{2-}$	0.7

SurfwOH and SurfsOH represent low and high affinity bonding sites. Surface site density in the model (Dzombak and Morel, 1990) for SurfwOH was 0.83 μM/g and was 0.02 μM/g for SurfsOH. The surface area was assumed to be 600 m^2/g (Gustafsson, 2003; Stollenwerk, 1998).

5.3 Results

5.3.1 Adsorption experiments

Results of the Mo – HFO batch experiments (Fig. 5.1 and Table 5.2) indicated that the adsorption affinity of Mo onto HFO was highly pH dependent. Nearly 100% Mo was adsorbed at low pH, whereas little Mo adsorption occurred at pH above 8. Initial Mo concentration in the solutoin was 10 mg/L. Adsorption of As(III) and As(V) onto HFO was strongly pH dependent (Fig. 5.2 and Table 5.3). Compared to Mo, As(III) and As(V) were adsorbed much more strongly onto HFO at pH 7 to 9, which corresponded to the pH range of the study area. Initial concentration of both As(III) and As(V) in the solution was 15 mg/L.

The chemical equilibrium program, Visual MINTEQ, was employed to produce model fits for the Mo and As data. For As(V) and As(III), some scatter was observed in the adsorption envelopes. However, a better fit was obtained for Mo when Dzombak and Morel's (1990), diffuse layer model (DLM) constants was used (Fig. 5.1 and Fig. 5.2).

Table 5.2: Measured pH and concentrations of dissolved Mo, As(III) and As(V) in the batch experiments.

pH	Mo	As(III)	As(V)
3.67	n.d.	n.d.	n.d.
4.36	n.d.	n.d.	0.2
5.65	0.1	n.d.	0.3
6.2	0.5	n.d.	0.8
6.75	0.4	0.1	0.3
7.15	5.0	n.d.	1.1
8.15	8.5	0.8	1.5
8.4	8.0	0.2	1.5
9.39	9.0	0.3	3.0

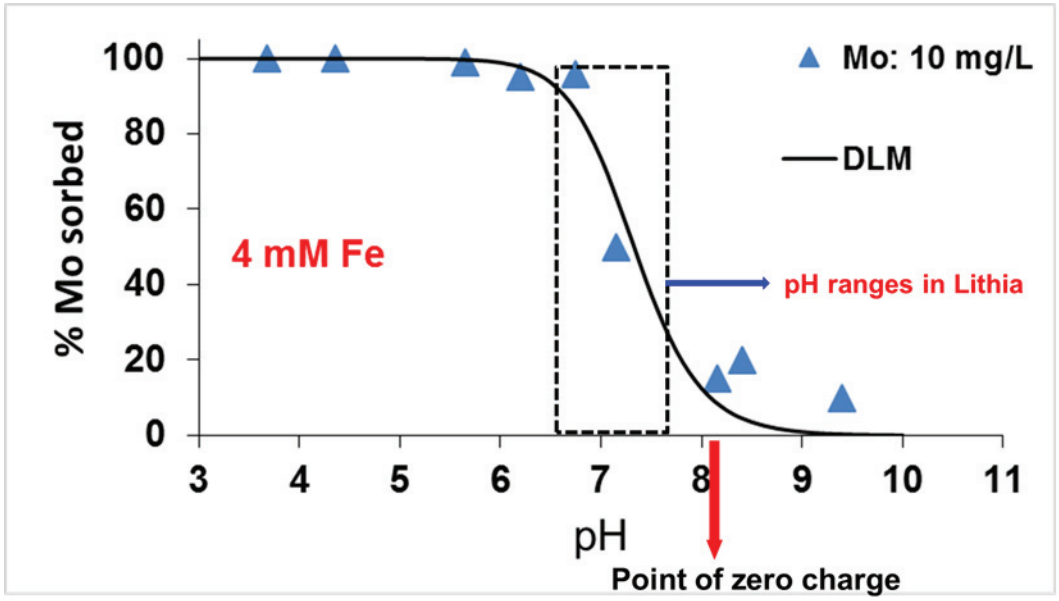

Fig. 5.1 Molybdenum adsorption onto HFO. Diffuse layer model (Dzombak and Morel, 1990) specifications: weak sites 0.83 μM/g and strong sites: 0.02 μM/g, surface area: 600 m^2/g. Points are observations (initial molybdenum concentration of 10 mg/L) and the curve is the fit for diffuse layer model model (DLM).

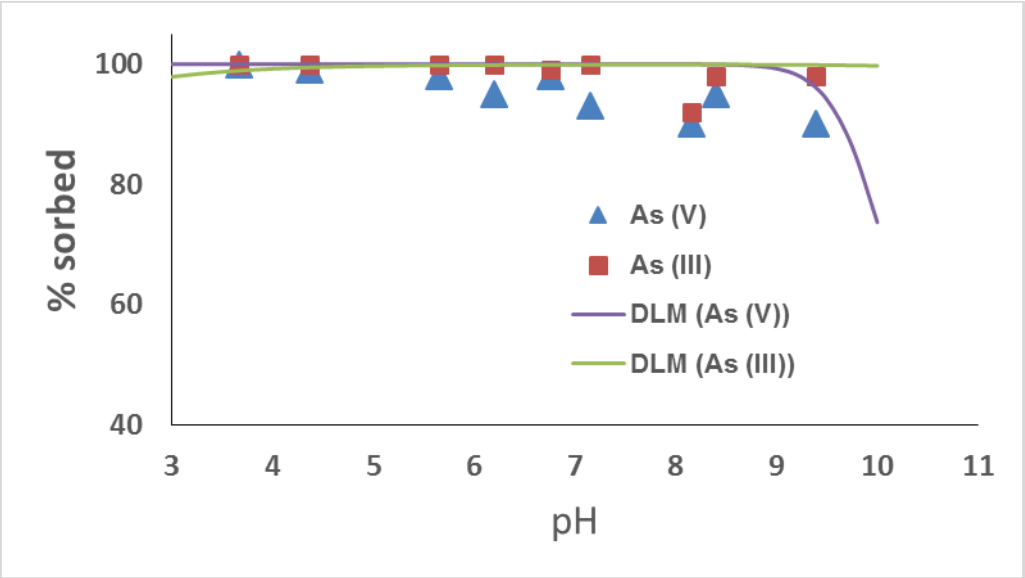

Fig. 5.2 Arsenite and arsenate adsorption onto HFO. Points are observations (arsenite and arsenate initial concentration of 15 mg/L) and the lines fit the diffuse layer model (DLM).

Adsorption of Mo onto HA and PHA was strongly pH dependent (Table 5.3 and Fig. 5.3). The highest Mo adsorption was at around pH 3.5. Molybdenum adsorption decreased exponentially with increasing pH and remained constant at pH above 7. The difference between Mo adsorption onto HA and PHA was related to impurities in HA such as clay minerals.

Table 5.3: Amounts and percentages of Mo adsorbed on HA and PHA.

pH	HA		PHA	
	sorbed mg/kg	sorbed %	sorbed mg/kg	sorbed %
3.5	7.7	51	7.1	47
4	6.0	40	4.5	30
4.6	4.1	27	1.8	12
5.3	2.4	16	2.0	13
6.1	2.6	17	1.2	8
7	0.6	4	0.6	4.3
8	1.1	7	0.7	4.4

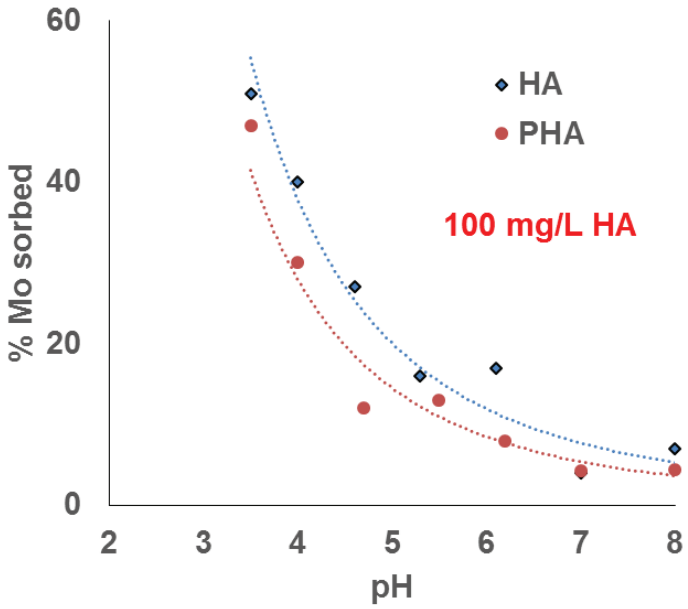

Fig. 5.3 Molybdenum adsorption on HA and PHA.

5.3.2 Desorption experiments

Desorption batch experiments were conducted by using clean and fresh DDI water to determine the reversibility of Mo and As adsorbed onto HFO. In addition, 4 samples from the aquifer matrix were selected and analyzed in the same manner as HFO's samples to assess the role of HFO as a host for Mo and As. The results of these experiments can be seen in Tables 5.4, 5.5, and Fig. 5.4 (A, B).

Table 5.4: Amounts of Mo released from the aquifer matrix and HFO samples by reaction with DDI water at different pH ranges.

pH	DEP-1 45-46		DEP-1 70-71		DEP-2 18-19		DEP-5 50-51		HFO (10, 15 mg/L)
	mg/kg	%	mg/kg	%	mg/kg	%	mg/kg	%	
3.67	116	96	357	71	20	53	20	86	n.d.
4.36	116	96	361	72	21	55	21	94	n.d.
5.65	112	93	353	71	20	53	20	83	n.d.
6.2	117	97	344	69	23	56	23	81	n.d.
6.75	114	94	340	68	19	50	19	86	n.d.
7.15	113	93	332	67	20	53	20	92	n.d.
8.15	114	94	344	69	21	55	21	89	n.d.
8.4	116	96	342	68	19	51	19	81	n.d.
9.39	117	97	354	71	22	57	22	83	n.d.

n.d. = not detected

Table 5.5: Amounts of As released from the aquifer matrix and HFO samples by reaction with DDI water at different pH ranges.

pH	DEP-1 45-46		DEP-1 70-71		DEP-2 18-19		DEP-5 50-51		HFO (10, 15 mg/L)
	mg/kg	%	mg/kg	%	mg/kg	%	mg/kg	%	
3.67	13	43	40	30	2	9	7	23	n.d.
4.36	13.4	45	39.5	30	2	9	8	26	n.d.
5.65	14	47	40	30	3	12	7	23	n.d.
6.2	14	47	40	30	2	9	5	17	n.d.
6.75	13	43	37	28	2	9	6	19	n.d.
7.15	12.5	42	37	30	1	5	6	19	n.d.
8.15	13.4	45	39.5	28	2	9	5	18	n.d.
8.4	14	47	37	28	1	5	6	19	n.d.
9.39	9.9	33	37.6	28	1	5	7	23	n.d.

n.d. = not detected

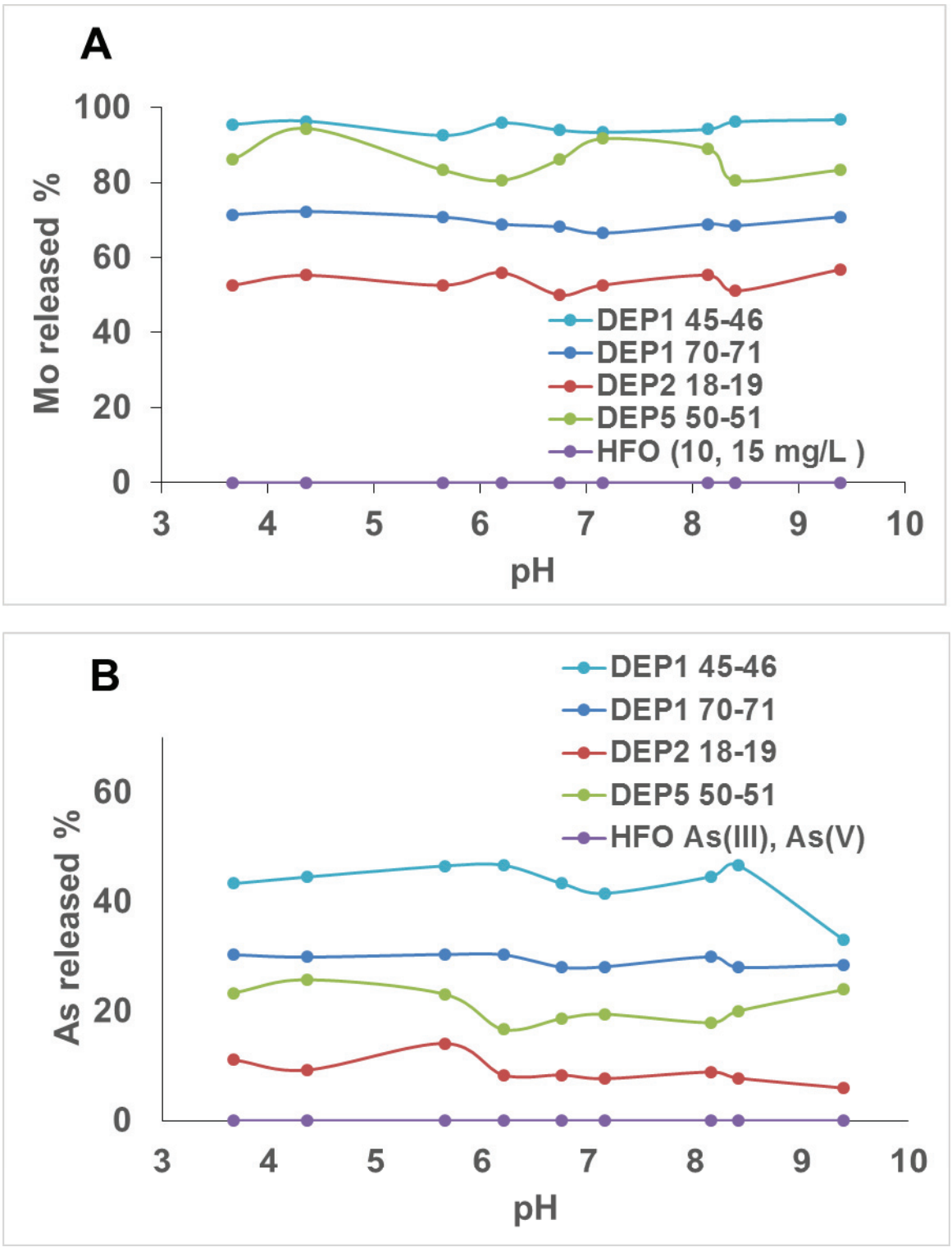

Fig. 5.4 (A, B) Percentage of Mo and As mobilized from the aquifer matrix as a result of the reaction with DDI water. The data corresponds to Tables 5.4 and 5.5.

5.3.3 Evaluation of adsorption types using sequential extraction

Hydrous ferric oxide possesses high specific surface area and is scattered everywhere in an aquifer matrix. Thus, it provides large sorption sites for toxic elements including Mo and As. The elements could be adsorbed onto HFO by forming inner and outer-sphere surface complexes. In order to investigate the adsorption type of Mo and As onto HFO, the first three steps of the SEP was applied to the residue of the desorption experiments. The results are presented in Tables 5.6, 5.7 and Fig. 5.5.

Table 5.6: Amounts of Mo extracted by the first three steps of the SEP.

Sample	Step1		Step 2		Step 3		Total
	mg/kg	%	mg/kg	%	mg/kg	%	mg/kg
DEP-1 45-46	n.d.		n.d.		n.d.		122
DEP-1 70-71	2.2	0.42	1.8	0.34	1.8	0.35	499
DEP-2 18-19	1.0	2.63	1.0	2.63	n.d.		38
DEP-5 50-51	0.2	0.59	0.3	0.88	0.3	0,79	36
HFO-1	0.1	1.1	1.6	15.8	8.0	77.4	10
HFO-2	0.4	2.5	3.0	19	11.5	71.9	15

n.d.= not detected

Table 5.7: Amounts of As extracted by the first three steps of the SEP.

Sample	Step1		Step 2		Step 3		Total
	mg/kg	%	mg/kg	%	mg/kg	%	mg/kg
DEP-1 45-46	3	10	4	13	6	20	30
DEP-1 70-71	4	3	2	2	30	23	132
DEP-2 18-19	1.5	8	1	6	7	39	18
DEP-5 50-51	3	10	4	13	17	57	30
HFO - As(III)	n.d.		n.d.		14	93	15
HFO - As(V)	n.d.		n.d.		13	87	15

n.d.= not detected

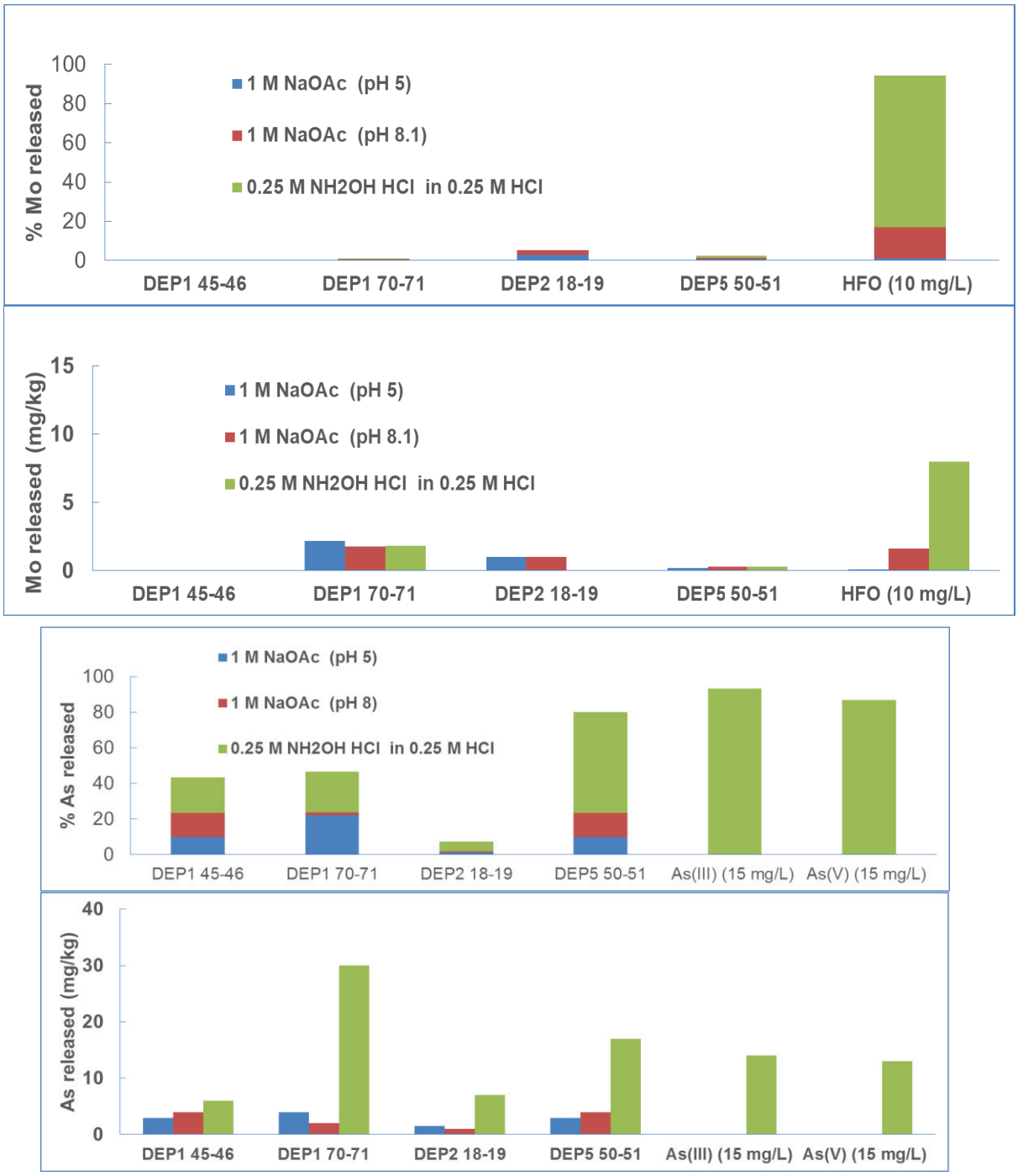

Fig. 5.5 Amounts and percentages of Mo and As released as a result of the application of the first three steps of the SEP to the residue of the desorption experiments. The data corresponds to Tables 5.6 and 5.7.

5.3.3 Geochemical modeling and adsorption isotherms

The adsorption of molybdate (MoO_4^{2-}), phosphate (PO_4^{3-}), and sulfate (SO_4^{2-}) onto HFO in DEP-1 well sample was simulated by PHREEQC using Dzombak and Morel (1990) form of diffuse double layer surface complexation model. The model provided a direct relation between molybdate adsorption and solution chemistry. The consequences of change in pH, phosphate, and sulfate on molybdate adsorption can be described with a relatively small number of mass action expressions. The sorption isotherms for the three anions as a function of pH are depicted in Figures 5.6 and 5.7. There was a decrease in sorption with an increase in pH of the groundwater solution. At any given pH and solution concentration, phosphate was sorbed more strongly than molybdate. Adsorption of molybdate decreased with increase in pH, a behavior typical of anion adsorption onto iron oxide. Sulfate also competed for sorption sites but to a lesser degree than phosphate. Adsorption of molybdate was nonlinear; the amount adsorbed decreased with increase in aqueous concentration. Adsorption isotherms also became more linear with increase in pH.

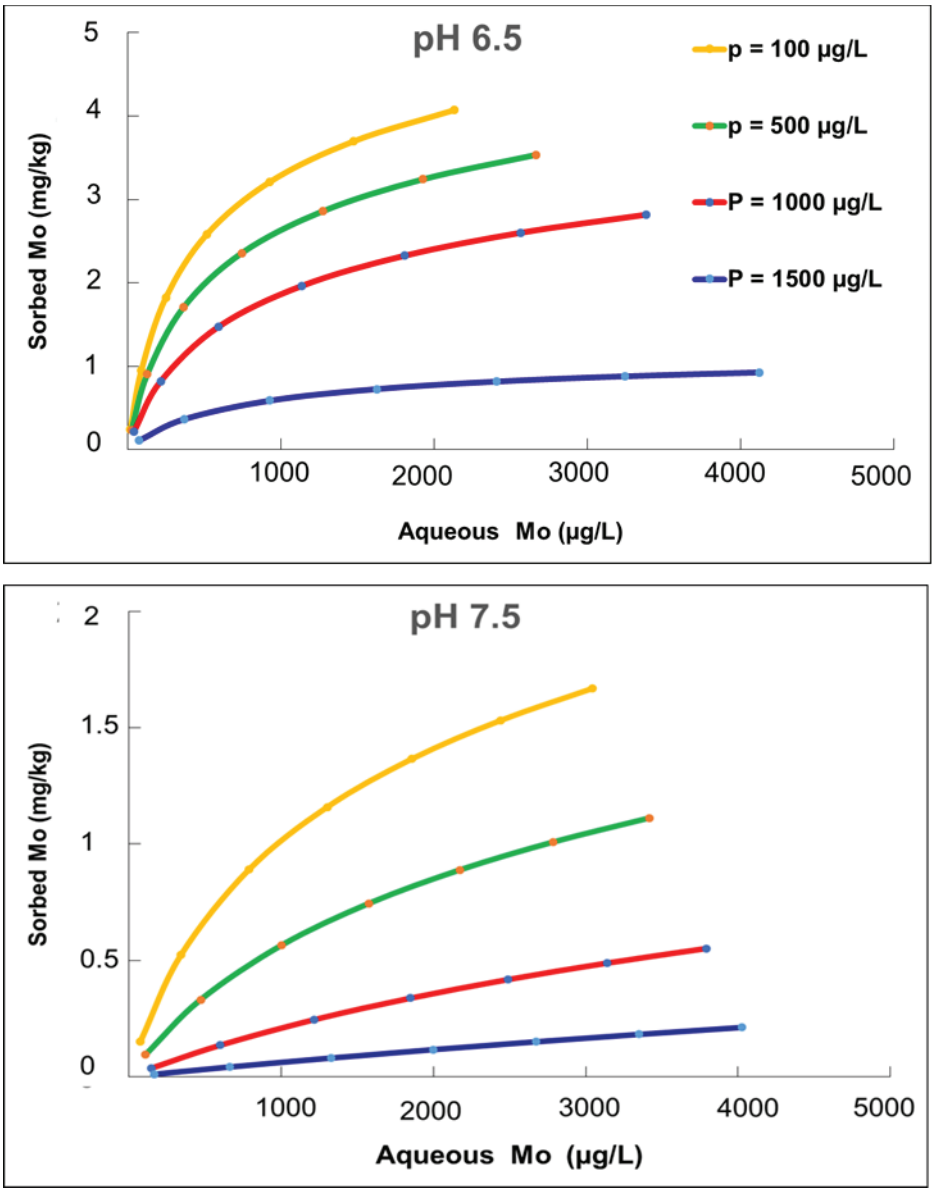

Fig. 5.6 Adsorption isotherms for molybdate in competition with phosphate in DEP-1 groundwater sample for HFO sites. The pH values (6.5 and 7.5) and anion concentrations in the solution were chosen as such to resemble the expected range of the study area.

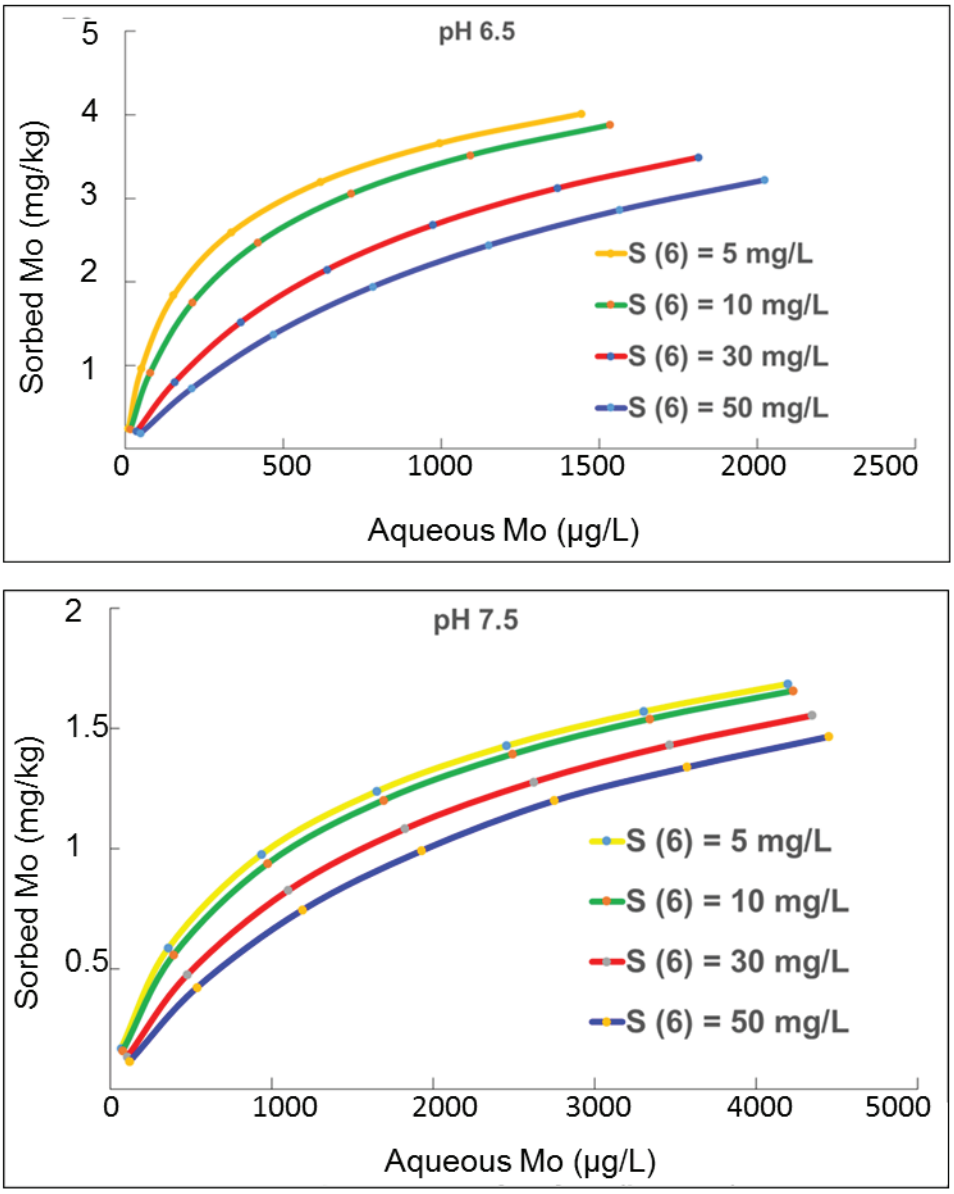

Fig. 5.7 Adsorption isotherms for molybdate in competition with sulfate in DEP-1 groundwater sample for HFO sites. The pH values (6.5 and 7.5) and anion concentrations in solution were chosen as such to resemble the expected range of the study area.

5.4 Discussion

5.4.1 Possible molybdate, arsenite and arsenate sorption sites

Adsorption is the main reaction which controls the mobility of many inorganic solutes including Mo and As. The extent of adsorption is highly dependent on the chemical composition of both the aqueous and solid phases. Variations in pH, concentration of the competing solutes, overall groundwater composition, and surface properties of the adsorbent have been shown to influence the mobility of anions and cations (Das and Jim Hendry, 2013; Gustafsson, 2003; Schaller et al., 2009; Wu et al., 2000).

In the aquatic environment, the major sorption sites for Mo and As include HFO (Goldberg et al., 1996; Gustafsson, 2003), pyrite (Bostick et al., 2003; Xu et al., 2006), Fe and Al oxides and clay minerals (Goldberg, 1985, 2010), calcite (Goldberg et al., 1996), anatase (Prasad Saripalli et al., 2002) and OM (Bibak and Borggaard, 1994a). Of all these minerals and materials which may act as sorption sites, the aquifer matrix in the Lithia area contained relatively high amount of HFO, clay minerals, carbonates and OM (Pichler and Mozaffari, 2015). The mentioned sorption sites are discussed in more detail in the order of their importance below here.

Hydrous ferric oxides: It has been known for a long time that Mo may be bound to Fe and Al oxides in soils and sediments (Bibak and Borggaard, 1994b; Ferreiro et al., 1985; Goldberg, 1985; Goldberg et al., 1996; Stollenwerk, 1998). It is the main adsorbent for Mo and As in the oxic environment. Molybdenum adsorption onto HFO exhibits a maximum value at low pH extending to about a pH of 4 (Goldberg et al., 1996; Stollenwerk, 1998). The rate of Mo adsorption onto HFO decreases with increase in the concentration of Mo in the solution (Stollenwerk, 1998). Ferreiro et al., (1985) showed that the sorption of Mo by HFO depends largely on pH, reaching maximum value at a pH of 4.

Of the two naturally occurring forms of As, i.e. arsenate, As(V), and arsenite, As(III), As(V) shows maximum sorption onto HFO at a pH of 4 while As(III) shows maximum sorption at the pH range of 7 to 8.4 (Pierce and Moore, 1982). Arsenate forms inner sphere surface complexes on HFO and shows very little ionic strength dependence on solution's pH. In contrast, arsenite forms outer sphere surface complexes on HFO and can be released into the environment easier than arsenate (Goldberg and Johnston, 2001).

Clay minerals: It is a well-known fact that clay minerals play an important part in the retardation of Mo and As in the environment. Molybdenum adsorption onto clay minerals showed pH dependence and maximum adsorption peak near a pH of 4 (Goldberg, 1985, 2010; Jones, 1957). Several studies showed that the relative adsorption of Mo onto clay minerals increased in the order: illite < kaolinite < kaolinite and montmorillonite < nontronite < metahalloysite (Jones, 1957; Theng, 1971; Motta and Miranda, 1989). Similarly, Goldberg et al., (1996) reported that the magnitude of Mo adsorption in an increasing order is: kaolinite < illite < montmorillonite. However, it is difficult to compare the adsorption affinity per unit mass or per unit surface area since the suspension density varies between adsorbents in different experiments. The mentioned study concluded that Mo adsorption onto clay minerals exhibited a peak near pH 3 and then decreased rapidly with increasing pH until adsorption was virtually zero near pH 7. Adsorption of Mo onto clay mineral can occur through a variety of mechanisms, including adsorption on outer- or inner-sphere complexes as well as precipitation. Outer-sphere adsorption is a weak electrostatic attraction between an ion and the surface of clay mineral. Inner-sphere adsorption occurs through the formation of one or more chemical bonds between the surface in question and the adsorbate. For Mo adsorption onto kaolinite, the point of zero charge (PZC) was shifted to a more acid pH value, indicating an inner-sphere adsorption mechanism.

Carbonates: In sediments, carbonate is not a major sink for Mo (Goldberg et al., 1996). Fox and Doner (2002) conducted relevant experiments and found that the sorption of Mo onto

calcite was low. In contrast, it has been revealed that As may be removed from the aquatic environments by carbonates.

Organic matter: To our knowledge, there is only one research regarding Mo adsorption onto OM (Bibak and Borggaard, 1994b). However, a considerable number of research has been focused on the enrichment of Mo by OM in the marine environments (Adelson et al., 2002; Bostick et al., 2003; Brumsack, 2006; Chappaz et al., 2014; Crusius et al., 1996; Dahl et al., 2010; Dahl et al., 2013; Erickson and Helz, 2000). On the other hand, numerous studies have already been conducted on As adsorption onto OM (Giménez et al., 2007; Mohan and Pittman Jr, 2007; Nickson et al., 1998; Nriagu et al., 2007; Peterson and Carpenter, 1986; Pierce and Moore, 1982).

Other oxyanions: Some oxyanions such as phosphate, silicate and sulfate compete with molybdate and arsenate for sorption sites (Goldberg, 1985, 2010; Jones, 1957; Pichler and Mozaffari, 2015). Roy et al., (1986) showed that the adsorption of molybdate is noticeably reduced by the competitive adsorption of phosphate on the surfaces of clay minerals. Molybdate adsorption onto gibbsite is not influenced by sulfate, but the adsorption of sulfate is significantly inhibited by molybdate (Wu et al., 2000). Silicate has a minor competitive effect on molybdate adsorption onto goethite while sulfate does not impart any competitive effect (Xu et al., 2006).

5.4.2 Hydrous iron oxides

The maximum, average and median concentration of Fein the Lithia area were 87311 mg/kg, 3535 mg/kg and 940 mg/kg, respectively. In the matrix of the local aquifer which underlies the town of Lithia in Central Florida, Fe concentration was high in two specific horizons, particularly at depths of 5 to 20 m in DEP-2 and depths of 50 to 70 m in DEP-1, DEP-2 and DEP-5 cores (Pichler and Mozaffari, 2015). The calculated correlation coefficients between Mo and Fe, as well as between As and Fe, within the measurement intervals were 0.1 and 0.71, respectively.

Therefore, Fe variations were generally in agreement with As and to a low extent with Mo. The mineralogy and petrology studies in the Lithia area showed that Fe in the sedimentary rocks have originated from crystalline iron oxide, pyrite and HFO (Pichler and Mozaffari, 2015). The results from the SEP experiments (data not shown) in Chapter 3 proved that approximately only 10% of the total Fe content in the Lithia area was in the form of HFO. The adsorption batch experiments demonstrated that maximum Mo adsorption occurred at low pH, up to pH 6, which decreased sharply with increase in pH (Fig. 5.1). The neutrality of the study area' pH led to the neutralization of the available surface sites and as a result, the adsorption of Mo and As was reduced. Since, the PZC for HFO is 8.1 (Goldberg, 2010), at pH ranges of 6.5-8, the protonated surface sites tended to transform to neutralized surface, and Mo adsorption onto HFO was consequently negligible.

Applying the first three steps of the SEP to the residues of initial stage of desorption experiments confirmed that HFO did not provide a significant adsorption site for Mo (Fig. 5.5). Although, about 20% Mo was desorbed from the synthesized HFO surface site in step 1 of the SEP, little, if any, was released from the aquifer matrix. This, which was against our expectations, clearly indicated that the majority of the retained Mo existed in the primary sources, including OM and pyrite. Such finding was also confirmed by the SEP in step 3 where HFO and powellite were dissolved but no Mo was released from the aquifer matrix sample (Fig. 5.5). Therefore, neither HFO nor powellite could be considered as a significant source for Mo in the Lithia area.

5.4.2.1 The novelty of the methodology implemented in this research

In geochemical texts, surface complexations are classified into inner-spherical complexes in which the ions directly bound to the surface of the solid phase, and outer-spherical complexes in which a hydration layer covers the ions. One way to detect the presence of an outer-sphere complex in a solution is to increase the ionic strength during the batch experiments, and monitor the PZC. Some researchers suggested that no shifting in the PZC is a reasonable

evidence of outer-sphere complexes (Ferreiro et al., 1985; Goldberg, 2010; Stollenwerk, 1998). In contrast, the ions adsorbed via inner-sphere surface complexes show insignificant dependence on ion strength (Zhang and Sparks, 1989). However, there are also contrary scientific documents which indicate that lack of shift in the PZC can result from the formation of inner-sphere surface complexes that do not produce a change in the net surface charge (Goldberg et al., 2009; Manning and Goldberg, 1996). To help overcoming the above mentioned discrepancy and to find an easier method to distinguish between inner and outer sphere complexes, special experiments were carried out for the first time in the present study as described above, i.e. applying the first three steps of the SEP to the residue of the samples after being in contact for 48 h with DDI water in a shaker. Our experiments not only proved that there are two types of Mo adsorption but also provided a precise estimation of the amount of each adsorption type. To further explain the novelty of our methodology, we propose the following rationale about the amount of Mo which was extracted in step 1 of the SEP:

(Mo extracted in step 1) % ≈ 20% of total adsorbed on HFO (outer-sphere surface complexes) + X% of total adsorbed on other adsorbents such as clay minerals, OM, and etc.

Such methodology is of appreciable practical application because it is quicker, cheaper and simpler with much less complexity. It is believed that the implemented methodology is important, not only for the study area but also for all ecological projects and environmental pollution studies which may involve Mo in one way or another. Further, these findings are novel and contrary to the previous works which reported that Mo adsorption onto HFO occurs in inner sphere complexes only (Ferreiro et al., 1985; Goldberg et al., 1996; Xu et al., 2006). In line with the above experiments, an isotherm modeling exercise with competing anions including molybdate, phosphate, and sulfate was undertaken to identify why Mo extraction in step 3, which was dissolved HFO, was so low. These ions which were present in the Lithia area, were released from the phosphorite, anhydrite and gypsum lenses of the sedimentary rocks (Pichler and Mozaffari, 2015). The amount of Mo adsorbed onto HFO decreased with increasing Mo

concentration in the solution (Figs. 5.6 and 5.7). Phosphate and to a lower extent sulfate, competed with molybdate for adsorption sites. Competitive interactions between phosphate, molybdate and sulfate indicated that phosphate occupied more HFO sorption sites than molybdate and sulfate (Figures 5.6 and 5.7). The main reason for this behavior of molybdate was attributed to the PZC of HFO (pH 8.1). The pH values of the groundwater in the study area were close to the PZC of HFO. This argument was also supported by the very low Mo extraction in step 3 of the SEP described in Chapter 3 (Fig. 3.2).

5.4.3 Organic matter

Numerous researches have revealed that sediments deposited beneath oxygen-deficient marine waters compared to oxic marine sediments and continental crust are more enriched in Mo. For example, Brumsack (1986) noticed a high correlation between OM and V, Mo and Zn for Cretaceous black shales from Cape Verde Basin drill cores. Werne et al,. (2002) showed striking covariance between OM and Mo/Al ratios in Devonian euxinic shales from western New York. Additionally, Brumsack (2006) discussed the general OM–trace metal relationship using Pliocene examples. However, to our knowledge only one research has been carried out to investigate Mo adsorption onto OM, i.e., Bibak and Borggaard, (1994). They found that in the alkaline pH range, Mo adsorption onto OM is too low. Such observation is in good agreement with the results of our study (Fig. 5.3). Thus, OM could not be considered a significant adsorbent in the study area. However, this may not be the ultimate role of OM in the aquifer in question because OM has high ability for complexing metal ions, formation of colloids and coating the mineral surface sites which have high potential to influence Mo behavior in the study area. Extensive research are needed to better understand all these phenomena.

5.5 Conclusions

In this part of the study it has been shown that considerable amount of Mo (50 to 96%) were removed from the Lithia area aquifer matrix samples by dissolving the samples in DDI water. In contrast, Arsenic showed much less mobility. By undertaking adsorption and desorption experiments, it became clear that Mo was not significantly adsorbed onto HFO and OM in the study area. However, OM could affect the speciation of Mo and As species including molybdate, arsenite and arsenate, and consequently influencing the migration of these pollutants in the environment.

A novel application of SEP method has been demonstrated in this study. By applying the first three steps of SEP to the residues of DDI extracted samples, two types of Mo adsorption mechanisms on HFO were recognized which include inner-sphere and outer-sphere surface complexes. This technique is superior to the earlier methods in determining the type of adsorption and in differentiating between inner and outer complexes. Hence, this is the novelty of this study. The three first step of the SEP analysis demonstrated that approximately only 20% of Mo adsorbed on HFO took place via forming outer-sphere complexes. In contrast, As was strongly absorbed by HFO and its adsorption mechanism could therefore be considered as inner-sphere complexes.

6. Conclusions, outlooks and recommendations for further research

6.1 Conclusions

This study investigated the chemical fractionation, primary sources and adsorption/desorption behavior of molybdenum (Mo) and arsenic (As) by/from hydrous ferric oxides (HFO) and humic acid (only for Mo) in the Lithia area and Avon Park Formation (APF), Florida, USA. This was the first such study for Mo and one of only a few similar studies for As. The findings are summarized in the following paragraphs:

1) Molybdenum and As were found at elevated levels in the aquifer matrix and groundwater in the study area. Molybdenum was present mostly in highly soluble phases (adsorbed/exchangeable) while As showed somewhat equal concentrations in all fractions including adsorbed/exchangeable, carbonates, HFO, crystalline iron oxides, sulfides and OM.
2) The primary source of Mo found in the aquifer matrix and groundwater was mainly attributed to the OM rather than pyrite, whereas As originated mainly from pyrite as a primary source as well as from HFO in the adsorbed forms. There was a positive correlation between Mo and OM (R^2 = 0.71 and $p < 0.001$). The results of chromium-reducible sulfur (CRS) did not point to the presence of Mo in pyrite in DEP drill cores, but as a minor source in the APF.
3) Geochemical modeling indicated that powellite was super-saturated in the Lithia water wells. The dissolution of the synthesized powellite which was already mixed with sample R13 1090 (Mo and As free sample) in DDI water and groundwater demonstrated that only minor amounts of powellite were released from the aquifer matrix sample. Powellite was not dissolvable in the pH range of the groundwater of study area. All these findings indicated that powellite could not be considered as a source for Mo.

4) Geochemical modeling also showed that in the Lithia area, Mo sorption onto HFO decreased with an increase in the groundwater pH. Also, adsorption of Mo was initially nonlinear but adsorption isotherms became more linear as pH increased. The amount of Mo adsorbed decreased with increasing aqueous concentration. Phosphate strongly competed with molybdate for adsorption onto HFO. Similarly, sulfate competed for HFO sorption sites, but less than phosphate.

5) The batch experiments of the Mo–HFO systems indicated that the adsorption affinity of Mo onto HFO was highly dependent on pH. Almost 100% of Mo was adsorbed at low pH, whereas little Mo adsorption occurred at pH above 8 at all surface coverage. Arsenic(III) and As(V) adsorption onto HFO was strongly pH dependent. Compared to Mo, As(III) and As(V) were adsorbed much more strongly to HFO at pH range of 7 to 9, which corresponded to the pH range of the groundwater in the study area. Molybdenum sorption onto HFO happened mainly via forming inner-sphere complexes. Arsenic(III) and As(V) sorption onto HFO were, in contrary, through inner-spherical complexes.

6) The Mo adsorption capacity of humic acid (HA) and purified humic acid (PHA) was high at around pH 3 but decreased exponentially with increasing pH; it remained constant at pH above 7. However, this may not be the ultimate role of OM in the aquifer in question because OM has high ability for complexing metal ions, formation of colloids and coating the mineral surface sites which have high potential to influence Mo behavior in the study area.

7) Hydrous ferric oxide was not a main sink for Mo but a significant secondary source for As. Dissolved oxygen inflicted no significant impact on the concentration of dissolved Mo and As in the Lithia area and APF.

6. 2 Outlooks and recommendations for further research

This study has dealt with geogenic Mo and As as potential contaminants in a limestone aquifer in Central Florida, USA. While there are some similar studies with respect to As, this is the first study of its kind with respect to Mo. Thus, more efforts are still required to study geochemistry of Mo along the following lines:

1) Organic matter was proved to be the main primary source for Mo. Consequently, its oxidation and degradation is the main cause of groundwater contamination. However, processes leading to the fixation and association of Mo with OM are still not well understood. One approach to deal with this phenomenon is to scavenge Mo with HA in the laboratory. There are two general approaches; synthetic and analytic. In the synthetic approach, one would dig into the literature of organic chemistry to list known reactions of molybdate, thiomolybdate, etc. with organic molecules. Alternatively, one might postulates what organic natural products are likely to scavenge Mo, and then design experiments to prove that accordingly. In the analytic approach, one would look for new ways of establishing the nature of Mo binding to OM. For example, finding new ways to chromatographically separating the organic extracts in a sequential extraction procedure (SEP) to see where Mo moves to? There are some very interesting syncrotron-based microscopic methods available that could be very useful.

2) Although, SEP provides useful information about chemical speciation of the elements but from adsorption point of view this technique is insufficient. For example, we designed experiments and found that about 20% of total Mo which was co-precipitated with HFO was released in step1 (exchangeable phase, Chapter 3), while HFO itself dissolves in step 3. Similar behavior are expected from other adsorbents such as carbonate, Al oxides, clay minerals, OM, and etc. Therefore, these complexities need to be addressed by conducting extensive research.

3) The simultaneous/competitive adsorption behavior of Mo with other paragenesis elements (As, P, V, U, S) which is affected by factors such as the sequence of addition of species,

adsorbate/adsorbent ratios, and ionic strength with/without the presence of natural organic matters.

With respect to Lithia area in Central Florida, it is recommended to provide more adsorption surfaces to reduce Mo and As health risk for the drinking water. Such practice could be carried out, for example, by injecting HFO into the groundwater. It is also necessary to manage fertilizers application which contain phosphate to reduce its concentration in the groundwater as a strong competitor for sorption sites. A potential remedy for the As and Mo problem in the Lithia area may be to install water wells with discrete screens in the Suwannee Limestone or deeper. It is recommended to include Mo in the analytical program whenever elevated As concentrations are encountered in aquifers of marine origin.

Acknowledgements

I would like to offer my greatest appreciations to my advisor Prof. Dr. Thomas Pichler, for all the help and support he generously provided during my PhD studies. Thank you Thomas for encouraging me during my research and for inspiring me to grow as a research scientist; your precise advices for my research as well as for my career have been priceless.

Writing a thesis is a difficult task and I could not have finished this project without the support of Prof. Dr Gholam Abbas Kazemi. Words cannot express my gratitude and appreciation to him for all his candid editorial comments and valuable knowledge.

I also thank Dr. Kay Hamer for his advices and discussions during the last few years. Furthermore, I am indebted to the members of the AG Geochemistry and Hydrogeology, for their assistance and support. Many thanks go especially to Laura Knigge for the support with all the time consuming complicated laboratory works. Thanks are also due to Dr. Maria Jose Ruiz for her assistance during the earlier stage of my study to get familiar with the laboratory. Thanks to Dr. Lars-Eric Heimbürgeron for analyzing some of my samples. I am grateful to Britta Hinz-Stolle for translating the thesis abstract into German and for all the efforts and time. It was a pleasure for me to do PhD studies along with my fellow students including Dr. Christian Breuer, Dr. Wu Debo, Dr. Budi Joko Purnomo, Dr. Qi Pengfei, Andereas Kubier and Estelle Kemayou Tchamako. I would also like to thank Dr. Nabil Khan Niyazi for kindly accepting to review this thesis.

Finally, special thanks go out to my family, for their support, encouragement and patience during my study. To my lovely wife, Maryam, who inspired me and provided constant encouragement during the entire process. To my little daughter, Elina, who brought us blessings and happiness. I sincerely thank both of them for their patience and love which was beyond my imagination.

References

Abernathy, C.O., Liu, Y.-P., Longfellow, D., Aposhian, H.V., Beck, B., Fowler, B., Goyer, R., Menzer, R., Rossman, T., Thompson, C., 1999. Arsenic: health effects, mechanisms of actions, and research issues. Environmental health perspectives 107, 593-597.

Adelson, J.M., Helz, G.R., Miller, C.V., 2002. Reconstructing the rise of recent coastal anoxia; molybdenum in Chesapeake Bay sediments. Geochimica Et Cosmochimica Acta 66, 4367-4367.

Amini, M., Abbaspour, K.C., Berg, M., Winkel, L., Hug, S.J., Hoehn, E., Yang, H., Johnson, C.A., 2008. Statistical modeling of global geogenic arsenic contamination in groundwater. Environ Sci Technol 42, 3669-3675.

Anbar, A.D., 2004. Molybdenum stable isotopes: observations, interpretations and directions. Reviews in Mineralogy and Geochemistry 55, 429-454.

Andrew R. Felmy, Dhanpat Rai, Mason, a.M.J., 1992. The solubility of powellite and an aqueous thermodynamic model for calcium-molybdate ion-interactions. Journal of Solution Chemistry 21.

Appleyard, S., Angeloni, J., Watkins, R., 2006. Arsenic-rich groundwater in an urban area experiencing drought and increasing population density, Perth, Australia. Applied Geochemistry 21, 83-97.

Arthur, J.D., Wood, H.A.R., Baker, A.E., Cichon, J.R., Raines, G.L., 2007. Development and implementation of a Bayesian-based aquifer vulnerability assessment in Florida. Natural Resources Research 16, 93-107.

Banning, A., Rüde, T.R., 2010. Enrichment processes of arsenic in oxidic sedimentary rocks–From geochemical and genetic characterization to potential mobility. Water Research 44, 5512-5531.

Berislav, M., 1999. A case report of acute human molybdenum toxicity from a dietary molybdenum supplement--a new member of the "Lucor metallicum" family. Arhiv za higijenu rada i toksikologiju 50, 289-297.

Bertine, K.K., Turekian, K.K., 1973. Molybdenum in marine deposits. Geochimica Et Cosmochimica Acta 37, 1415-1434.

Bibak, A., Borggaard, O., 1994. Molybdenum adsorption by aluminum and iron oxides and humic acid. Soil Science 158, 323-328.

Borah, D., Senapati, K., 2006. Adsorption of Cd (II) from aqueous solution onto pyrite. Fuel 85, 1929-1934.

Bostick, B.C., Fendorf, S., Helz, G.R., 2003. Differential adsorption of molybdate and tetrathiomolybdate on pyrite Environ Sci Technol 37, 285-291.

Brumsack, H.-J., 2006. The trace metal content of recent organic carbon-rich sediments: Implications for Cretaceous black shale formation. Palaeogeography, Palaeoclimatology, Palaeoecology 232, 344-361.

Budd, D.A., Vacher, H., 2004. Matrix permeability of the confined Floridan Aquifer, Florida, USA. Hydrogeology Journal 12, 531-549.

Burton, E.D., Sullivan, L.A., Bush, R.T., Johnston, S.G., Keene, A.F., 2008. A simple and inexpensive chromium-reducible sulfur method for acid-sulfate soils. Applied Geochemistry 23, 2759-2766.

Campillo, N., López-García, I., Viñas, P., Arnau-Jerez, I., Hernández-Córdoba, M., 2002. Determination of vanadium, molybdenum and chromium in soils, sediments and sludges by electrothermal atomic absorption spectrometry with slurry sample introduction. Journal of Analytical Atomic Spectrometry 17, 1429-1433.

Canfield, D.E., Raiswell, R., Westrich, J.T., Reaves, C.M., Berner, R.A., 1986. The use of chromium reduction in the analysis of reduced inorganic sulfur in sediments and shales. Chemical Geology 54, 149-155.

Carroll, K.C., Artiola, J.F., Brusseau, M.L., 2006. Transport of molybdenum in a biosolid-amended alkaline soil. Chemosphere 65, 778-785.

Cederkvist, K., Holm, P.E., Jensen, M.B., 2010. Full-scale removal of arsenate and chromate from water using a limestone and ochreous sludge mixture as a low-cost sorbent material. Water Environment Research 82, 401-408.

Chappaz, A., Lyons, T.W., Gregory, D.D., Reinhard, C.T., Gill, B.C., Li, C., Large, R.R., 2014. Does pyrite act as an important host for molybdenum in modern and ancient euxinic sediments? Geochimica et Cosmochimica Acta 126, 112-122.

Clark, K., 1972. Stockwork molybdenum deposits in the western Cordillera of North America. Economic Geology 67, 731-758.

Cornell, R., Giovanoli, R., Schindler, P., 1987. Effect of silicate species on the transformation of ferrihydrite into goethite and hematite in alkaline media. Clays and Clay Minerals 35, 21-28.

Cot, 2003. Expert Group on Vitamins and Minerals (2003).Risk assessment: Molybdenum.

Couture, R.-M., Wallschläger, D., Rose, J., Van Cappellen, P., 2013. Arsenic binding to organic and inorganic sulfur species during microbial sulfate reduction: a sediment flow-through reactor experiment. Environmental Chemistry 10, 285-294.

Crusius, J., Calvert, S., Pedersen, T., Sage, D., 1996. Rhenium and molybdenum enrichments in sediments as indicators of oxic, suboxic and sulfidic conditions of deposition. Earth and Planetary Science Letters 145, 65-78.

Dahl, T.W., Anbar, A.D., Gordon, G.W., Rosing, M.T., Frei, R., Canfield, D.E., 2010. The behavior of molybdenum and its isotopes across the chemocline and in the sediments of sulfidic Lake Cadagno, Switzerland. Geochimica Et Cosmochimica Acta 74, 144-163.

Dahl, T.W., Chappaz, A., Fitts, J.P., Lyons, T.W., 2013. Molybdenum reduction in a sulfidic lake: Evidence from X-ray absorption fine-structure spectroscopy and implications for the Mo paleoproxy. Geochimica et Cosmochimica Acta 103, 213-231.

Das, A.K., Chakraborty, R., Cervera, M.L., De la Guardia, M., 2007. A review on molybdenum determination in solid geological samples. Talanta 71, 987-1000.

Das, S., Jim Hendry, M., 2013. Adsorption of molybdate by synthetic hematite under alkaline conditions: Effects of aging. Applied Geochemistry 28, 194-201.

Datta, D and Subramanian, V. (1997). Texture and Mineralogy of sedimentsfrom the Ganges-BrahmaputraMeghna river system in the Bengal Basin, Bangladesh and their environmentalimplications. Env. Geology, 30(3/4): 181--188

Davis, J.A., 1984. Complexation of trace metals by adsorbed natural organic matter. Geochimica Et Cosmochimica Acta 48, 679-691.

Davis, J.A., James, R.O., Leckie, J.O., 1978. Surface ionization and complexation at the oxide/water interface: I. Computation of electrical double layer properties in simple electrolytes. Journal of Colloid and Interface Science 63, 480-499.

Diels, L., Vanbroekhoven, K., 2008. Remediation of metal and metalloid contaminated groundwater, methods and techniques for cleaning-up contaminated sites. Springer, pp. 1-23.

Drever, J.I., 1988. The geochemistry of natural waters. Prentice Hall New Jersey.

Dzombak, D.A., Morel, F.M., 1990. Surface complexation modeling: hydrous ferric oxide. John Wiley & Sons.

Einsle, O., Kroneck, P.M.H., 2004. Structural basis of denitrification. Biol Chem 385, 875-883.

Elliott, H.A., Taylor, M., 2000. Molybdenum montent of water treatment residuals. J. Environ. Qual. 29, 1835-1839.

Erickson, B.E., Helz, G.R., 2000. Molybdenum(VI) speciation in sulfidic waters: Stability and lability of thiomolybdates. Geochimica Et Cosmochimica Acta 64, 1149-1158.

Ferguson, J.F., Gavis, J., 1972. A review of the arsenic cycle in natural waters. Water Research 6, 1259-1274.

Ferreiro, E., Helmy, A., De Bussetti, S., 1985. Molybdate sorption by oxides of aluminium and iron. Zeitschrift für Pflanzenernährung und Bodenkunde 148, 559-566.

Giménez, J., Martínez, M., de Pablo, J., Rovira, M., Duro, L., 2007. Arsenic sorption onto natural hematite, magnetite, and goethite. Journal of Hazardous Materials 141, 575-580.

Glass, J.B., Chappaz, A., Eustis, B., Heyvaert, A.C., Waetjen, D.P., Hartnett, H.E., Anbar, A.D., 2013. Molybdenum geochemistry in a seasonally dysoxic Mo-limited lacustrine ecosystem. Geochimica Et Cosmochimica Acta 114, 204-219.

Goldberg, S., 1985. Chemical modeling of anion competition on goethite using the constant capacitance model. Soil Science Society of America Journal 49, 851-856.

Goldberg, S., 2010. Competitive adsorption of molybdenum in the presence of phosphorus or sulfur on gibbsite. Soil Science 175, 105-110.

Goldberg, S., Forster, H., 1998. Factors affecting molybdenum adsorption by soils and minerals. Soil Science 163, 109-114.

Goldberg, S., Forster, H.S., Godfrey, C.L., 1996. Molybdenum adsorption on oxides, clay minerals, and soils. Soil Sci. Soc. Am. J. 60, 425-432.

Goldberg, S., Johnston, C.T., 2001. Mechanisms of arsenic adsorption on amorphous oxides evaluated using macroscopic measurements, vibrational spectroscopy, and surface complexation modeling. Journal of Colloid and Interface Science 234, 204-216.

Goldberg, T., Archer, C., Vance, D., Poulton, S.W., 2009. Mo isotope fractionation during adsorption to Fe (oxyhydr)oxides. Geochimica et Cosmochimica Acta 73, 6502-6516.

Gröger, J., Franke, J., Hamer, K., Schulz, H.D., 2009. Quantitative recovery of elemental sulfur and improved selectivity in a chromium-reducible sulfur distillation. Geostandards and Geoanalytical Research 33, 17-27.

Gustafsson, J.P., 2003. Modelling molybdate and tungstate adsorption to ferrihydrite. Chemical Geology 200, 105-115.

Haack, S.K., Rachol, C.M., 2000. Arsenic in groundwater in Washtenaw County, Michigan. US Dept. of the Interior, US Geological Survey.

Hall, G.E.M., Vaive, J.E., Beer, R., Hoashi, M., 1996. Selective leaches revisited, with emphasis on the amorphous Fe oxyhydroxide phase extraction. Journal of Geochemical Exploration 56, 59-78.

Harvey, C.F., Swartz, C.H., Badruzzaman, A., Keon-Blute, N., Yu, W., Ali, M.A., Jay, J., Beckie, R., Niedan, V., Brabander, D., 2002. Arsenic mobility and groundwater extraction in Bangladesh. Science 298, 1602-1606.

Hayes, K.F., Leckie, J.O., 1987. Modeling ionic strength effects on cation adsorption at hydrous oxide/solution interfaces. Journal of Colloid and Interface Science 115, 564-572.

Hayes, K.F., Papelis, C., Leckie, J.O., 1988. Modeling ionic strength effects on anion adsorption at hydrous oxide/solution interfaces. Journal of Colloid and Interface Science 125, 717-726.

Heinrichs, G., Udluft, P., 1999. Natural arsenic in Triassic rocks: a source of drinking-water contamination in Bavaria, Germany. Hydrogeology Journal 7, 468-476.

Helz, G.R., Bura-Nakić, E., Mikac, N., Ciglenečki, I., 2011. New model for molybdenum behavior in euxinic waters. Chemical Geology 284, 323-332.

Helz, G.R., Miller, C.V., Charnock, J.M., Mosselmans, J.F.W., Pattrick, R.A.D., Garner, C.D., Vaughan, D.J., 1996. Mechanism of molybdenum removal from the sea and its concentration in black shales: EXAFS evidence. Geochimica Et Cosmochimica Acta 60, 3631-3642.

Helz, G.R., Vorlicek, T.P., Kahn, M.D., 2004. Molybdenum scavenging by iron monosulfide. Environ Sci Technol 38, 4263-4268.

Hiemstra, T., Van Riemsdijk, W., Bolt, G., 1989. Multisite proton adsorption modeling at the solid/solution interface of (hydr) oxides: A new approach: I. Model description and evaluation of intrinsic reaction constants. Journal of Colloid and Interface Science 133, 91-104.

Hollister, V.F., 1978. Geology of the porphyry copper deposits of the western hemisphere. Society for Mining Metallurgy.

Johnson, C., Breward, N., Ander, E., Ault, L., 2005. G-BASE: baseline geochemical mapping of Great Britain and Northern Ireland. Geochemistry: Exploration, Environment, Analysis 5, 347-357.

Jones, L., 1957. The solubility of molybdenum in simplified systems and aqueous soil suspensions. Journal of Soil Science 8, 313-327.

Kaback, D.S., Runnells, D.D., 1980. Geochemistry of molybdenum in some stream sediments and waters. Geochimica et Cosmochimica Acta 44, 447-&.

Karimian, N., Cox, F., 1978. Adsorption and extractability of molybdenum in relation to some chemical properties of soil. Soil Science Society of America Journal 42, 757-761.

Kaspar, H., 1983. Denitrification, nitrate reduction to ammonium, and inoganic nitrogen pools in intetidal sediments. Marine biology 74, 133-139.

Kersten, M., Karabacheva, S., Vlasova, N., Branscheid, R., Schurk, K., Stanjek, H., 2014. Surface complexation modeling of arsenate adsorption by akagenéite (β-FeOOH)-dominant granular ferric hydroxide. Colloids and Surfaces A: Physicochemical and Engineering Aspects 448, 73-80.

Kinniburgh, D.G., Newell, A.J., Davies, J., Smedley, P.L., Milodowski, A.E., Ingram, J.A., Merrin, P.D., 2006. The arsenic concentration in groundwater from the Abbey Arms Wood observation borehole, Delamere, Cheshire, UK. Geological Society, London, Special Publications 263, 265-284.

Kosmulski, M., 2002. The pH-dependent surface charging and the points of zero charge. Journal of Colloid and Interface Science 253, 77-87.

Kraus, T.E., Dahlgren, R.A., Zasoski, R.J., 2003. Tannins in nutrient dynamics of forest ecosystems-a review. Plant and Soil 256, 41-66.

Krishnamachari KA, K.K., 1974. An epidemiological study of the syndrome of genu valgum among residents ofendemic areas for fluorosis in Andhra Pradesh. Indian journal of medical research 62, 1415-1423.

Krishnamachari, K.A., Krishnaswamy, K., 1974. An epidemiological study of the syndrome of genu valgum among residents of endemic areas for fluorosis in Andhra Pradesh. Indian J Med Res 62, 1415-1423.

Legeleux, F., Reyss, J.-L., Schmidt, S., 1994. Particle mixing rates in sediments of the northeast tropical Atlantic: evidence from 210 Pb xs, 137 Cs, 228 Th xs and 234 Th xs downcore distributions. Earth and Planetary Science Letters 128, 545-562.

Lenoble, V., Bouras, O., Deluchat, V., Serpaud, B., Bollinger, J.-C., 2002. Arsenic adsorption onto Pillared clays and iron oxides. Journal of Colloid and Interface Science 255, 52-58.

Li, Y.-H., 2000. A compendium of geochemistry: from solar nebula to the human brain. Princeton University Press.

Lyons, T.W., Werne, J.P., Hollander, D.J., Murray, R.W., 2003. Contrasting sulfur geochemistry and Fe/Al and Mo/Al ratios across the last oxic-to-anoxic transition in the Cariaco Basin, Venezuela. Chemical Geology 195, 131-157.

Mamindy-Pajany, Y., Hurel, C., Marmier, N., Roméo, M., 2009. Arsenic adsorption onto hematite and goethite. Comptes Rendus Chimie 12, 876-881.

Manning, B.A., Goldberg, S., 1996. Modeling competitive adsorption of arsenate with phosphate and molybdate on oxide minerals. Soil Science Society of America Journal 60, 121-131.

Marks, J.A., Perakis, S.S., King, E.K., Pett-Ridge, J., 2015. Soil organic matter regulates molybdenum storage and mobility in forests. Biogeochemistry 125, 167-183.

Matern, K., Mansfeldt, T., 2015. Molybdate adsorption by birnessite. Applied Clay Science 108, 78-83.

McEwan, A.G., Ridge, J.P., McDevitt, C.A., Hugenholtz, P., 2002. The DMSO reductase family of microbial molybdenum enzymes; Molecular properties and role in the dissimilatory reduction of toxic elements. Geomicrobiol J 19, 3-21.

McNeill, L.S., Edwards, M., 1995. Soluble arsenic removal at water treatment plants. Journal of the American Water Works Association 87.

Meng, X., Bang, S., Korfiatis, G.P., 2000. Effects of silicate, sulfate, and carbonate on arsenic removal by ferric chloride. Water Research 34, 1255-1261.

Merkel, B.J., Planer-Friedrich, B., Nordstrom, D., 2005. Groundwater geochemistry. A practical guide to modeling of natural and contaminated aquatic systems 2.

Mikkonen, A., Tummavuori, J., 1993. Retention of vanadium (V), molybdenum (VI) and tungsten (VI) by kaolin. Acta Agriculturae Scandinavica B-Plant Soil Sciences 43, 11-15.

Miller, C.A., Peucker-Ehrenbrink, B., Walker, B.D., Marcantonio, F., 2011. Re-assessing the surface cycling of molybdenum and rhenium. Geochimica Et Cosmochimica Acta 75, 7146-7179.

Mitry, E., Baudin, E., Ducreux, M., Sabourin, J., Rufie, P., Aparicio, T., Lasser, P., Elias, D., Duvillard, P., Schlumberger, M., 1999. Treatment of poorly differentiated neuroendocrine tumours with etoposide and cisplatin. British Journal of Cancer 81, 1351.

Mohan, D., Pittman Jr, C.U., 2007. Arsenic removal from water/wastewater using adsorbents—A critical review. Journal of Hazardous Materials 142, 1-53.

Momcilovic, B., 2000. Acute human molybdenum toxicity from a dietary molybdenum supplement—a new member of the “lucor metallicum” family, Trace Elements in Man and Animals 10. Springer, pp. 699-700.

Mongenot, T., Tribovillard, N.-P., Desprairies, A., Lallier-Vergès, E., Laggoun-Defarge, F., 1996. Trace elements as palaeoenvironmental markers in strongly mature hydrocarbon source rocks: the Cretaceous La Luna Formation of Venezuela. Sedimentary Geology 103, 23-37.

Moore, L., Machlan, L., Shields, W., Garner, E., 1974. Internal normalization techniques for high accuracy isotope dilution analyses. Application to molybdenum and nickel in standard reference materials. Analytical Chemistry 46, 1082-1089.

Morford, J.L., Emerson, S., 1999. The geochemistry of redox sensitive trace metals in sediments. Geochimica Et Cosmochimica Acta 63, 1735-1750.

Morrison, S.J., Mushovic, P.S., Niesen, P.L., 2006. Early breakthrough of molybdenum and uranium in a permeable reactive barrier. Environ Sci Technol 40, 2018-2024.

Morrison, S.J., Spangler, R.R., 1992. Extraction of uranium and molybdenum from aqueous-solutions - a survey of industrial materials for use in chemical barriers for uranium mill tailings remediation. Environ Sci Technol 26, 1922-1931.

Motta, M.M., Miranda, C., 1989. Molybdate adsorption on kaolinite, montmorillonite, and illite: Constant capacitance modeling. Soil Science Society of America Journal 53, 380-385.

Nickson, R., McArthur, J., Burgess, W., Ahmed, K.M., Ravenscroft, P., Rahmann, M., 1998. Arsenic poisoning of Bangladesh groundwater. Nature 395, 338-338.

Nickson, R., McArthur, J., Ravenscroft, P., Burgess, W., Ahmed, K., 2000. Mechanism of arsenic release to groundwater, Bangladesh and West Bengal. Applied Geochemistry 15, 403-413.

Nriagu, J.O., Bhattacharya, P., Mukherjee, A.B., Bundschuh, J., Zevenhoven, R., Loeppert, R.H., 2007. Arsenic in soil and groundwater: an overview, Trace metals and other contaminants in the environment. Elsevier, pp. 3-60.

O'Shea, B., Jankowski, J., Sammut, J., 2007. The source of naturally occurring arsenic in a coastal sand aquifer of eastern Australia. Science of the Total Environment 379, 151-166.

Passier, H., Böttcher, M., Lange, G.D., 1999. Sulfur enrichment in organic matter of eastern mediterranean sapropels: a study of sulfur isotope partitioning. Aquatic Geochemistry 5, 99-118.

Peterson, M., Carpenter, R., 1986. Arsenic distributions in porewaters and sediments of Puget Sound, Lake Washington, the Washington coast and Saanich Inlet, BC. Geochimica Et Cosmochimica Acta 50, 353-369.

Philippot, L., Hojberg, O., 1999. Dissimilatory nitrate reductases in bacteria. Bba-Gene Struct Expr 1446, 1-23.

Pichler, T., Hendry, M.J., Hall, G.E.M., 2001. The mineralogy of arsenic in uranium mine tailings at the Rabbit Lake in-pit Facility, northern Saskatchewan, Canada. Environmental Geology 40, 495-506.

Pichler, T., Mozaffari, A., 2015. Distribution and mobility of geogenic molybdenum and arsenic in a limestone aquifer matrix. Applied Geochemistry 63, 623-633.

Pichler, T., Renshaw, C.E., Sültenfuß, J., 2016. Geogenic As and Mo groundwater contamination caused by an abundance of domestic supply wells. Applied Geochemistry.

Pierce, M.L., Moore, C.B., 1982. Adsorption of arsenite and arsenate on amorphous iron hydroxide. Water Research 16, 1247-1253.

Planer-Friedrich, B., Fisher, J.C., Hollibaugh, J.T., Suss, E., Wallschlager, D., 2009. Oxidative Transformation of trithioarsenate along alkaline geothermal drainages abiotic versus microbially mediated processes. Geomicrobiol J 26, 339-350.

Planer-Friedrich, B., London, J., McCleskey, R.B., Nordstrom, D.K., Wallschlager, D., 2007. Thioarsenates in geothermal waters of yellowstone national park: Determination, preservation, and geochemical importance. Environ Sci Technol 41, 5245-5251.

Prasad Saripalli, K., McGrail, B.P., Girvin, D.C., 2002. Adsorption of molybdenum on to anatase from dilute aqueous solutions. Applied Geochemistry 17, 649-656.

Price, R.E., Pichler, T., 2006. Abundance and mineralogical associations of naturally occurring arsenic in the Suwannee Limestone, Upper Floridan Aquifer. Chemical Geology 228, 44-56.

Qi, P., Pichler, T., 2014. Closer Look at As (III) and As (V) Adsorption onto Ferrihydrite under Competitive Conditions. Langmuir 30, 11110-11116.

Randazzo, A.F., Jones, D.S., 1997. The geology of Florida. University Press of Florida.

Reza, A.H.M.S., Jean, J.S., Yang, H.J., Lee, M.K., Woodall, B., Liu, C.C., Lee, J.F., Luo, S.D., 2010. Occurrence of arsenic in core sediments and groundwater in the Chapai-Nawabganj District, northwestern Bangladesh. Water Research 44, 2021-2037.

Riboulleau, A., Derenne, S., Sarret, G., Largeau, C., Baudin, F., Connan, J., 2000. Pyrolytic and spectroscopic study of a sulfur-rich kerogen from the “Kashpir oil shales”(Upper Jurassic, Russian platform). Organic Geochemistry 31, 1641-1661.

Roy, W., Hassett, J., Griffin, R., 1986. Competitive coefficients for the adsorption of arsenate, molybdate, and phosphate mixtures by soils. Soil Science Society of America Journal 50, 1176-1182.

Saada, A., Breeze, D., Crouzet, C., Cornu, S., Baranger, P., 2003. Adsorption of arsenic (V) on kaolinite and on kaolinite–humic acid complexes: Role of humic acid nitrogen groups. Chemosphere 51, 757-763.

Schaller, M.S., Koretsky, C.M., Lund, T.J., Landry, C.J., 2009. Surface complexation modeling of Cd(II) adsorption on mixtures of hydrous ferric oxide, quartz and kaolinite. Journal of Colloid and Interface Science 339, 302-309.

Schindler, P., Gamsjäger, H., 1972. Acid—base reactions of the anatase - water interface and the point of zero charge of anatase suspensions. Kolloid-Zeitschrift und Zeitschrift für Polymere 250, 759-763.

Schreiber, M.E., Simo, J.A., Freiberg, P.G., 2000. Stratigraphic and geochemical controls on naturally occurring arsenic in groundwater, eastern Wisconsin, USA. Hydrogeology Journal 8, 161-176.

Scott, T.M., Arthur, J., Rupert, F., Upchurch, S., Randazzo, A., 1989. The lithostratigraphy and hydrostratigraphy of the Floridan Aquifer System in Florida. Wiley Online Library.

Shan, H., Ma, T., Wang, Y., Zhao, J., Han, H., Deng, Y., He, X., Dong, Y., 2013. A cost-effective system for in-situ geological arsenic adsorption from groundwater. Journal of Contaminant Hydrology 154, 1-9.

Shimp, N.F., Schleicher, J.A., Ruch, R., Heck, D.B., Leland, H.V., 1971. Trace element and organic carbon accumulation in the most recent sediments of southern Lake Michigan. Environmental geology no. 041.

Singh, D.B., Prasad, G., Rupainwar, D.C., 1996. Adsorption technique for the treatment of As(V)-rich effluents. Colloids and Surfaces A: Physicochemical and engineering aspects 111, 49-56.

Slaveykova, V.I., Wilkinson, K.J., 2005. Predicting the bioavailability of metals and metal complexes: Critical review of the biotic ligand model. Environmental Chemistry 2, 9-24.

Smedley, P.L., Kinniburgh, D.G., 2001. Source and behavior of arsenic in natural waters. United Nations synthesis report on arsenic in drinking water. World Health Organization, Geneva, Switzerland. http://www. who. int/water_sanitation_health/dwq/arsenicun1. pdf, 1-61.

Smedley, P.L., Kinniburgh, D.G., 2002. A review of the source, behavior and distribution of arsenic in natural waters. Applied Geochemistry 17, 517-568.

Somasundaran, P., Agar, G.E., 1967. The zero point of charge of calcite. Journal of Colloid and Interface Science 24, 433-440.

Sposito, G., 1984. The surface chemistry of soils. Oxford University Press.

Stiefel, E.I., 1996. Molybdenum Bolsters the Bioinorganic Brigade. Science 272, 1599-1600.

Stollenwerk, K.G., 1998. Molybdate transport in a chemically complex aquifer: Field measurements compared with solute-transport model predictions. Water Resources Research 34, 2727-2740.

Swedlund, P.J., Webster, J.G., 1999. Adsorption and polymerisation of silicic acid on ferrihydrite, and its effect on arsenic adsorption. Water Research 33, 3413-3422.

Takeno, N., 2005. Atlas of Eh-pH diagrams. Geological survey of Japan open file report 419, 102.

Taylor, R., Hammarstrom, J., Piatak, N., Seal, R., 2012. Arc-related porphyry molybdenum deposit model. US Geological Survey Scientific Investigations Report, 64.

Taylor, S.R., McLennan, S.M., 1985. The continental crust: its composition and evolution.

Thornburg, K., Sahai, N., 2004. Arsenic occurrence, mobility, and retardation in sandstone and dolomite formations of the Fox River Valley, Eastern Wisconsin. Environ Sci Technol 38, 5087-5094.

Tiberg, C., Sjöstedt, C., Persson, I., Gustafsson, J.P., 2013. Phosphate effects on copper (II) and lead (II) sorption to ferrihydrite. Geochimica Et Cosmochimica Acta 120, 140-157.

Tribovillard, N., Lyons, T.W., Riboulleau, A., Bout-Roumazeilles, V., 2008. A possible capture of molybdenum during early diagenesis of dysoxic sediments. B Soc Geol Fr 179, 3-12.

Tribovillard, N., Riboulleau, A., Lyons, T., Baudin, F.O., 2004. Enhanced trapping of molybdenum by sulfurized marine organic matter of marine origin in Mesozoic limestones and shales. Chemical Geology 213, 385-401.

Ure, A., Berrow, M., 1982. Environmental chemistry. Spec. Period. Rep 2, 94-204.

Vorlicek, T.P., Helz, G.R., 2002. Kaolinite-catalyzed sulfidation of trithiomolybdate: Comparison of rates measured and predicted from the reverse reaction. Abstracts of papers of the American Chemical Society 223, U617-U617.

Vorlicek, T.P., Kahn, M.D., Kasuza, Y., Helz, G.R., 2004. . , 547– 556. , 2004. Capture of Mo in pyriteforming sediments: role of ligandinduced reduction by polysulfides. Geochimica et Cosmochimica Acta 68, 547– 556.

Wang, M., Zheng, B., Wang, B., Li, S., Wu, D., Hu, J., 2006. Arsenic concentrations in Chinese coals. Science of the total environment 357, 96-102.

Wasay, S.A., Haron, M.J., Uchiumi, A., Tokunaga, S., 1996. Removal of arsenite and arsenate ions from aqueous solution by basic yttrium carbonate. Water Research 30, 1143-1148.

Weng, C., Wang, J., Huang, C., 1997. Adsorption of Cr (VI) onto titanium from dilute aqueous solutions. Water science and technology 35, 55-62.

Werne, J.P., Lyons, T.W., Hollander, D.J., Schouten, S., Hopmans, E.C., Damste, J.S.S., 2008. Investigating pathways of diagenetic organic matter sulfurization using compound-specific sulfur isotope analysis. Geochimica Et Cosmochimica Acta 72, 3489-3502.

WHO, 1993. Guidelines for drinking-water quality. World Health Organization, Geneva.

WHO, 2011. Guidelines for drinking-water quality. Geneva: world health organization.

Wichard, T., Mishra, B., Myneni, S.C., Bellenger, J.-P., Kraepiel, A.M., 2009. Storage and bioavailability of molybdenum in soils increased by organic matter complexation. Nature Geoscience 2, 625-629.

Wilde, P., Lyons, T.W., Quinby-Hunt, M.S., 2004. Organic carbon proxies in black shales: molybdenum. Chemical Geology 206, 167-176.

Williams, J.H., Paillet, F.L., 2002. Using flowmeter pulse tests to define hydraulic connections in the subsurface: a fractured shale example. Journal of Hydrology 265, 100-117.

Wolthers, M., Charlet, L., van Der Weijden, C.H., van der Linde, P.R., Rickard, D., 2005. Arsenic mobility in the ambient sulfidic environment: Sorption of arsenic(V) and arsenic(III) onto disordered mackinawite. Geochimica Et Cosmochimica Acta 69, 3483-3492.

Wu, C.-H., Lo, S.-L., Lin, C.-F., 2000. Competitive adsorption of molybdate, chromate, sulfate, selenate, and selenite on γ-Al 2 O 3. Colloids and Surfaces A: Physicochemical and Engineering Aspects 166, 251-259.

Wu, C.-H., Lo, S.-L., Lin, C.-F., Kuo, C.-Y., 2001. Modeling competitive adsorption of molybdate, sulfate, and selenate on γ-Al2O3 by the Triple-Layer Model. Journal of Colloid and Interface Science 233, 259-264.

Xu, N., Christodoulatos, C., Braida, W., 2006. Adsorption of molybdate and tetrathiomolybdate onto pyrite and goethite: effect of pH and competitive anions. Chemosphere 62, 1726-1735.

Yudovich, Y.E., Ketris, M.P., 2005. Arsenic in coal: a review. International Journal of Coal Geology 61, 141-196.

Zhang, P.C., Sparks, D.L., 1989. Kinetics and mechanisms of molybdate adsorption/desorption at the goethite/water interface using pressure-jump relaxation. Soil Science Society of America Journal 53, 1028-1034.

Zheng, Y., Anderson, R.F., van Geen, A., Kuwabara, J., 2000. Authigenic molybdenum formation in marine sediments: A link to pore water sulfide in the Santa Barbara Basin. Geochim Cosmochim Ac 64, 4165-4178.

CD Appendix

This CD appendix contains the whole thesis.

Appendix 1

Applied Geochemistry xxx (2015) 1–11

Contents lists available at ScienceDirect

Applied Geochemistry

journal homepage: www.elsevier.com/locate/apgeochem

Distribution and mobility of geogenic molybdenum and arsenic in a limestone aquifer matrix

Thomas Pichler*, Ali Mozaffari

Geochemistry and Hydrogeology, Department of Geosciences, University of Bremen, Klagenfurter Straße, 28359 Bremen, Germany

ARTICLE INFO

Article history:
Received 31 May 2015
Received in revised form
27 July 2015
Accepted 8 August 2015
Available online xxx

Keywords:
Geogenic
Arsenic
Molybdenum
Aquifer matrix
Limestone
Groundwater

ABSTRACT

To investigate the potential of Mo and As as possible geogenic contaminants, three sediment cores were examined to evaluate their mineralogical association, distribution and mobility. The cores were described and analyzed for total organic carbon (TOC), Ca, Mg, Si, Al, P, Sr, As, Mo, Fe, and S content. Except in the uppermost segment, limestone was the main lithology with the occasional presence of dolomite and clay. That change in lithology was also observed in the bulk chemical composition, where Ca, Mg and Sr concentrations increased with depth, while Si, Al and P concentrations decreased with depth. Minor minerals included pyrite (FeS_2), powellite ($CaMoO_4$) and ferrihydrite. The minimum, maximum, median and standard deviations for all analyzed elements, including As and Mo were comparable for all three cores. Molybdenum and As, however, varied significantly with depth and median As and Mo values were above their respective crustal averages of approximately 1.1 mg/kg and 1.5 mg/kg. The median values for As were 1.9 mg/kg in core DEP-1, 3.3 mg/kg in DEP-2 and 1 mg/kg in DEP-5. The median values for Mo were 2.3 mg/kg in core DEP-1, 2.5 mg/kg in DEP-2 and 2.5 mg/kg in DEP-5. Maximum concentrations for As were 101.9 mg/kg, 47.5 mg/kg and 56.2 mg/kg in cores DEP-1, DEP-2 and DEP-5, respectively. Maximum concentrations for Mo were 880 mg/kg, 123 mg/kg and 225 mg/kg in cores DEP-1, DEP-2 and DEP-5, respectively. Electron microprobe analyses of individual minerals revealed variable concentrations of As ranging from approximately 300 to 9000 mg/kg, in pyrite and up to 17,600 mg/kg in powellite ($CaMoO_4$). The Mo concentration in pyrite was consistently below the detection limit of approximately 100 mg/kg. In powellite the Mo concentration was up to 42 wt%.

A subset of 10 samples from different stratigraphic sections and with different As and Mo concentrations was further investigated to assess As and Mo mobility under changing physicochemical conditions. Leaching the aquifer matrix with a 1 M NaOAc solution at a pH of 8.1 removed more than 70% Mo in 8 of the 10 samples. The maximum value was 97%. In contrast to Mo, As was mobilized to a lesser degree. In 8 of the samples less than 30% were removed and the maximum was only 50%. Molybdenum, which seemed to be loosely bound to mineral and organic matter surfaces thus could easily be removed from the aquifer matrix, while As on the other hand should be much less mobile, because it occurred either tightly adsorbed by hydrous ferric oxide or as an impurity in pyrite. Thus, it is advisable to include Mo in the analytical program whenever elevated As concentrations are encountered in groundwater.

1. Introduction

Molybdenum (Mo) is considered an essential element, whose daily requirement for humans is approximately 0.3 mg (WHO, 2011), while at the same time high doses of Mo could be detrimental to human health. The recommendation by the World Health Organization (WHO) for drinking water is that Mo should not exceed 70 μg/L (WHO, 2011). Currently only anthropogenic Mo contamination seems to be of environmental interest and particularly in mining areas it is a well-known contaminant (Davies et al., 2005; Heijerick et al., 2012; Smedley et al., 2014; Zhai et al., 2013) where it is released during mining operations and due to weathering of mine tailings (Price et al., 1999). The deterioration of groundwater, however, is not exclusively due to the direct input of anthropogenic contaminants, such as the discharge of Pb due to battery recycling (e.g., Pichler, 2005). Another process leading to

* Corresponding author.
E-mail address: pichler@uni-bremen.de (T. Pichler).

http://dx.doi.org/10.1016/j.apgeochem.2015.08.006
0883-2927/

groundwater deterioration can be the mobilization of naturally occurring (geogenic) elements induced by anthropogenic perturbations of the physicochemical conditions in the aquifer (e.g., Amini et al., 2008; Ferguson and Gavis, 1972; Korte and Fernando, 1991; McNeill et al., 2002; Peters and Blum, 2003). This type of anthropogenic-induced contamination is a public health issue worldwide. In particular the ongoing catastrophic problems with arsenic (As) in Bangladesh and West Bengal are front-page stories in newspapers and scientific journals (e.g., Ahmed et al., 2006). There is the potential that geogenic Mo could be candidate for anthropogenic-induced widespread groundwater contamination as well. Marine sediments are known to accumulate Mo in organic matter (e.g., Tribovillard et al., 2004) and in pyrite (e.g., Helz et al., 2011, 1996). Since As is known to accumulate in the same two phases the physicochemical conditions that cause the release of As from the aquifer matrix should also release Mo.

Elevated arsenic (As) is a well-known problem in Floridan groundwater, whenever the physicochemical conditions in the aquifer are perturbed due to anthropogenic activities (Arthur et al., 2007; Jones and Pichler, 2007; Katz et al., 2009; Wallis et al., 2011). Thus As is routinely analyzed after completion of new wells, which led to the discovery of elevated As and Mo concentrations in groundwater in a rural area in central Florida (Pichler and Sültenfuß, 2010). There As concentrations of up to 350 μg/L and Mo concentrations of up to 5000 μg/L were measured. The value of 5000 μg/L is substantially above what could be considered "normal" for Mo concentrations in groundwater. Smedley et al. (2014) who studied Mo in Great Britain found a 10 to 90th percentile range of 0.08–2.44 μg/L with a median of 0.57 μg/L and a maximum observation of 230 μg/L in stream water samples (n = 11,600). In groundwater samples the 10 to 90th percentile ranged from 0.035 to 1.80 μg/L with a median of 0.20 μg/L and a maximum observation of 89 μg/L (n = 1735).

While some information about the occurrence and distribution of As in the Floridan aquifer matrix exists (e.g., Pichler et al., 2011), next to nothing is known about Mo. In this study, we present a first look at the distribution and mineralogical association of As together with Mo in a limestone aquifer of marine origin. To estimate As and Mo mobility, a modified extraction was carried out according to the procedure recommended by Pichler et al. (2001).

2. Study area

The study area is located in the municipality of Lithia southeast of Tampa Bay in the United Sates (Fig. 1). There, a multilayered aquifer system exists, which can be subdivided into three distinct hydrostratigraphic units, which are, from the top down: the Surficial Aquifer System (SAS), the Intermediate Aquifer System (IAS), and the Upper Floridan Aquifer System (UFA). Katz et al. (2007) provided detailed mineralogical and lithological descriptions of these units and their regional hydrogeology in central Florida, which were recently reviewed (Hughes et al., 2009). Relevant hydrogeological characteristics of these units are briefly summarized here.

The unconfined SAS consists of unconsolidated to poorly indurated clastic deposits with depths to the water table ranging from about 3 m to 15 m below land surface (Katz et al., 2009). The upper surface of the SAS is defined by the surface topography, which near the wells with high As concentrations is generally about 30 m above mean sea level (amsl) and ranges from about 65 m just to east of the high-As wells to near zero where it intersects Hillsborough Bay about 35 km to the west. Near the high-As concentration wells, the base of the SAS is 10 m amsl and dips to the west at a slope of approximately 0.001. The SAS generally is not used as a major source of water supply because of relatively low yields (less than 19 L/min), high Fe content, and the potential for contamination from the surface. Water table elevations in the SAS generally are above the potentiometric surface of the UFA, indicating downward groundwater flow through the IAS from the SAS to the UFA (Katz et al., 2009).

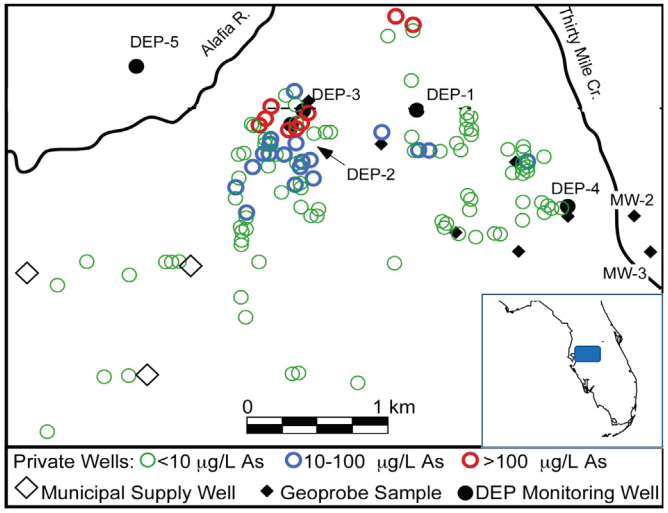

Fig. 1. Location of the study area showing domestic supply wells and their approximate As concentrations and the locations of the three cores, which were sampled for this study (DEP-1, DEP-2 and DEP-5).

The IAS consists of several water-bearing units separated by confining units, which are composed mainly of the siliciclastic Hawthorn Group with interlayered sequences of more and less permeable carbonates, sands and clays (Scott, 1988, 1990). The extent, thickness, and permeability of the IAS are variable, but generally control the downward leakage between the SAS and the UFA (Katz et al., 2009). Pyrite is found unevenly distributed throughout the Hawthorn Group and occurs mainly in its framboidal form (Lazareva and Pichler, 2007). Arsenic concentrations in the Hawthorn Group are generally less than 5 mg/kg, but can reach up to 69 mg/kg in samples with abundant pyrite (Lazareva and Pichler, 2007; Pichler et al., 2011). Near the highest As concentrations, the bottom of the IAS is about −30 m amsl and dips to the west at a slope of approximately 0.001.

The UFA is the major source of water supply within the study area and consists of permeable limestone and dolomite deposited in a shallow marine environment (Green et al., 1995; Miller, 1986). Carbonate deposition was interrupted at first periodically, and finally completely, with the influx of the siliciclastic sediments eroded from the Appalachian Mountains that form the IAS. Within the region of high As concentrations, the bottom of the UFA is about − 400 m amsl and dips to the west at a slope of approximately 0.001. Because of its high permeability, the Florida Geological Survey has been testing the UFA to serve as an underground reservoir for aquifer storage and recovery (ASR) systems. Detailed lithological, mineralogical, and geochemical studies of the two uppermost formations of the UFA, the Tampa Member and the Suwannee Limestone, showed that As is generally present in low concentrations (a few mg/kg), but is concentrated in minor minerals, such as pyrite, which may contain up to 11,200 mg/kg As (Lazareva and Pichler, 2007; Price and Pichler, 2006). The Tampa Member of the Arcadia Formation hydrostratigraphically belongs to the UFA, although it is the lowermost stratigraphic unit of the Hawthorn Group (Miller, 1986).

Please cite this article in press as: Pichler, T., Mozaffari, A., Distribution and mobility of geogenic molybdenum and arsenic in a limestone aquifer matrix, Applied Geochemistry (2015), http://dx.doi.org/10.1016/j.apgeochem.2015.08.006

3. Materials and methods

3.1. Core description

To assess the occurrence, distribution and mineralogical association of As and Mo in the aquifer matrix in the study area three cores were analyzed (Fig. 1). Core DEP-1 was drilled inside the area of contamination to a depth of 114 m below surface and sampled between 44 m and 114 m. Core DEP-2 was drilled inside the area of contamination to a depth of 103 m below surface and sampled between 4 and 103 m. As a reference, core DEP-5 was drilled outside the area of contamination to a depth of 103 m below surface and sampled between 27 m and 103 m. The cores were described in detail, which included the chemical analyses for total organic carbon (TOC), Ca, Mg, Si, Al, P, Sr, As, Mo, Fe, and S content and the preparation of thin sections. Each core was sampled at a spacing of approximately 0.5 m to ensure representation of all stratigraphic units. In addition to those interval samples, targeted samples were taken along each core from sections with visible pyrite, hydrous ferric oxide, clays, or organic material. These sections were suspected to have higher As concentrations than the bulk carbonate or clay matrix. This sampling approach was successfully applied to assess the importance of pyrite as the source of As in the UFA (Lazareva and Pichler, 2007; Pichler et al., 2011; Price and Pichler, 2006). The samples were dried at room temperature and subsequently powdered and dissolved using a digestion method modified from van der Veen et al. (1985). Once cooled, the digestates were diluted to 50 mL with deionized water (DI) and allowed to settle for at least 24 h before being passed through a 2.0 μm Teflon filter. Two mL of the filtered samples were diluted with 8 mL of DI for determination of Ca, Mg, Si, Al, P, Sr, Mo, Fe, and S on a Perkin Elmer Optima 2000 DV inductively coupled plasma-optical emission spectrometer (ICP-OES). A 10 mL aliquot of each sample was prepared for As analysis by hydride generation-atomic fluorescence spectrometry (HG-AFS) on a PSA 10.055 Millennium Excalibur instrument following (Price and Pichler, 2006). To assure quality control, approximately 10% duplicate samples were randomly selected. Sample blanks, which were added every 5–10 samples, did not show detectable concentrations of As (<0.2 μg/L). To test recovery, 2 samples from each batch were spiked in liquid form with the equivalent 25 mg/kg As before digestion. Recovery of As from the spiked samples was always between 90% and 110%.

Polished thin sections were made for 20 samples high in As and Mo for further analyses of discrete mineral phases by optical microscopy, scanning electron microscopy (SEM) using a Zeiss Supra 40 instrument equipped with a Bruker EDX detector and electron microprobe analysis (EMPA) using a JEOL JXA-8900R instrument. Reference materials consisted of natural and synthetic sulfide, sulfate, silicate, and oxide. Due to logistic limitations, only core DEP-2 was analyzed top to bottom. The other two cores, DEP-1 and DEP-5, were analyzed starting at a depth of approximately 45 m (below surface) and had essentially the same stratigraphy, element patterns and concentrations as DEP-2 (Appendix A and B).

Total carbon (TC), inorganic carbon (IC) and total organic carbon (TOC) were determined as follows: (1) The samples were dried at 105 °C, (2) TC was determined by combusting a dried sample at 1350 °C in an oxygen atmosphere using a LECO CR-412 instrument, (3) TOC was determined by the same combustion method after removal of IC with phosphoric acid (1:1) and (4) IC was determined by difference.

3.2. Mobilization test for weakly bound As and Mo

To assess the mobilization potential of As and Mo from the aquifer matrix 10 samples were chosen for a chemical extraction experiment based on the following criteria: (1) high total Mo concentration, (2) high total As concentration and (3) geographic representation of the study area (Fig. 1). The extraction experiment was carried out on duplicate samples following step 1 of an established sequential extraction procedure (Pichler et al., 2001; Price and Pichler, 2005). All chemicals used were reactant grade or better and solutions were prepared with double deionized water (DDI) of at least 18 MΩ cm^{-1}.

The purpose of this procedure was to assess the amount of exchangeable (i.e., easily mobilized) As and Mo in the aquifer matrix. To carry out the extraction 20 mL of 1.0 M sodium acetate (NaOAc) adjusted to a pH of 8.1 were added to 1 g of powdered sample in a 50 mL screw cap centrifuge tube and shaken for 2 h at room temperature in a mechanical shaker operating at 250 motions min^{-1}. The extract was separated from the solid residue by centrifugation at 4000 RPM for 10 min. The supernatant was decanted into a 50 mL tube, diluted to 50 mL and prepared for chemical analyses (i.e., filtration, dilution if necessary). To wash the residuals they were re-suspended in 5 mL of DI water then centrifuged and the supernatant was discarded.

4. Results

4.1. Stratigraphy, mineralogy and chemical composition of the cores

The stratigraphy from top to bottom was approximately as follows: 0–18 m surficial sediments (SAS), 18–60 m Hawthorn Group (IAS), 60–70 m Tampa Member (UFA) and below 70 m Suwannee Limestone (UFA). Except in the uppermost segment, limestone was the main lithology. Occasionally dolomite and clay minerals were present. That lithology was also observed in the bulk chemical composition, where Ca, Mg and Sr concentrations increased with depth, while Si, Al and P decreased, indicating the decreasing siliciclastic and clay content (Appendix A and B). Core lithology, Arsenic and Mo concentrations in DEP-5, which was the reference core from outside the area of contamination, did not differ from those cores drilled inside the area of contamination (DEP-1 and DEP-2). The minimum, maximum, median and standard deviations for all analyzed elements, including As and Mo were comparable for all three cores (Figs. 2 and 3, Appendix B). Molybdenum, As, S and Fe, however, varied significantly with depth and median As and Mo values were above their respective crustal averages of approximately 1.1 mg/kg and 1.5 mg/kg (Li, 2000). The median values for As were 3.4 mg/kg in DEP-1, 4.7 mg/kg in DEP-2 and 3 mg/kg in DEP-5 (Appendix A, Fig. 3). The median values for Mo were 4.4 mg/kg in DEP-1, 6 mg/kg in DEP-2 and 3.1 mg/kg in DEP-5 (Appendix A,

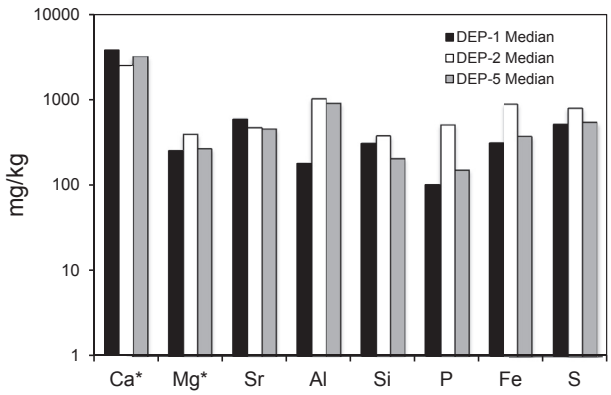

Fig. 2. Comparison of the median concentrations of Ca, Mg, Sr, Al, Si, P, Fe and S in sediments samples from the three cores DEP-1, DEP-2 and DEP-5. *To allow for better presentation Ca and Mg values were divided by 100 and 10, respectively.

Please cite this article in press as: Pichler, T., Mozaffari, A., Distribution and mobility of geogenic molybdenum and arsenic in a limestone aquifer matrix, Applied Geochemistry (2015), http://dx.doi.org/10.1016/j.apgeochem.2015.08.006

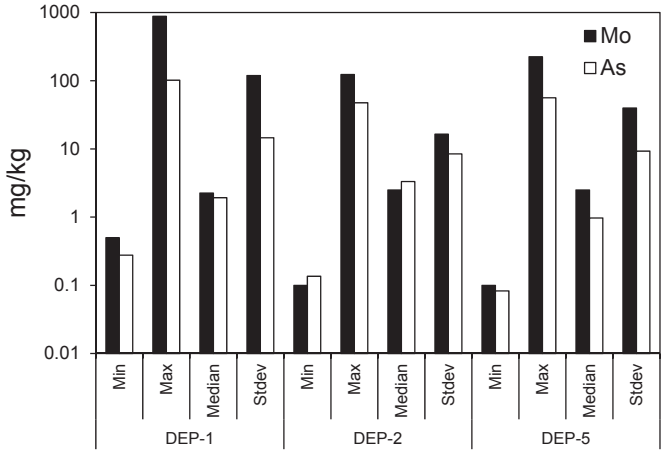

Fig. 3. Comparison of the minimum, maximum, median and standard deviations of As and Mo concentrations in sediment samples from cores DEP-1, DEP-2 and DEP-3. Although there are differences in minimum and maximum concentrations, the median values are more or less identical.

Fig. 3). However, these median values are heavily skewed due to occasionally high values of up to 100 mg/kg for As and up to 880 mg/kg for Mo (Appendix A).

The concentrations were highest in the SAS and IAS and returned to "normal", i.e., expected values for crustal carbonate rocks, in the UFA below a depth of 60–70 m below surface (Fig. 4). The concentrations of Fe and S seemed to follow the same pattern, being elevated in each of the cores at approximately the same depth (Fig. 5). In core DEP-1 As was elevated at depths of approximately 45 m and 55 m (Fig. 5). In core DEP-2 As varied significantly between 5 m and 35 m and then had two pronounced high concentrations at 45 m and 60 m (Fig. 5). In core DEP-5 As was elevated at depths of approximately 50 m and 65 m (Fig. 5). In core DEP-1 Mo was elevated at depths of approximately 45 m and 70 m (Fig. 5). In core DEP-2 Mo showed the same pattern as As. It varied significantly between 5 m and 35 m and then had two pronounced high concentrations at approximately 45 m and 70 m (Fig. 5). In core DEP-5 was elevated at several depths, the highest values at approximately 50 m and 75 m (Fig. 5).

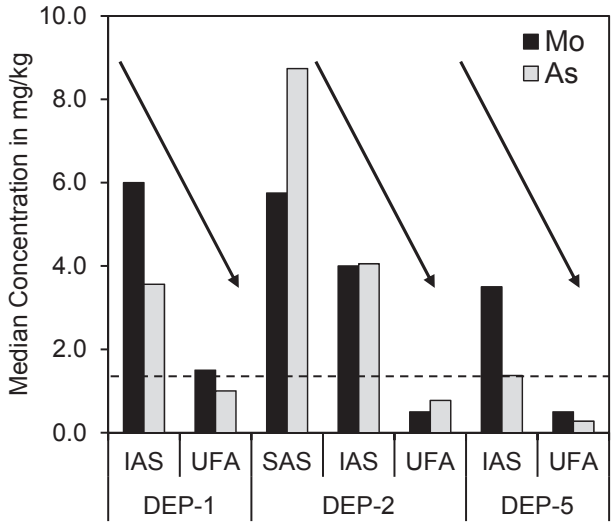

Fig. 4. Comparison of the medians of As and Mo concentrations in each hydrostratigraphic section in sediment samples from cores DEP-1, DEP-2 and DEP-3. The median values decrease with increasing depth. The dashed line approximately depicts the average concentration of As and Mo in crustal rocks.

Euhedral and framboidal pyrite was identified as a minor mineral in the IAS and UFA sections (Fig. 6), where it generally filled void spaces. Sometimes occurring together with hydrous ferric oxide (HFO) (Fig. 6A) or with powellite (Fig. 6B). Electron microprobe analyses revealed variable concentrations of As in pyrite ranging from approximately 300 to 9000 mg/kg (Table 1). The molybdenum concentration in pyrite was consistently below the detection limit of approximately 100 mg/kg and the highest values for Zn and Sb were 806 mg/kg and 730 mg/kg, respectively. These values were in the same range as those previously reported for the IAS (Lazareva and Pichler, 2007) and Suwannee Limestone (Price and Pichler, 2006). HFO was identified mainly in the upper sections of the cores.

In core DEP-1 the calcium molybdate powellite ($CaMoO_4$) was identified at a depth of approximately 45 m. It occurred as very small grains of approximately 20 μm in diameter filling void spaces and enclosing primary mineral grains of the aquifer matrix indicating that powellite was the latest stage of mineral formation (Fig. 6B). Based on the average of 5 EMPA measurements, its chemical composition by mass was approximately 21% Ca, 42% Mo and 1.76% As, while other elements were less than 0.2% (Table 2). The elevated As concentration could also be observed by energy dispersive X-ray spectroscopy (EDX) (Fig. 6D).

Organic carbon was present throughout the cores, ranging from 0.1 to 3.3% (Appendix C). Its occurrence in each of the three cores was almost identical. Core DEP-1 had a maximum concentration of 2.6% and a median of 1.4% ($n = 22$), core DEP-2 had a maximum concentration of 3.0% and a median of 1.4% ($n = 27$) and core DEP-5 had a maximum concentration of 3.3% and a median of 1.4% ($n = 26$).

4.2. Mobilization experiment

The results for the mobilization of Mo and As are shown in Table 3. Analytical quality was evaluated by including a replicate and a blank in each analytical batch. The results showed high precision for replicate samples (average standard deviation of replicates were 2.8 for Mo and 0.86) for As and the blanks did not contain detectable concentrations of either element.

During the experiment with NaOAc at a pH of 8.1, which had the purpose to identify easily mobilized Mo in the aquifer matrix up to 97% were removed (Fig. 7). More than 80% Mo was removed from samples 45–46, 46–47, 70–71, 31–32, 42–43 and 51–52 and approximately 65%–70% Mo was removed from samples 18–19 and 75–76. Despite the high extraction from these samples, two samples 10–11 and 69–70 showed much lower Mo extraction of 5% and 21%, respectively. The percentages were calculated using the corresponding Mo concentrations from the total analyses (Appendix A).

In contrast to Mo, As was mobilized to a lesser degree and the samples could be divided into three groups. Between 21% and 50% As were removed from samples 42–43, 45–46, 46–47, 70–71 and 31–32 and approximately 10%–24% As were removed from samples and 50–51, while little to nothing was removed from the remaining samples, 10–11, 18–19 and 69–70 (Table 3). The percentages were calculated using the corresponding As concentrations from the total analyses (Appendix A).

5. Discussion

5.1. Molybdenum

In the aquifer matrix below the town of Lithia in central Florida cores, Mo was elevated in certain horizons, particularly at depths of

Please cite this article in press as: Pichler, T., Mozaffari, A., Distribution and mobility of geogenic molybdenum and arsenic in a limestone aquifer matrix, Applied Geochemistry (2015), http://dx.doi.org/10.1016/j.apgeochem.2015.08.006

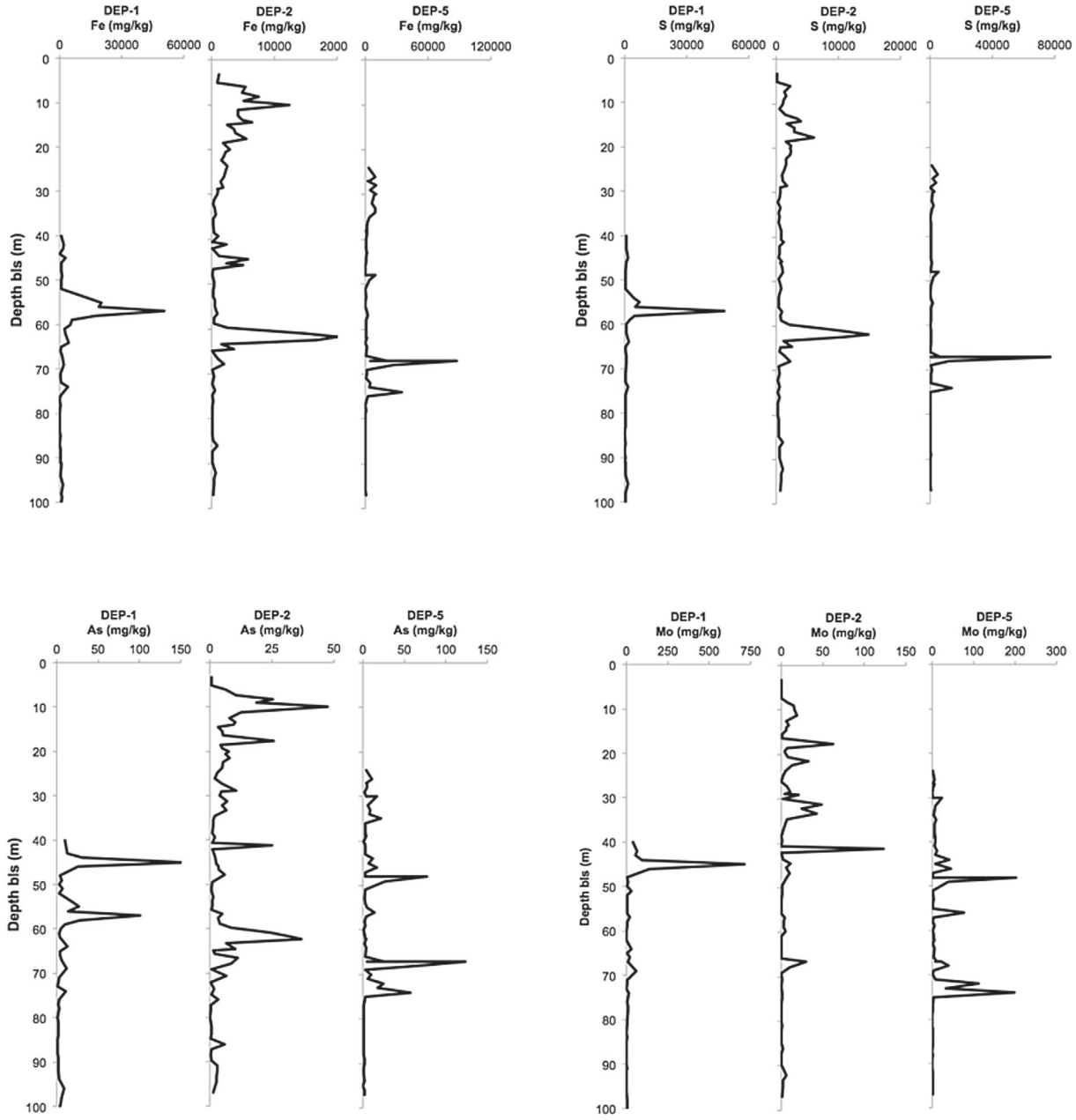

Fig. 5. Approximate stratigraphy and depth profiles for the concentration of iron (Fe), sulfur (S), arsenic (As) and molybdenum (Mo) in cores DEP-1, DEP-2 and DEP-5.

approximately 40–60 m below surface in all three cores (Fig. 5). Values were comparable between the cores with maximum values above 100 mg/kg and median values of around 3 mg/kg. These values were higher than what was considered to be the mean concentration of Mo in the Earth's crust of around 1–2 mg/kg (Li, 2000). However, Mo concentrations can be significantly higher in sediments, which were deposited under oxygen-depleted conditions. Hatch and Leventhal (1992) reported up to 850 mg/kg Mo for the Stark Shale Member of the Dennis Limestone in Kansas and Calvert and Pedersen (1993) reported a range from 21 to 160 mg/kg Mo for sediments from several anoxic basins. In purely oxic sediments of marine origin Mo concentrations are generally much lower (Bertine and Turekian, 1973; Crusius et al., 1996) and thus changing redox conditions during deposition may cause the Mo variation seen in the DEP cores (Fig. 4). According to Scott (1988) the depositional environment of the Hawthorn Group changed constantly from marine or peri-marine conditions that seemed to have ranged from prodeltaic and shallow to sub-tidal marine, to intertidal and supratidal with occasional deposition of terrestrial sediments in the form of paleosoils and weathered residuum of the Hawthorn sediments. In addition the existence of phosphorite deposits in the Hawthorn Group points towards upwelling and the associated changes in redox conditions (Riggs, 1984), as well as the varying abundance of organic carbon in the sediments (Appendix B).

The exact mineralogical association of Mo in the aquifer matrix remains unclear, although the mineral powellite ($CaMoO_4$) was observed in the aquifer matrix (Fig. 6). Based on crystal habit it is unlikely that powellite is a primary mineral that would have precipitated during sediment deposition or early diagenesis. In Fig. 6B powellite encloses primary calcite fragments indicating that it was the latest or one of the latest mineral phases to precipitate in

Please cite this article in press as: Pichler, T., Mozaffari, A., Distribution and mobility of geogenic molybdenum and arsenic in a limestone aquifer matrix, Applied Geochemistry (2015), http://dx.doi.org/10.1016/j.apgeochem.2015.08.006

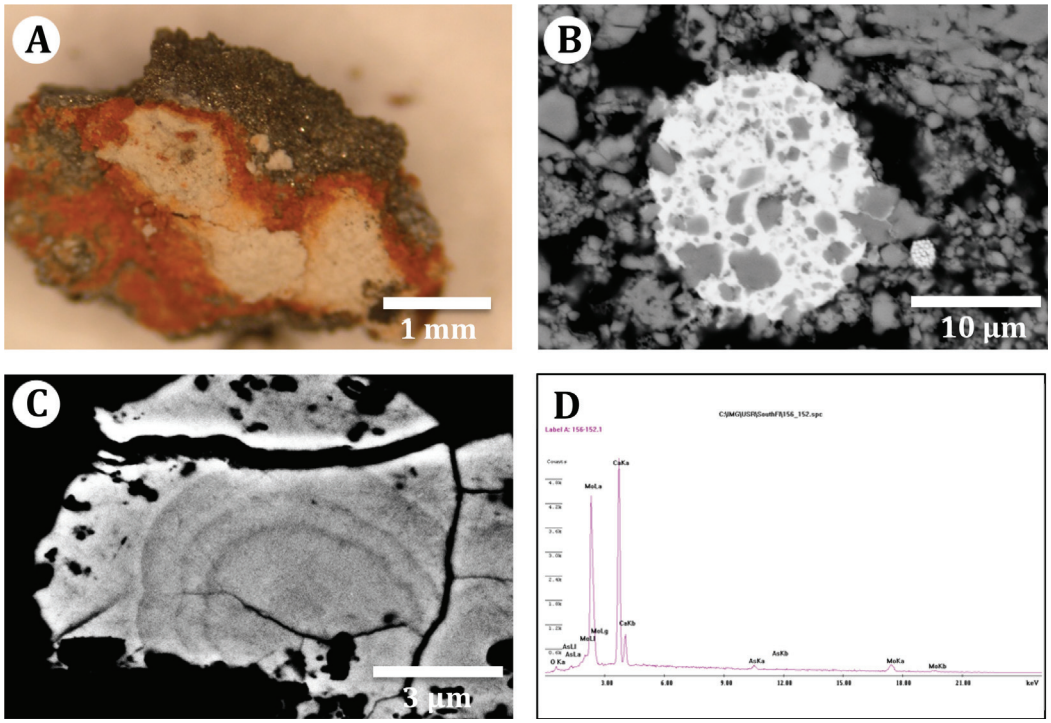

Fig. 6. (A) Optical microscopy image of pyrite and HFO in core DEP-1 at a depth of 60 m. (B) Back scatter electron image of powellite and a framboidal pyrite from core DEP-1 (46 m depth) of powellite in a clay/carbonate matrix. (C) Secondary electron microprobe image (polished thin section) of a powellite crystal showing fine growth banding. (D) EDX spectra for the powellite in image B.

the aquifer matrix. Precipitation of powellite due to evaporative concentration of Mo in the pore water during drying of the samples could have happened. However, several powellites showed very delicate banding, which appeared to be growth banding (Fig. 6C). The fine scale of the bands and their uniformity precludes the type of rapid deposition one would expect from evaporation during core handling. Thus it is conceivable that powellite is a sink for Mo, rather than a source. Thermodynamic modeling with the computer code Geochemist's Workbench (GWB), using recent thermodynamic data for aqueous Mo species, powellite and molybdenite, showed that powellite was super-saturated in groundwater samples with Mo concentrations above 2000–3000 µg/L. Precipitation of powellite from super-saturated groundwater was observed elsewhere as well (e.g., Conlan et al., 2012). Thus, the likely primary source for Mo is organic matter, which is sufficiently abundant in the aquifer matrix. The mean concentration was in each of the three cores was 1.4%, which is significantly higher than 0.24%, which is considered the mean concentration in limestone (Gehman, 1962). Organic matter has a high adsorption potential for Mo (Jenne, 1998) and is known to incorporate and concentrate Mo (e.g., Tribovillard et al., 2004).

Under reducing conditions at the time of sediment deposition, Mn refluxing has the potential to concentrate dissolved MoO_4^{2-} at the sediment–water interface. In cases where anoxia extends upward into the water column, Mn^{2+} oxidizes to particulate MnO_x (solid) just above the chemocline. The particulate Mn settles into the anoxic waters, and re-dissolved Mn^{2+} diffuses back through the chemocline, thus completing a redox cycle (Adelson et al., 2002). In this case Mo can be co-precipitated by Mn and Fe oxides. However, no evidence was found to indicate that Mo was co-precipitated with Mn and Fe oxides during time of sediment deposition. The Mn concentrations were rather low and more or less uniformly distributed throughout the study area with median values of 24, 37 and 34 for Cores DEP-1, DEP-2 and DEP-5, respectively. The possible explanation is that the physicochemical conditions in the sedimentary environment did not change sufficiently. On the other hand, in sulfidic settings, pyrite and organic matter (OM) have a greater capability to fix Mo from seawater and retain it during diagenesis (Adelson et al., 2002; Helz et al., 2011, 1996; Tribovillard

Table 1
Average chemical compositions of pyrite (FeS_2) in thin sections from cores DEP-1 and DEP-2.

Core	Sample	Fe	S	As	Sb	Zn	Mo	Ca	Total
		wt%	wt%	mg/kg	mg/kg	mg/kg	mg/kg	wt%	wt%
DEP-1	45–46	42	52	8788	730	320	<0.5	0.19	95
DEP-1	45–46b	47	52	2113	0	48	<0.5	0.53	99
DEP-1	57–58	47	52	1281	18	40	<0.5	0.04	99
DEP-1	57–58	48	53	360	0	15	<0.5	0.03	101
DEP-1	64–65b	47	53	451	9	68	<0.5	0.15	100
DEP-1	64–65	46	52	1412	16	54	<0.5	0.24	98
DEP-2	17–18a	47	53	794	9	59	<0.5	0.22	99
DEP-2	17–18b	46	52	1164	11	806	<0.5	0.39	98
DEP-2	41–42	38	51	6597	57	19	<0.5	0.52	90
DEP-2	62–63d	47	53	1846	32	28	<0.5	0.03	100
DEP-2	62–63b	47	52	1713	25	98	<0.5	0.11	99
DEP-2	67–68	46	54	681	66	21	<0.5	0.76	101
DEP-2	68–69	48	53	285	13	6	<0.5	0.06	101

Table 2
Average chemical compositions of powellite ($CaMoO_4$) in thin sections from core DEP-1.

Core	Sample	Fe	S	As	Sb	Zn	Mo	Ca	Total
		mg/kg	mg/kg	mg/kg	mg/kg	mg/kg	wt%	wt%	wt%
DEP-1	45–46	5935	4690	15,050	<0.5	755	23	15	41
DEP-1	47–48	472	3216	17,640	34	1312	42	21	66

Please cite this article in press as: Pichler, T., Mozaffari, A., Distribution and mobility of geogenic molybdenum and arsenic in a limestone aquifer matrix, Applied Geochemistry (2015), http://dx.doi.org/10.1016/j.apgeochem.2015.08.006

Table 3
Amounts of Mo and As mobilized from the aquifer matrix sediments by reaction with NaOAc at pH 8.1 compared to total Mo and As.

Core	Sample	Mo^A	Mo^A	Mo^T	As^A	As^A	As^T
		mg/kg	%	mg/kg	mg/kg	%	mg/kg
DEP-1	45–46	114	94	122	11	39	30
DEP-1	46–47	750	91	825	72	50	144
DEP-1	70–71	399	80	499	28	22	132
DEP-2	10–11	1	4	25	n.d.	n.d.	29
DEP-2	18–19	21	55	38	n.d.	n.d.	18
DEP-2	31–32	52	97	53	3	29	9
DEP-2	42–43	76	98	78	4	21	20
DEP-5	50–51	30	83	36	2	6	30
DEP-5	69–70	6	20	30	n.d.	n.d.	60
DEP-5	75–76	85	62	136	2	3	52

Note: Mo^A is mobilized Mo and Mo^T is total Mo in the sample; the same for As; n.d. = not detected.

et al., 2008). Of the two possible sources OM is considered the dominant source for Mo (Chappaz et al., 2014). A closer look at the element distribution in core DEP-2 (Fig. 7) corroborates OM in the sense that hydrous ferric oxide and pyrite are excluded as major sources. If those two minerals were a source for Mo then either Fe or S or both should have been elevated at depth of 40 m where Mo has its maximum concentration. Pyrite was also ruled out because no Mo was detected during the electron microprobe analyses of pyrite.

5.2. Arsenic

In the aquifer matrix below the town of Lithia in central Florida cores, As was elevated in certain horizons, particularly at depths of approximately 10 m, 45 m, 60 m and 70 m below surface in all three cores (Fig. 4). Values were comparable for all three cores with maximum values above 100 mg/kg and median values of around 3 mg/kg. These values are higher than what is considered the mean concentration of As in the Earth's crust of around 1–2 mg/kg (Li, 2000). The observed distribution and concentration values are similar to previous studies of As occurrence in the Floridan Aquifer System (FAS) (Lazareva and Pichler, 2007; Pichler et al., 2011). According to Taylor and McLennan (Taylor and McLennan, 1985) the abundance of As in the upper continental crust is approximately 1.5 ppm. This value is somewhat controversial, because most of the individual rock types that were analyzed for As have higher values. The mean abundance in the common igneous rocks, basalt and granite, are 8.3 and 7.6 ppm, respectively (Taylor, 1964). The average for shale and its related materials, such as loess and mud, is approximately 10.6 ppm (Li, 2000). The average composition for sandstone is too difficult to determine, but the value for the commonly used geostandard GSR-4 is 9.1 ppm (Govindaraju, 1994). The average value for limestone/dolomite is 2.6 ppm (Baur and Onishi, 1969). Arsenic is considered a chalcophile element and therefore often found in As-rich pyrite, although discrete As minerals, such as arsenopyrite and reaglar are common if As concentrations are sufficiently high (e.g., Borba et al., 2003; Price et al., 2013; Price and Pichler, 2006). In oxic sediments As shows a high affinity for adsorption or co-precipitation with hydrous ferric oxide (HFO), such as ferrihydrite, goethite and hematite (Dixit and Hering, 2003; Lenoble et al., 2002; Pierce and Moore, 1982).

In the subsurface As was found as a minor element in pyrite and powellite (Tables 1 and 2), while in the SAS where the conditions are more oxygenated, As was likely bound to HFO, hence the association of As and Fe (Fig. 8). In the IAS, As occurs together with powellite and in the UFA where Fe and S were elevated As should predominantly occur in As-rich pyrite. This inferred As mineralogy follows the expected redox gradient for groundwater from

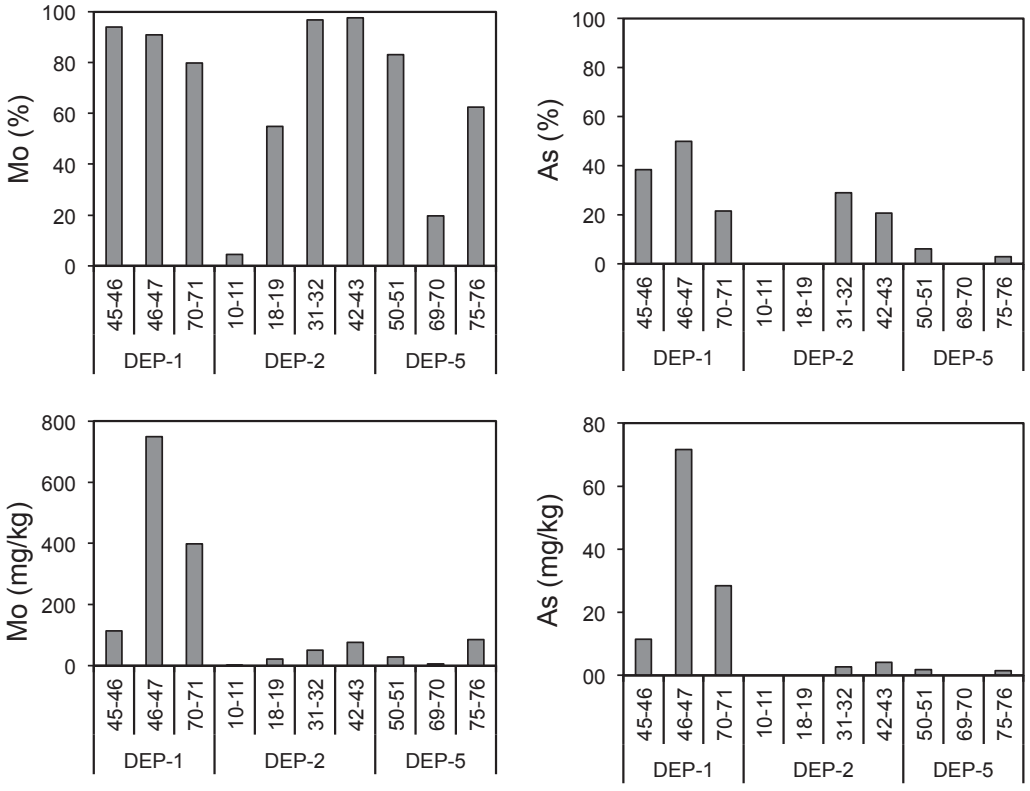

Fig. 7. Percentage and absolute amount of Mo and As mobilized during the reaction with a NaOAc solution at pH 8.1. The data corresponds to Table 3.

Please cite this article in press as: Pichler, T., Mozaffari, A., Distribution and mobility of geogenic molybdenum and arsenic in a limestone aquifer matrix, Applied Geochemistry (2015), http://dx.doi.org/10.1016/j.apgeochem.2015.08.006

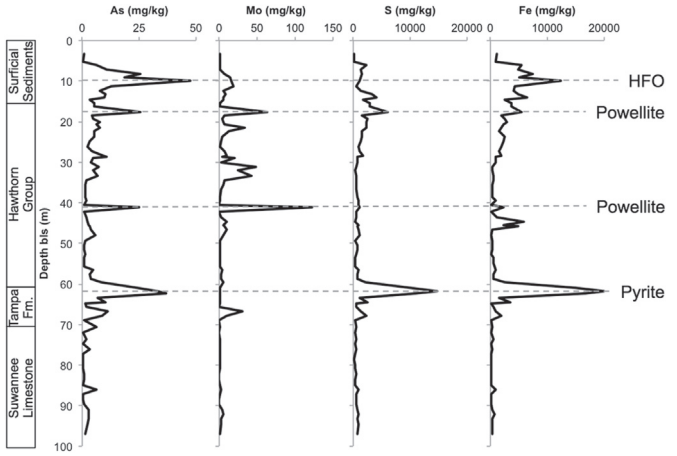

Fig. 8. Stratigraphy and depth profiles for the concentration of arsenic (As), molybdenum (Mo), sulfur (S) and iron (Fe) in core DEP-2. The dashed lines are an aid to correlate peaks across the graph and the minerals names on the right side indicate the possible source.

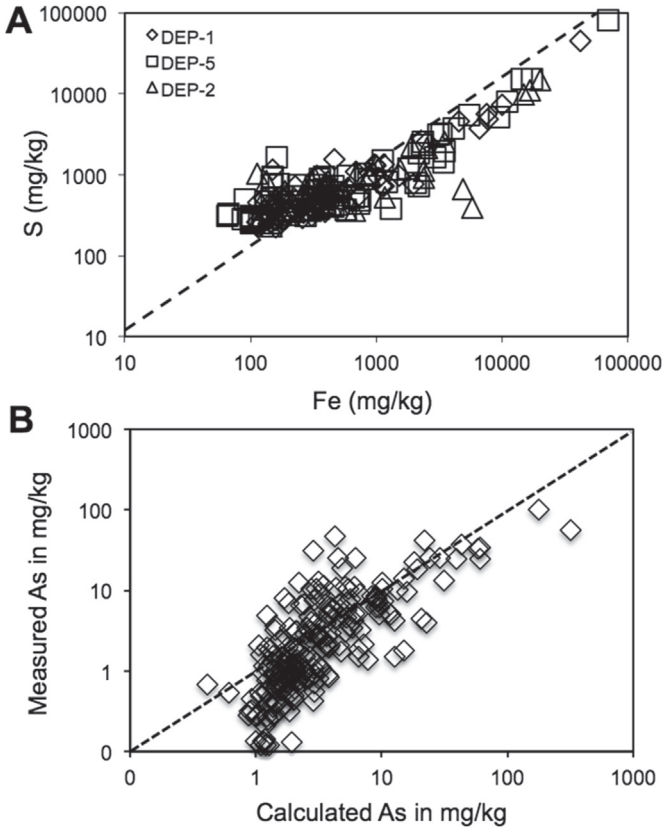

Fig. 9. (A) Plot of Fe vs. S for the three monitoring well clusters DEP-1, DEP-2 and DEP-5. The dashed line represents the "pyrite line", i.e., if pyrite would be the single source of Fe and S in a sample then all analyses would plot on this line. (B) Plot of As measured vs. As calculated, based on As abundance in pyrite (see text for more explanation). The dashed line represents the ideal case of As measured = As calculated. Data points that fall above this line contain more bulk As than expected, considering pyrite as the only source of As, and are made up of mostly samples containing clay. Data points below the line are due to high S contents in organic material and therefore have higher calculated As values.

oxygenated near the surface to more reducing conditions at depth. HFO is generally stable under oxygen-rich conditions (Jambor and Dutrizac, 1998), while pyrite is stable under the reduced conditions in the UFA (e.g., Jones and Pichler, 2007). The redox stability of powellite is not well known, however, reducing (sulfidic) conditions seem to have little influence on powellite stability, since powellite and pyrite coexist in close proximity (Fig. 6B). Unfortunately there is nothing known about abiotic molybdate reduction but sulfate its structural analog is well studied and abiotic sulfate reduction can only proceed at temperatures above 160 °C (Machel, 2001). It appears, however, that pyrite is the primary source of As in the subsurface below Lithia, because only little powellite was present in the aquifer matrix. This assumption can be verified with a massbalance approach using the bulk concentrations of Fe, S, and As combined with As concentrations in individual pyrites. Due to the correlation between S and Fe ($R^2 = 0.94$), it can be assumed that Fe and S concentrations were controlled largely by the presence of pyrite (Fig. 9A). The pyrite line (Fe = 2S) represents Fe/S ratios that are exclusively controlled by the presence of pyrite (Fig. 9A). Thus, using the values of S and Fe, the abundance of pyrite in each sample was calculated and the calculated amount of pyrite was multiplied by the mean arsenic concentration of pyrite obtained by electron microprobe analyses (Table 1) and compared to the actual analyzed bulk arsenic concentrations (Appendix A). Calculated and measured arsenic are compared in Fig. 9B. Many samples show good agreement between the measured and calculated As concentrations, i.e., they follow the dashed line in Fig. 9B. For those samples that lie significantly above the equal concentration line, calculated arsenic concentrations were lower than those measured in the bulk sample. These results can be explained by existence of other As sources such as, clays, organic material, hydrous ferrous oxides and powellite or an underestimation of the amount of pyrite. Samples that show a much higher calculated arsenic concentration compared to a measured result probably due to overestimation of pyrite abundance due to the presence of S from sources other than pyrite, e.g., gypsum or anhydrite.

5.3. Mobilization of As and Mo

Until present, no effort was made to investigate the geogenic or anthropogenic mobilization of Mo from sedimentary rocks and its impact on groundwater quality. In anoxic/sulfidic sediments, Mo is mainly associated with iron sulfides and/or OM (Chappaz et al., 2014; Dahl et al., 2013; Erickson and Helz, 2000; Glass et al., 2013; Zheng et al., 2000). In normal seawater, Mo is stable as MoO_4^{2-} with a resident time of approximately 440 thousand years (Miller et al., 2011). Its enrichment is much lower compared to sulfidic sediments and it can be preserved in marine oxic sediments by adsorption onto Fe/Mn-oxyhydroxides (Goldberg et al., 2009; Zheng et al., 2000).

Considering how As and Mo are bound in the aquifer matrix below Lithia (i.e., organic matter, pyrite, powellite and HFO; Fig. 8), changing the physicochemical conditions should cause the mobilization of As and Mo in three ways: i) the introduction of oxygen into the aquifer could result in the oxidation of pyrite and organic matter (e.g., Alberic and Lepiller, 1998); ii) consumption of oxygen by biotic and abiotic processes could result in the reduction of HFO (Amirbahman et al., 1997; Welch and Lico, 1998); and iii) non-equilibrium saturation could eventually lead to the aqueous dissolution of powellite (e.g., Conlan et al., 2012). On the other hand, the same three scenarios could also cause the precipitation of As and Mo: i) the introduction of oxidative conditions could result in the adsorption of As onto newly precipitated HFO (e.g., Pichler et al., 1999); ii) the change to reducing conditions could result in the incorporation of As into newly precipitated pyrite (Bostick and Fendorf, 2003) or adsorption of As and Mo onto pyrite (Bostick et al., 2003); and iii) non-equilibrium

Please cite this article in press as: Pichler, T., Mozaffari, A., Distribution and mobility of geogenic molybdenum and arsenic in a limestone aquifer matrix, Applied Geochemistry (2015), http://dx.doi.org/10.1016/j.apgeochem.2015.08.006

saturation could result in the precipitation of powellite from super-saturated groundwater (e.g., Conlan et al., 2012). Any of these changes in the physicochemical conditions beneath Lithia can be caused by mixing between shallow, oxygenated and deep, oxygen-depleted groundwater. In Lithia each home has its own water well, because the township is not connected to the public water supply system. Thus there is the potential that the abundance of private supply wells in this area may short-circuit the hydraulic gradient across the confining layer in the Hawthorne group (IAS), e.g., bringing oxygen-depleted water from the deep aquifer into the shallow aquifer and vice versa. While there is little known about Mo mobilization, there is abundant knowledge about the release of geogenic As under oxidizing, as well as reducing conditions. Since Mo can be present in similar solid phases, such as HFO, pyrite and organic matter (e.g., Tribovillard et al., 2004), the release mechanisms of As should be a good analog. For example, Delemos et al. (2006) argued that leakage of organic contaminants from a landfill in New England, USA mobilized geogenic As by driving the reduction of As-bearing oxides. At other sites, pumping-induced hydraulic gradient changes can perturb physiochemical conditions in the aquifer, mobilizing geogenic As. Harvey et al. (2006) argue that geogenic As at their field site in Bangladesh is mobilized because pumping for irrigation draws fresh organic carbon into the aquifer, which subsequently drives the reduction of As-bearing oxides. The introduction of oxygen-rich surface water into an anoxic aquifer during aquifer storage and recovery (ASR) caused the dissolution of As-rich pyrite and thus increased As concentration in recovered water above the drinking water limit of 10 μg/L (e.g., Wallis et al., 2011). Since in an anoxic aquifer the inferred association of Mo is with organic matter (e.g., Tribovillard et al., 2004), the introduction of oxygen into an anoxic aquifer would oxidize the organic matter and liberate Mo.

From the leaching experiment it becomes clear that Mo should be easier mobilized from the aquifer matrix than As (Fig. 7). Up to 90% of Mo were removed during the reaction with 1.0 M sodium acetate (NaOAc) adjusted to a pH of 8.1, while at the same time only up to 50% As were mobilized. This indicates that the majority of Mo in the aquifer matrix is adsorbed onto mineral surfaces and organic matter, while As should be present as impurities in minerals, i.e., As in pyrite and powellite and co-precipitated with HFO. Thus the mobilization of Mo can proceed along several pathways, which are oxidation of organic matter, desorption from mineral surfaces and re-dissolution of powellite. However, only Mo mobilized through oxidation of organic matter should be considered primary Mo. There was evidence for redox disequilibrium in the IAS in the study area, i.e., co-occurrence of pyrite and HFO and pyrite and powellite in the aquifer matrix (Fig. 2). Thus, following the initial release from the aquifer matrix Mo could be adsorbed by either pyrite or HFO under uncertain redox conditions and later released from either. Since its stability is mainly controlled by the ion activity product (IAP) of Ca^{2+} and MoO_4^{2-} dissolution of secondary powellite is possible once the IAP of the groundwater is less than the K_{sp} (e.g., Conlan et al., 2012). Thus we propose that the release of Mo to groundwater in the IAS intervals could be a combination of changing redox conditions and changing ion activity product (IAP) due to mixing between shallow and deep groundwater, as well as the reversal from oxygenated to reducing conditions. Considering the observed redox disequilibrium, which indicated at least a single but most likely several redox changes, As should be mobilized similarly. During the infiltration of oxygenated surface water pyrite oxidation causes the release of As, while during periods of upward flow of oxygen-depleted groundwater, HFO is reduced and co-precipitated (sorbed) As is released.

6. Summary and conclusions

Arsenic (As) and molybdenum (Mo) were found at elevated levels in the aquifer matrix of the Surficial Aquifer System (SAS) and the Intermediate Aquifer System (IAS). Median values for both were approximately 3–6 times higher that their respective crustal averages. In the upper part of the Upper Floridan Aquifer System (UFA) median values were below their corresponding crustal averages. Thus the distribution of As and Mo in the study area seems to be controlled by the clastic and clay content of the aquifer matrix. With depth the aquifer matrix changes from (1) poorly indurated clastic deposits, to (2) interlayered sequences of carbonates, sands and clays and to (3) limestone and dolomite. That lithological change was also observed in the bulk sediment chemical composition, where Ca, Mg and Sr concentrations increased with depth, while Si, Al and P concentrations decreased with depth.

In the SAS As mainly occurred adsorbed onto hydrous ferric oxide (HFO) and in the IAS and UFA As was found as an impurity in pyrite, with concentrations of up to 9000 mg/kg. Although Mo generally has a high affinity for incorporation into pyrite, in the study area pyrite was virtually Mo-free. Thus pyrite formed during a period when Mo was either not present in the aquifer matrix or when physic-chemical conditions were such that Mo was securely bound by organic matter. In a few samples the mineral powellite ($CaMoO_4$) was discovered, which was not considered a source of Mo, but rather a sink. Geochemical modeling indicated that in the study area powellite was supersaturated and its crystal habit dismissed precipitation during sediment deposition or early diagenesis. Thus organic matter is the likely primary source of Mo in the aquifer matrix. The difference of where and how Mo and As were present in the aquifer matrix impacted their behavior during the mobilization experiments. Molybdenum, which seemed to be loosely bound to mineral and organic matter surfaces, was easily removed from the aquifer matrix. Arsenic on the other hand was much less mobile, because it occurred either tightly absorbed by HFO or as an impurity in pyrite.

Currently this study stands alone and thus it remains questionable if Mo is of similar concern as As, nevertheless it would be advisable to include Mo in the analytical program whenever elevated As concentrations are encountered in aquifers of marine origin.

Acknowledgments

We thank the Florida Department of Environmental Protection Site Investigation Section for making this study possible. Particularly the participation and support by Robert Cilek, Jeff Newton and William Martin was greatly appreciated. Olesya Lazareva, Daniela Stebbins, Angela Dippold, David Budd and Bastian Kuehl are thanked for their participation in the laboratory analyses and core descriptions. This project was partially funded by the German Research Foundation (DFG-Projekt PI 746/1-1).

Appendix A. Supplementary data

Supplementary data related to this article can be found at http://dx.doi.org/10.1016/j.apgeochem.2015.08.006.

References

Adelson, J.M., Helz, G.R., Miller, C.V., 2002. Reconstructing the rise of recent coastal anoxia; molybdenum in Chesapeake Bay sediments. Geochim. Cosmochim. Acta 66, 4367.

Ahmed, M.F., Ahuja, S., Alauddin, M., Hug, S.J., Lloyd, J.R., Pfaff, A., Pichler, T., Saltikov, C., Stute, M., van Geen, A., 2006. Ensuring safe drinking water in

Bangladesh. Science 314, 1687–1688.
Alberic, P., Lepiller, M., 1998. Oxydation de la matière organique dans un système hydrologique karstique alimenté par des pertes fluviales (Loiret, France) (Oxidation of organic matter in a karstic hydrologic unit supplied through stream sinks (Loiret, France)). Water Res. 32, 2051–2064.
Amini, M., Abbaspour, K.C., Berg, M., Winkel, L., Hug, S.J., Hoehn, E., Yang, H., Johnson, C.A., 2008. Statistical modeling of global geogenic arsenic contamination in groundwater. Environ. Sci. Technol. 42, 3669–3675.
Amirbahman, A., Sigg, L., Gunten, U.V., 1997. Reductive dissolution of Fe(III) (hydr) oxides by cysteine: kinetics and mechanism. J. Colloid Interface Sci. 194, 194–206.
Arthur, J.D., Dabous, A.A., Fischler, C., 2007. Aquifer storage and recovery in Florida: geochemical assessment of potential storage zones. In: Fox, P. (Ed.), Management of Aquifer Recharge for Sustainability, Proceedings of the International Symposium on Managed Aquifer Recharge, Scottsdale, Arizona.
Baur, W.H., Onishi, B.H., 1969. Arsenic. In: Wedepohl, K.H. (Ed.), Handbook of Geochemistry. Springer Verlag, Berlin, pp. A1–A33.
Bertine, K.K., Turekian, K.K., 1973. Molybdenum in marine deposits. Geochim. Cosmochim. Acta 37, 1415–1434.
Borba, R.P., Figueiredo, B.R., Matschullat, J., 2003. Geochemical distribution of arsenic in waters, sediments and weathered gold mineralized rocks from iron quadrangle, Brazil. Environ. Geol. 44, 39–52.
Bostick, B.C., Fendorf, S., 2003. Arsenite sorption on troilite (FeS) and pyrite (FeS2). Geochim. Cosmochim. Acta 67, 909–921.
Bostick, B.C., Fendorf, S., Helz, G.R., 2003. Differential adsorption of molybdate and tetrathiomolybdate on pyrite (FeS2). Environ. Sci. Technol. 37, 285–291.
Calvert, S.E., Pedersen, T.F., 1993. Geochemistry of recent oxic and anoxic marine sediments: implications for the geological record. Mar. Geol. 113, 67–88.
Chappaz, A., Lyons, T.W., Gregory, D.D., Reinhard, C.T., Gill, B.C., Li, C., Large, R.R., 2014. Does pyrite act as an important host for molybdenum in modern and ancient euxinic sediments? Geochim. Cosmochim. Acta 126, 112–122.
Conlan, M.J.W., Mayer, K.U., Blaskovich, R., Beckie, R.D., 2012. Solubility controls for molybdenum in neutral rock drainage. Geochem. Explor. Environ. Anal. 12, 21–32.
Crusius, J., Calvert, S., Pedersen, T., Sage, D., 1996. Rhenium and molybdenum enrichments in sediments as indicators of oxic, suboxic and sulfidic conditions of deposition. Earth Planet. Sci. Lett. 145, 65–78.
Dahl, T.W., Chappaz, A., Fitts, J.P., Lyons, T.W., 2013. Molybdenum reduction in a sulfidic lake: evidence from X-ray absorption fine-structure spectroscopy and implications for the Mo paleoproxy. Geochim. Cosmochim. Acta 103, 213–231.
Davies, T.D., Pickard, J., Hall, K.J., 2005. Acute molybdenum toxicity to rainbow trout and other fish. J. Environ. Eng. Sci. 4, 481–485.
Delemos, J.L., Bostick, B.C., Renshaw, C.E., Stürup, S., Feng, X., 2006. Landfill-stimulated iron reduction and arsenic release at the Coakley superfund site (NH). Environ. Sci. Technol. 40, 67–73.
Dixit, S., Hering, J.G., 2003. Comparison of arsenic(V) and arsenic(III) sorption onto iron oxide minerals: implications for arsenic mobility. Environ. Sci. Technol. 37, 4182–4189.
Erickson, B.E., Helz, G.R., 2000. Molybdenum(VI) speciation in sulfidic waters: stability and lability of thiomolybdates. Geochim. Cosmochim. Acta 64, 1149–1158.
Ferguson, J.F., Gavis, J., 1972. A Review of the Arsenic Cycle in Natural Waters, 6. Water Research Pergamon Press, pp. 1259–1274.
Gehman Jr., H.M., 1962. Organic matter in limestones. Geochim. Cosmochim. Acta 26, 885–897.
Glass, J.B., Chappaz, A., Eustis, B., Heyvaert, A.C., Waetjen, D.P., Hartnett, H.E., Anbar, A.D., 2013. Molybdenum geochemistry in a seasonally dysoxic Mo-limited lacustrine ecosystem. Geochim. Cosmochim. Acta 114, 204–219.
Goldberg, T., Archer, C., Vance, D., Poulton, S.W., 2009. Mo isotope fractionation during adsorption to Fe (oxyhydr)oxides. Geochim. Cosmochim. Acta 73, 6502–6516.
Govindaraju, K., 1994. 1994 compilation of working values and and sample description for 383 geostandards. Geostand. Newsl. 18, 1–158.
Green, R., Arthur, J.D., DeWitt, D., 1995. Lithostratigraphic and Hydrostratigraphic Cross Sections Through Pinellas and Hillsborough Counties, Southwest Florida. United States Geological Survey Open File Report, p. 26.
Harvey, C.F., Ashfaque, K.N., Yu, W., Badruzzaman, A.B.M., Ali, M.A., Oates, P.M., Michael, H.A., Neumann, R.B., Beckie, R., Islam, S., Ahmed, M.F., 2006. Groundwater dynamics and arsenic contamination in Bangladesh. Chem. Geol. 228, 112–136.
Hatch, J.R., Leventhal, J.S., 1992. Relationship between inferred redox potential of the depositional environment and geochemistry of the upper Pennsylvanian (Missourian) stark shale member of the Dennis limestone, Wabaunsee Country, Kansas, U.S.A. Chem. Geol. 99, 65–82.
Heijerick, D.G., Regoli, L., Carey, S., 2012. The toxicity of molybdate to freshwater and marine organisms. II. Effects assessment of molybdate in the aquatic environment under REACH. Sci. Total Environ. 435, 179–187.
Helz, G.R., Bura-Nakić, E., Mikac, N., Ciglenečki, I., 2011. New model for molybdenum behavior in euxinic waters. Chem. Geol. 284, 323–332.
Helz, G.R., Miller, C.V., Charnock, J.M., Mosselmans, J.F.W., Pattrick, R.A.D., Garner, C.D., Vaughan, D.J., 1996. Mechanism of molybdenum removal from the sea and its concentration in black shales: EXAFS evidence. Geochim. Cosmochim. Acta 60, 3631–3642.
Hughes, J.D., Vacher, H.L., Sanford, W.E., 2009. Temporal response of hydraulic head, temperature, and chloride concentrations to sea-level changes, Floridan aquifer system, USA. Hyrogeol. J. 17, 793–815.
Jambor, J.L., Dutrizac, J.E., 1998. Occurrence and constitution of natural and synthetic ferrihydrite, a widespread iron oxyhydroxide. Chem. Rev. 98, 2549–2585.
Jenne, E.A., 1998. Adsorption of Metals by Geomedia: Variables, Mechanisms, and Model Applications. Academic Press, San Diego.
Jones, G.W., Pichler, T., 2007. The relationship between pyrite stability and arsenic mobility during aquifer storage and recovery in southwest central Florida. Environ. Sci. Technol. 41, 723–730.
Katz, B.G., Crandall, C.A., Metz, P.A., McBride, W.S., Berndt, M.P., 2007. Chemical Characteristics, Water Sources and Pathways, and Age Distribution of Ground Water in the Contributing Recharge Area of a Public-supply Well Near Tampa, Florida, 2002–05. USGS Scientific Investigations Report 2007-5139, 85 pp.
Katz, B.G., McBride, W.S., Hunt, A.G., Crandall, C.A., Metz, P.A., Eberts, S.M., Berndt, M.P., 2009. Vulnerability of a public supply well in a karstic aquifer to contamination. Ground Water 47, 438–452.
Korte, N.E., Fernando, Q., 1991. A review of arsenic(III) in groundwater. Crit. Rev. Environ. Control 21, 1–36.
Lazareva, O., Pichler, T., 2007. Naturally occurring arsenic in the Miocene hawthorn group, Southwestern Florida: implication for phosphate mining. Appl. Geochem. 22, 953–973.
Lenoble, V., Bouras, O., Deluchat, V., Serpaud, B., Bollinger, J.-C., 2002. Arsenic adsorption onto pillared clays and iron oxides. J. Colloid Interface Sci. 255, 52–58.
Li, Y.-H., 2000. A Compendium of Geochemistry: from Solar Nebula to the Human Brain. Princeton University Press, Princeton.
Machel, H.-G., 2001. Bacterial and thermochemical sulfate reduction in diagenetic settings – old and new insights. Sediment. Geol. 140, 143–175.
McNeill, L.S., Hsiao-wen, C., Edwards, M., 2002. Aspects of arsenic chemistry in relation to occurrence, health and treatment. In: Frankenberger Jr., W.T. (Ed.), Environmental Chemistry of Arsenic. Marcel Dekker, New York, pp. 141–154.
Miller, C.A., Peucker-Ehrenbrink, B., Walker, B.D., Marcantonio, F., 2011. Re-assessing the surface cycling of molybdenum and rhenium. Geochim. Cosmochim. Acta 75, 7146–7179.
Miller, J.A., 1986. Hydrogeologic Framework of the Floridan Aquifer System in Florida, Georgia, South Carolina and Alabama.
Peters, S.C., Blum, J.D., 2003. The source and transport of arsenic in a bedrock aquifer, New Hampshire, USA. Appl. Geochem. 18, 1773–1787.
Pichler, T., 2005. $\delta^{34}S$ isotope values of dissolved sulfate (SO_4^{2-}) as a tracer for battery acid (H_2SO_4) contamination. Environ. Geol. 47, 215–224.
Pichler, T., Hendry, J., Hall, G.E.M., 2001. The mineralogy of arsenic in uranium mine tailings at the Rabbit Lake in-pit facility, Northern Saskatchewan, Canada. Environ. Geol. 40, 495–506.
Pichler, T., Price, R.E., Lazareva, O., Dippold, A., 2011. Determination of arsenic concentration and distribution in the Floridan aquifer System. J. Geochem. Explor. 111, 84–96.
Pichler, T., Sültenfuß, J., 2010. A stable and radioactive isotope study of geogenic arsenic contamination in a limestone aquifer. In: Levin, C., Grathwohl, P., Kappler, A., Kaufmann-Knoke, R., Rügner, H. (Eds.), Grundwasser für die Zukunft. E. Schweizerbart, Tübingen, p. 62.
Pichler, T., Veizer, J., Hall, G.E.M., 1999. Natural input of arsenic into a coral-reef ecosystem by hydrothermal fluids and its removal by Fe(III) oxyhydroxides. Environ. Sci. Technol. 33, 1373–1378.
Pierce, M.L., Moore, C.B., 1982. Adsorption of arsenite and arsenate on amorphous iron hydroxide. Water Res. 16, 1247–1253.
Price, R.E., S, I., Planer-Friedrich, B., Bühring, S.I., Amend, J., Pichler, T., 2013. Processes influencing extreme As enrichment in shallow-sea hydrothermal fluids of Milos Island, Greece. Chem. Geol. 348, 15–26.
Price, R.E., Pichler, T., 2005. Distribution, speciation and bioavailability of arsenic in a shallow-water submarine hydrothermal system, Tutum Bay, Ambitle Island, PNG. Chem. Geol. 224, 122–135.
Price, R.E., Pichler, T., 2006. Abundance and mineralogical association of arsenic in the Suwannee limestone (Florida): implications for arsenic release during water–rock interaction. Chem. Geol. 228, 44–56.
Price, W.A., Hart, B., Howell, C., 1999. Proceedings of the 1999 Workshop on Molybdenum Issues in Reclamation. British Columbia Technical and Research Committee on Reclamation, p. 144.
Riggs, S.R., 1984. Paleoceanographic model of Neogene phosphorite deposition, U.S. Atlantic Continental margin. Science 223, 123–131.
Scott, T.M., 1988. Lithostratigraphy of the hawthorn group (Miocene) of Florida. Fla. Geol. Surv. Bull. 1–148.
Scott, T.M., 1990. The Lithostratigraphy of the Hawthorn Group of Peninsular Florida. Florida Geologica Survey Open File Report 36, Open file report. FGS.
Smedley, P.L., Cooper, D.M., Ander, E.L., Milne, C.J., Lapworth, D.J., 2014. Occurrence of molybdenum in British surface water and groundwater: distributions, controls and implications for water supply. Appl. Geochem. 40, 144–154.
Taylor, S.R., 1964. Abundance of elements in the crust: a new table. Geochim. Cosmochim. Acta 28, 1273–1285.
Taylor, S.R., McLennan, S.M., 1985. The Continental Crust: Its Composition and Evolution. Blackwell Scientific Publications, Oxford.
Tribovillard, N., Lyons, T.W., Riboulleau, A., Bout-Roumazeilles, V., 2008. A possible capture of molybdenum during early diagenesis of dysoxic sediments. Bull. De. La Soc. Geol. De. Fr. 179, 3–12.
Tribovillard, N., Riboulleau, A., Lyons, T., Baudin, F., 2004. Enhanced trapping of molybdenum by sulfurized marine organic matter of marine origin in Mesozoic limestones and shales. Chem. Geol. 213, 385–401.

Please cite this article in press as: Pichler, T., Mozaffari, A., Distribution and mobility of geogenic molybdenum and arsenic in a limestone aquifer matrix, Applied Geochemistry (2015), http://dx.doi.org/10.1016/j.apgeochem.2015.08.006

van der Veen, N.G., Keukens, H.J., Vos, G., 1985. Comparison of ten digestion procedures for the determination of arsenic in soils by hydride-generation atomic absorption spectrometry. Anal. Chim. Acta 171, 285–291.

Wallis, I., Prommer, H., Pichler, T., Post, V., Norton, S.B., Annable, M.D., Simmons, C.T., 2011. Process-based reactive transport model to quantify arsenic mobility during aquifer storage and recovery of potable water. Environ. Sci. Technol. 45, 6924–6931.

Welch, A.H., Lico, M.S., 1998. Factors controlling As and U in shallow ground water, southern Carson Desert, Nevada. Appl. Geochem. 13, 521–539.

WHO, 2011. Guidelines for Drinking-water Quality, fourth ed. World Health Organization, Geneva.

Zhai, X.W., Zhang, Y.L., Qi, Q., Bai, Y., Chen, X.L., Jin, L.J., Ma, X.G., Shu, R.Z., Yang, Z.J., Liu, F.J., 2013. Effects of molybdenum on sperm quality and testis oxidative stress. Syst. Biol. Reprod. Med. 59, 251–255.

Zheng, Y., Anderson, R.F., van Geen, A., Kuwabara, J., 2000. Authigenic molybdenum formation in marine sediments: a link to pore water sulfide in the Santa Barbara Basin. Geochim. Cosmochim. Acta 64, 4165–4178.

Please cite this article in press as: Pichler, T., Mozaffari, A., Distribution and mobility of geogenic molybdenum and arsenic in a limestone aquifer matrix, Applied Geochemistry (2015), http://dx.doi.org/10.1016/j.apgeochem.2015.08.006